Stony Brook University

Functions of Interferon Stimulated Gene, ISG54

A Dissertation Presented

by

Marcin Stawowczyk

to

The Graduate School

in Partial Fulfillment of the

Requirements

for the Degree of

Doctor of Philosophy

in

Molecular and Cellular Biology

Stony Brook University

August 2012

Stony Brook University

The Graduate School

Marcin Stawowczyk

We, the dissertation committee for the above candidate for the

Doctor of Philosophy degree, hereby recommend

acceptance of this dissertation.

Nancy C Reich Marshall Ph.D. – Dissertation Advisor
Professor, Department of Molecular Genetics and Microbiology

Eckard Wimmer Ph.D. - Chairperson of Defense
Distinguished Professor, Department of Molecular Genetics and Microbiology

Erwin London, PhD
Professor, Department of Biochemistry and Cell Biology

Wei-Xing Zong, PhD
Associate Professor, Department of Molecular Genetics and Microbiology

James Bliska, PhD
Professor, Department of Molecular Genetics and Microbiology

This dissertation is accepted by the Graduate School

Charles Taber
Interim Dean of the Graduate School

Abstract of the Dissertation

Functions of Interferon Stimulated Gene, ISG54

by

Marcin Stawowczyk

Doctor of Philosophy

in

Molecular and Cellular Biology

Stony Brook University

2012

The ability of interferons to protect cells from viral infection depends on the activation of multiple interferon-stimulated genes that together induce an anti-viral state. One of the genes is Interferon Stimulated Gene 54 (ISG54/IFIT2), coding for a 54kDa protein with a highly segmented structure rich in tetratricopeptide (TPR) motifs. We discovered that ISG54 promotes apoptosis in cancer cell lines, and that shRNA knockdown of ISG54 significantly reduced cell death in response to interferon. ISG54-mediated apoptosis proceeds by the mitochondrial pathway and requires the presence of Bax and Bak proteins. The anti-apoptotic B-cell lymphoma (Bcl-xL) effectively blocks ISG54-mediated apoptosis. In addition, anti-apoptotic proteins: adenoviral E1B-19K, and gammaherpesvirus v-Bcl2 and M11, also block apoptosis induced by ISG54. Activation of caspase-3 was apparent in the ISG54 expressing cells, and the pan-caspase inhibitor ZVAD-FMK was found to block ISG54-induced cell death. A decrease of mitochondrial potential, and translocation of Bax into the mitochondrial compartment were also detected in ISG54 expressing cells. ISG54-mediated apoptosis was found to be p53 independent but could be partially inhibited by overexpression of H-Ras, PI3K and Akt.

Our further studies revealed that ISG54 interacts with other members of its family: ISG56 and ISG60 and that together they form an oligomeric structure at ~150-250kDa. ISG60 was found to inhibit the pro-apoptotic functions of ISG54 and that effect was dependent on a direct

interaction between ISG60 and the first TPR domain of ISG54. Moreover, ISG54 was found to interact with other binding partners such as STING, DLC1, PRDX5 and eEF1α.

We generated ISG54 knockout mice and evaluated the protective role of ISG54 during infection with Mouse Gamma Herpesvirus 68 (MHV68). We discovered that the ISG54 knockout facilitates MHV68 replication in embryonic fibroblasts in culture, especially at low multiplicities of infection. In vivo infections of the ISG54 knockout animals showed an increased viral latency as measured by viral genomes in the spleen and ex vivo viral reactivation. Together our data suggest that ISG54 may be important part of the interferon system responsible for both anti-viral and anti-cancer effects. Elucidating mechanisms of ISG54 action may help to improve existing therapies against cancer and viral diseases.

Dedication Page

I dedicate this thesis to my Family, especially to my Grandmas who passed away during my studies in grad school. It's due to their love and support that I can be here and write this thesis. You will be forever in my heart

Table of content

List of Figures

List of Abbreviations

3-MA	3-Methyladenine
aa	Aminoacid
Ab	Antibody
ADAR	Adenosine deaminase
AIF	Apoptosis inducing factor
ALG2	Apoptosis-Linked gene 2
APAF1	Apoptotic protease activating factor-1
APC	Allophycocyanin
ATF2	Activating transcription factor 2
ATP	Adenosine triphosphate
ATRA	All transretinoic acid
Bcl	B-cell lymphoma
BH domain	Bcl-2 homology domin
BSA	Bovine serum albumin
CAD	Caspase activated endonuclease
CASP	Caspase
CBP	Creb binding protein
CD	cluster of differentiation

cdk	cyclin dependent kinase
CML	Chronic myelogenous leukemia
COP	Coat protein complex
CPE	Cytopathic effect
CREB	cAMP response element-binding
DISC	Death-inducing signaling complex
DLC1	Dynein light chain 1
DMEM	Dulbecco's Modified Eagle Medium
DNA	Deoxyribonucleic acid
DR	Death Receptor
ds	Double stranded
EDTA	Ethylenediaminetetraacetic acid
eEF-1α	Eukaryotic elongation factor 1 alpha
EGFP	Enhanced Green Fluorescent Protein
EGTA	ethylene glycol tetraacetic acid
eIF2	Eukaryotic initiation factor 2
eIF3	Eukaryotic initiation factor 3
EMCV	Encephalomyocarditisvirus
ER	Endoplasmic reticulum
ERK	Extracellular signal regulated kinase

FBS	Fetal bovine serum
GAPDH	Glyceraldehyde 3-phosphate dehydrogenase
GAS	Gamma- IFN Activated Site
GFP	Green fluorescent protein
GTP	Guanine triphosphate
HBV	Hepatitis B virus
HCV	Hepatitis C virus
HIV	Human Immunodeficiency Virus
HOP	Hsp70-Hsp90 Organizing Protein
HPV	Human papillomavirus
HSP	Heat Shock Protein
IAP	Inhibitors of apoptotic proteins
iE-DAP	D-glutamyl-meso-diaminopimelic acid
IFIT	Interferon Induced Transcript
IFITM1	Interferon-induced transmembrane protein 1
IFN	Interferon
IFNAR	Interferon alpha receptor
Ig	Immunoglobulin
IkBα	Inhibitor of nuclear factor of kappa light chain gene enhancer in B-cells alpha)
IKK	IkappaB kinase

Il	Interleukin
IRAK	Interleukin-1 receptor-associated kinases
IRF	Interferon regulatory factor
ISG	Interferon Stimulated Gene
ISGF3	Interferon stimulated Gene Factor-3
ISRE	Interferon stimulated Response Element
JAB1	Jun-activation domain-binding protein 1
JAK	Janus Kinase
kDA	Kilodalton
KO	Knockout
KOMP	Knock-Out Mouse Project
KS	Kaposi's Sarcoma
KSHV	Kaposi Sarcoma Herpes Virus
LC3	Microtubule-associated protein 1A/1B-light chain 3
LCMV	Lymphocytic Choriomeningitis Virus
LDA	Limited Dilution Assay
LD-PCR	Limited Dilution PCR
LGP2	Laboratory of genetics and physiology 2 (protein)
LPS	Lipopolysaccharide
MAPK	Mitogen activated protein kinase

MAVS	Mitochondrial Antiviral-Signaling Protein
Mcl-1	Induced myeloid leukemia cell differentiation protein 1
MDA-5	Melanoma differentiation associated factor 5
MEFs	Mouse embryo fibroblasts
mGFP	monomeric form of Green Fluorescent Protein
MHC	Major Histocompatibility complex
MIP2	Macrophage inflammatory protein 2
MITA	Mediator of IRF3 activation
MKK6	MAP kinase kinase 6
mM	Milimolar
MMLV	Moloney Murine Leukemia Virus
MNK1	MAPK signal interating kinase-1
MOI	Multiplicity of Infection
MSK1	Mitogen- and stress-activated protein kinase
mTOR	Mammalian target of rapamycin
NF-κB.	Nuclear factor kappa-light-chain-enhancer of activated B cells
NK cells	Nature killer cells
NOD	Nucleotide Oligomerization Domain
NUB1	NEDD8 ultimate buster 1
OAS	2’5’ oligoadenylate synthase

OSCC	Oral squamous cell carcinoma
PAGE	Polyacrylamide gel electrophoresis
PAMP	Pathogen associated molecular pattern
PBS	Phosphate buffered saline
PCR	Polymerase chain reaction
Pfu	Plaque forming unit
PI	Propidium iodide
PI3K	Phosphatidylinositol kinase 3
PKR	Protein kinase R
PPP-RNA	Triphosphorylated RNA
PRDX5	Peroxiredoxin 5
PRR	Pathogen recognition receptor
Rb	Retinoblastoma
RIG-I	Retinoic acid inducible gene-I
RNA	Ribonucleic acid
ROS	Reactive oxigen species
SDS	Sodium dodecyl sulphate
SeV	Sendai Virus
SH2 domain	Src homology 2 domain
shRNA	Small hairpin ribonucleic acid

SLE	Systemic lupus erythematosus
SMAC	Second mitochondria-derived activator of caspase
SOD	Superoxide dismutase
STAT	Signal Transducer and activator of transcription
STING	Stimulator of interferon genes
TAC buffer	Tris ammonium chloride buffer
TANK	TRAF family member-associated NF-kB activator
TBK1	Tank-binding kinase 1
TBS	Tris buffered saline
TLR	Toll-like receptor
TNF	Tumor necrosis factor
TOM	Translocase of outer membrane
TPR	Tetratricopeptide
TRADD	Tumor necrosis factor receptor type 1-associated DEATH domain protein
TRAF	TNF recpetor associated factor
TRAIL	TNF-related apoptosis-inducing ligand
TRIF	TIR-domain-containing adapter-inducing interferon-β
tRNA	Transfer RNA
TYK2	Non-recpetor Tyrosine protein kinase 2

UTR	Untranslated Region
VACV	Vaccinia Virus
VDAC	Voltage dependent anion chanel
VEGF	Vascular endothelial growth factor
VISA	Virus-Induced Signaling Adaptor
vMAP	Viral mitochondrial antiapoptotic protein
VSV	Vesicular stomaits virus
WNV	West Nile Virus
wt	Wild-type
XAF-1	X-linked Inhibitor of Apoptosis Protein Associated Factor 1
YFP	Yellow fluorescent protein

Acknowledgments

I would like to express my gratitude to all the people whose tremendous help allowed me to complete this thesis. First of all, I would like to thank my Graduate Advisor, Dr Nancy Reich-Marshall for her continuous help and support throughout my studies. She was always there with her invaluable suggestions helping not only with designing experiments or writing papers but also with doing actual lab work and often working next to me hand in hand. Secondly I would like to thank all the past and present lab members for helping me with experiments, teaching me new methods and making the lab amazing, friendly place where you always wanted to come. Special thanks I owe to Sarah van Scoy who with unshaken patience kept introducing me to molecular techniques and to Dr Velasco Cimica who helped me with imaging experiments and was a great joyful friend. I am also extremely grateful to Dr Laurie Krug for her help with viral experiments and her students Brandon, and Nana who practically from the scratch taught me how to work with animals and viruses. Finally, I would like to thank my committee members: Dr Eckard Wimmer, Dr Wei-Xing Zong, Dr Erwin London and Dr Jim Bliska for their useful suggestions and critical remarks regarding both my experimental work and the thesis. And at last I would like to express my great gratitude to my girlfriend, Ania, who with her unconditioned love supported me during writing this thesis giving me reason to hold on and to do my best.

Chapter 1. Introduction

Throughout the evolution organisms became targets for many pathogens such as viruses, bacteria or parasites. To prevent growth and to inactivate infectious agents hosts developed multiple defense mechanisms

The interferon (IFN) system has evolved as a critical component of innate immunity first found in cartilagenous fish (1). There are three main classes of IFN that bind to distinct cell surface receptors and yet they all share the unique ability to confer resistance to viral infection(2).

The IFN receptors are associated with Janus kinases that are activated following ligand binding. The Janus kinases tyrosine phosphorylate a specific set of latent transcription factors, STATs that gain the ability to bind DNA of target genes (3). The target genes called Interferon Stimulated Genes (ISGs) are responsible for the unique biological properties of IFNs. IFNs promote an anti-viral response, stimulate immune cells and decrease cancer cell proliferation. Understanding the function of each of the ISGs is essential to understand the biological response to IFN and to pursue knowledge to improve its clinical use.

The objective of my thesis research was to determine the function of the one of ISGs, ISG54. This gene is induced directly by the STAT transcription factors following IFN stimulation (4). I have taken three approaches to investigate the function of ISG54: i) Ectopic expression of ISG54 in the absence of other ISGs was found to clearly promote apoptosis; ii) Protein-protein associations were used to identify a number of binding partners of ISG54, some of which are other ISGs; iii) We generated an ISG54 knockout mouse and found that it is more susceptible to viral latency following infection with murine gammaherpesvirus MHV68. These studies together indicate that ISG54 plays a critical role in viral defense likely by its ability to promote apoptosis. This function may also contribute to the anti-proliferative effect of IFN on cancer cells.

Interferons

The Interferon (IFN) system is a specific set of cytokines responsible for induction of an anti-viral response. Interferons are glycosylated and non-glycosylated proteins 165-200aa long

that are secreted from cells infected with pathogens and bind to cell surface receptors to signal in an autocrine or paracrine manner (on the neighboring cells) (5). There are three known types of IFNs. Type I and type III can be produced by most nucleated cells after viral infection while type II is synthesized by the activated T lymphocytes and Natural Killer (NK) cells. Type I and type III IFNs are produced shortly after pathogen entry and their function is to induce an anti-viral state in all types of cells. Type II is produced at later stages of infection and its main target are macrophages that are stimulated to destroy engulfed pathogens (5). Type I encompasses multiple IFN-α genes (thirteen in humans, fourteen in mice), a single IFN-β gene and group of other IFN genes: ε,κ,ω. Type II is represented by one IFN-γ gene and type III by two IFN-λ genes (5). IFN-αs are produced primarily by different types of leukocytes while IFN-β is synthesized by non-leukocytic cells. This review focuses mainly on the details of type-I IFN signaling that induces the ISG54 gene.

IFN action

Following secretion IFNs bind to specific cell surface receptors. Type IFNs bind to the type I receptors that consist of two subunits: Interferon Receptor Alpha 1 and Interferon Receptor Alpha 2 (IFNAR1 and IFNAR2) (6). Although all type-I IFNs bind to the same type-I receptor, they may have different effects on specific anti-viral response possibly due to different affinities. Downstream signaling events that lead to activation of IFN stimulated genes involve Janus Kinases (7) and Signal Transducer and Activator of Transcription (STAT) proteins. Janus kinases are non-receptor tyrosine kinases that contain kinase domain and a catalytically inactive pseudo-kinase domain. They associate with cytokine receptors in an inactive form and become activated after ligand binding (8). There are four Janus kinases in humans: JAK1, JAK2, JAK3 and TYK2, two of them, Tyrosine Kinase 2 (TYK2) and Janus Kinase 1 (JAK1), play a particularly important role in type I IFN signaling (3). STATs are a family of latent transcription factors involved in cytokine signaling that require tyrosine phosphorylation to bind a specific DNA target site. They are characterized by the ability to dimerize through reciprocal recognition of phosphotyrosine groups by their Src homology 2 (SH2) domains. A specific conserved tyrosine residue in SH2 domains of STAT protein is phosphorylated by JAK kinases. Phosphorylated STATs form homo- or heterodimers and translocate to the nucleus where they recruit transcription coactivators such as CREB binding protein (CBP)/p300 (9). Out of seven

known human STAT proteins, STAT1 and STAT2 play the most important role in type I IFN signaling.

Under physiological conditions JAK1/TYK2 kinases remain associated with subunits of IFN receptor: TYK2 with IFNAR1 and JAK1 with IFNAR2 (10) (see Figure 1). Binding of IFN molecule to the receptor brings JAK1 and TYK2 together and triggers their enzymatic activity. First they cross-phosphorylate each other and then in the next step they induce phosphorylation of tyrosine residues on the intracellular domain of IFN receptor (4,11). Phosphorylated receptors recruit STAT1 and STAT2 proteins that are subsequently phosphorylated by JAK1/TYK2. STAT2 is associated with another protein, IFN Regulatory Factor 9 (IRF9) and together with STAT1 they form trimer known as IFN-Stimulated Gamma Factor 3 (ISGF3) (12). ISGF3 translocates into the nucleus and binds to the regulatory element in promoter of IFN stimulated genes known as ISRE (IFN Stimulated Response Element). This recruits transcription machinery and initiates expression of ISGs (see Figure 1).

Other members of the STAT family: STAT3, STAT4, STAT5 and STAT6 have been also reported to be activated by type-I IFN (4), although they are not required for IFN anti-viral response. Combinations of homo and heterodimers of STATs can bind to another regulatory element referred to as GAS (Gamma- IFN Activated Site) that is characteristic for the genes activated by IFN-γ (10). Different combinations of STAT molecules and regulatory elements allow for precise regulation of gene expression. Together there are over 300 genes that can be upregulated in response to type I IFN signals (13). They are involved in multiple processes, such as host defence, adhesion, regulation of translation, and apoptosis (13). One of them is Interferon Regulatory Factor 7 (IRF7), transcription factor that stimulates further expression of IFN genes creating a loop of positive feedback (14). As a result more IFN is produced and secreted which leads to amplification and spreading of anti-viral message.

Induction of IFN genes

A typical mechanism of IFN response involves recognition of a intracellular pathogen (virus, intracellular bacteria or parasite) by one of cytosolic pathogen recognition receptors (PRRs). Activated PRR triggers a series of signaling events that result in activation of transcription factors and expression of IFN genes (see Figure 2).

Major transcription factors involved in expression of IFNα genes are Interferon Regulatory Factors 3 and 7 (IRF3, IRF7). The IFNβ promoter has also additional binding sites for NF-kB (nuclear factor kappa-light-chain-enhancer of activated B cells) and Activating transcription factor 2 (ATF2) /c-Jun dimer (15,16). Generally induction of IFN genes is initiated by activation of IRF3/7 and NF-κB. Regulation of those transcription factors is mediated by multiprotein complexes that include kinases and adapter proteins. In the cytosol NF-κB remains inactive bound to its inhibitor IkBα (Inhibitor of nuclear factor of kappa light chain gene enhancer in B-cells alpha) and must be released in order for NF-kB to enter the nucleus. Phosphorylation of IkBα by the IkappaB kinase (17) complex consisting of IKKα/IKKβ/IKKγ proteins causes its dissociation and proteaosomal degradation (18). On the other hand IRF3 and IRF7 are present as inactive monomers shuttling between cytosol and nucleus and require phosphorylation to dimerize and bind DNA in the nucleus. They are phosphorylated by TANK-Binding Kinase 1 (TBK1) and IkappaB kinase epsilon (IKKε) that are a part of a bigger protein complex including Tumor Necrosis Factor (TNF) receptor associated factor 3 (TRAF3), TRAF family member-associated NF-kB activator (TANK) and IKKγ (19-21).

Multiple PRRs induce IFN expression by activating TBK1 and IKK complexes. One of them is a family of Toll-like Receptors (TLRs) that recognize multiple Pathogen Associated Molecular Patterns (PAMPs) such as double stranded (ds)RNA, Lipopolysaccharide (22), flagellin or peptidoglycan (23). Among 10 TLR family members in humans TLR3, TLR4, TLR7 and TLR9 are known to induce type-I IFN response (24). TLR4 is a plasma membrane receptor while other three are the proteins associated with endosomes. TLR3 and TLR7 recognize viral RNA while TLR9 detects double stranded (ds) viral DNA (23). TLR4 is primary LPS sensor but can also be activated by some viral proteins and trigger IFN response. Signaling from most Toll-like receptors requires a presence of adapter protein MyD88. MyD88 directly or indirectly stimulates downstream effectors such as as TIR-domain-containing adapter-inducing interferon-β (TRIF) (24), Interleukin-1 receptor-associated kinases 1 and 4 (IRAK1/4) or TNF receptor associated factor 6 (TRAF6). TRIF binds to the TBK1 complex inducing phosphorylation of IRF3 and IRF7 while IRAK1 and TRAF6 can directly activate IRF7 by phosphorylation and ubiquitination respectively (25). TRIF and TRAF6 also indirectly stimulate IKK complex leading to NF- kB activation. TLR3 does not interact with MyD88 but it can still activate IRF3

by direct stimulation of TRIF as well as activation of phosphatidylinositol-3 kinase (PI3K) pathway that results in IRF3 phosphorylation (26).

Other PRRs are also effective inducers of IFN genes. A family of RIG-I–like helicases including: RIG-I (retinoic acid inducible gene I), MDA-5 (melanoma differentiation associated factor 5) and LGP2 (laboratory of genetics and physiology 2) work as the sensors of viral RNA (24). Both RIG-I and MDA-5 trigger expression of type I IFN genes while LGP2 lacks the activation domain and plays an inhibitory role. RIG-I can preferentially detect single stranded (ss)RNA with triphosphate group at its 5' end while MDA-5 is more specific to RNA containing poly I:C bases. Both can also detect different types of dsRNA (27). After binding viral RNA conformation of MDA-5 and RIG-I changes and their caspase recruitment domain (CARD) interacts with Mitochondrial Antiviral Signaling (MAVS) protein that is associated with mitochondrial membranes (20,27). MAVS is a very important adapter for induction of IFN genes. It recruits over 30 different adapter/effector proteins including TRADD (TNF receptor type 1-associated death domain protein) and TNF receptor associated factors 3 and 6 (TRAF3/6). These proteins together with their downstream effectors participate in activation of TBK1 and IKK complexes (20). One particularly important adapter protein that responds to DNA of pathogens and interacts with MAVS is Stimulator of IFN Gene (STING) also known as MITA (Mediator of IRF3 activation) (28,29). Role of STING and MAVS is schematically depicted in Figure 3. STING is bound to endoplasmic reticulum (ER) membranes surrounding mitochondria and functionally connects mitochondrial and ER compartments. STING binds TRAF3, MAVS and TBK1, it is phosphorylated by TBK1 complex and stimulates TBK1 to phosphorylate IRF3 (30). Moreover, STING was found to directly bind IRF3 probably triggering its phosphorylation by bridging it with TBK1 (30). STING is responsible for induction of IFNs in response to DNA pathogens (28). Without STING, synthesis of type I IFN in the cells infected with dsDNA viruses or transfected with dsDNA is severely impaired (31). Although STING also binds RIG-I and is involved in RIG-I dependent induction of IFN ,it is not essential for this process (30). Since signaling through STING is independent of TLRs, it suggests the existence of a cytoplasmic DNA sensor that can specifically activate STING. This sensor however, hasn't been yet discovered.

Synthesis of IFN can be also induced by PAMPs other than nucleic acids. Elements of Gram-negative peptidoglycan containing D-glutamyl-meso-diaminopimelic acid (iE-DAP)

moiety can activate IFN β production through action of NOD1 (Nucleotide-binding oligomerization domain-containing protein 1) receptor (32). NOD1 represents a family of over 20 NOD-like receptors (NLRs) that recognize different bacterial products including flagellin, muramyl dipeptide or bacterial toxins (23). NOD2, another member of the family, is known to induce IFN expression in response to ssRNA (33,34). Both NOD1 and NOD2 contain single CARD domains used for binding to RIP2 (Receptor interacting protein-2) adapter. RIP2 stimulates TRAF3 leading to the activation of TBK1 and phosphorylation of IRFs (32). Moreover, it forms a scaffold for transforming growth factor β-activated kinase-1 (TAK1), an enzyme responsible for stimulation of the IKK complex and activation of NF-kB (35). Interestingly, NOD2 was also reported to bind directly to MAVS and induce phosphorylation of IRF3/7 similarly to RIG-I/MDA-5 (33). Therefore it appears that diverse cytoplasmic sensors use multiple and often overlapping pathways to induce expression of interferons.

Once synthesized, IFNs are secreted and bind to the receptors on different types of cells. Stimulation with IFN influences many aspects of cell functioning often resulting in the induction of anti-viral or anti-cancer effects. Those effects define the biological significance of IFN and will be discussed in the next parts of this chapter.

Interferon and its anti-viral effect

A primary function of the IFN system is to protect cells from microbial infection. Animals that lack either IFN genes or IFN receptors are viable and fertile but show high susceptibility to microbial infection (36-38).

The STAT transcription factors activated by tyrosine phosphorylation bind and induce expression of a specific subsets of genes called IFN-stimulated genes. (ISGs). It is the products of these genes that confer the biological responses to IFN. ISGs confer anti-viral resistance by inhibiting various aspects of viral replication. Degradation of viral RNA is performed by 2’5’ oligoadenylate synthases (OAS) and RNase L. Both those enzymes are induced by interferon (39,40). OAS is activated by the recognition of dsRNA that is often a component of RNA virus replication. Upon its activation it synthesizes RNA oligonucletotides linked by a 2’5’ phosphodiester bond instead of the usual 3’5’ bond. Those oligonucleotides activate RNase L, an enzyme responsible for RNA degradation. While RNase L displays specificity to some kinds of

viral RNAs, in most cases it degrades both viral and cellular RNA, an event that often precedes apoptosis (41,42). RNA cleavage fragments produced by RNA-se L are known to induce IFN-β production and enhance the anti-viral state.

Interferons can also induce editing of viral RNAs. This is achieved by stimulation of RNA-Specific Adenosine Deaminase (ADAR1) that catalyzes transition of adenine into inosine. ADAR1 is normally present in the cells where it participates in editing of cellular RNAs but it has an isoform that becomes strongly induced by IFNs. Since IU pairs are less stable than AU pairs, viral dsRNAs become unwound and lose their ability to interact with ribosomes or other cellular structures. Also inosine is recognized more as guanine than adenine by transcriptional and translational machinery that leads to mutations in viral proteins and often makes them non-functional. While ADAR1 shows an inhibitory effect against some types of viruses like LMCV or hepatitis virus (43-45)some pathogens (HIV1, VSV, measles) hijack RNA editing and use it for increasing their virulence at the level of genetic changes (46,47).

Another level of IFN action is its influence on cellular translation. As viruses use host cell machinery, inhibition of viral protein synthesis is essential for slowing down the infection. Protein Kinase R activated by dsRNA (PKR) is an IFN induced enzyme responsible for that step. It becomes activated by binding dsRNA and it phosphorylates a number of substrates including eukaryotic initiation factor 2 (eIF2) thereby blocking early steps of translation (48).

Another group of anti-viral factors induced by IFN includes the Mx proteins. These are small GTP-ases that accumulate in the cytosol of IFN treated cells and can assemble into dynamin-like oligomers. In humans there are two members: MxA and MxB but only MxA was reported to have anti-viral properties. It displays antiviral activity against both RNA and DNA viruses by binding to the elements of viral nucleocapsids and blocking their transport and entry into the nucleus (49). Interestingly, animals lacking RNAse-L/PKR/Mx1 genes are still able to resist viral infection when treated with IFN (50). This suggests the presence of alternative IFN stimulated pathways that contribute significantly to anti-viral defense.

IFNs influence not only events inside the single cell but also act on the level of the entire immune system. Many genes belonging to Major Histocompatibility Complex I (MHCI) family are strongly induced by type I IFNs. Consequently this increases the number of antigen presenting molecules and facilitates activation of T and NK cells. IFN-α was found to promote

survival and proliferation of CD8+ cells in culture and to strongly induce differentiation of monocytes into dendritic cells (51). Also it was found to decrease proliferation of T regulatory (Treg) cells while inducing activation of T helper cells (52). IFN is known to stimulate antibody production by B cells, as well as isotype switching (53). Recent findings show that IFN-α has potent ability to induce and to enhance cross-presentation of antigens by modulating antigen survival, endocytic routing and processing (47).

Because of their anti-viral properties IFNs have been used in therapy of viral diseases. Recombinant IFN-α is used for therapy of both Hepatitis B and Hepatitis C (HBV and HCV) infections, it is also used for treatment of genital warts where it inhibits replication of human papillomaviruses (HPV) (54-56). Presently many clinical trials focus on use of IFNs as potential adjuvants to improve anti-cancer or anti-viral vaccines (57).

Interferon and cancer

While the biological action of IFNs targets pathogen, it also found use in cancer therapy. IFN-α has been used for therapy of over 14 types of cancer including renal cell carcinoma, AIDS related Kaposi's sarcoma (KS), follicular lymphoma, hairy cell leukemia, and chronic myelogenous leukemia (CML) (51,58,59). In spite of its anti-neoplastic effects, little is known about the mechanisms of IFN anti-cancer activity. One of the effects is enhancement of an immune response against tumors which can be a consequence of increased expression of MHCI molecules, stimulation of dendritic cells and enhanced cross-presentation of antigen. Patients treated with IFN showed an increase in tumor infiltrating T-lymphocytes, elevated NK cells activity and higher numbers of tumor specific CD8+ lymphocytes (51,59). However, since even seriously immunocompromised individuals could show a positive response to IFN, it seems that IFN's anti-cancer effect depends more on a direct influence on tumor cells.

Type-I IFNs were shown to have anti-proliferative effects on multiple cancer cell lines and to induce G1/G0 phase arrest (60). Transfection of cell lines resistant to IFN with the IFNAR genes made them sensitive to IFN stimulated growth inhibition. It was found that cells treated with IFN display decreased levels of phosphorylated Retinoblastoma (pRb) protein and lowered

activity of cdc25A phosphatase (60). IFN stimulation downregulated expression of cyclin D3 and simultaneously increased expression of p21, p15 and p27, proteins known as inhibitors of cyclin dependent kinases (cdks) (60-62). Study of cdks in IFN stimulated cells showed that an increased fraction of the cdks remained bound to inhibitors in an inactive state (61). Recently it was found that NEDD8 ultimate buster 1 **(**NUB1) protein, one of the IFN induced proteins, plays crucial role in inhibition of cell cycle (63). NUB1 regulates NEDD8, a ubiquitin like protein that forms conjugates with Cullin-family members and activates Skp-Cullin-Fbox (SCF) complexes. As a result NEDD8 is responsible for ubiquitination and degradation of cell cycle inhibitors such as p27, p21 and p73. NUB1 recruits NEDD8 and its conjugates to the proteasome and therefore helps in retaining high levels of cell-cycle regulators (63).

Besides its influence on the cell cycle, IFN is known to induce apoptosis in multiple cancer cell lines such as melanomas, ovarian carcinomas, multiple myelomas and leukemias (4). Observed effects are variable and dependent on the studied cell line. IFN-induced apoptosis is accompanied by activation of caspases both from mitochondrial (caspases-3,9) and ligand directed (caspase-8) pathways (64). Also XAF-1 (X-linked Inhibitor of Apoptosis Protein Associated Factor 1), a protein known to neutralize cellular caspase inhibitors is strongly upregulated by IFN (65). IFN-directed cell death can be efficiently neutralized by using different types of caspase inhibitors. Blocking caspase-8 has especially strong anti-apoptotic effects suggesting the role of death receptor signaling in the action of IFN (64). In fact IFN was found to upregulate TRAIL, Fas and caspase-8 in different cancer cell lines while inhibition of TRAIL reduced IFN-stimulated cell death (62,66,67)

Studies also showed that cells dying in response to IFN treatment display loss of mitochondrial potential and release of cytochrome c to the cytosol (64). This links IFN-induced apoptosis with the mitochondrial pathway but factors initiating that process still remain unknown. While type-I IFN induces production of p53, a protein that could enhance apoptosis (68), in many cases IFN directed cell death seems to be p53 independent (69). One of the possible mechanisms is the role of phosphatidylinositol-3 (PI3K) and mTOR kinase pathway (70). Inhibition of PI3K reduced IFN induced apoptosis and a similar effect was observed with inhibition of mTOR. Interestingly that phenomenon did not affect activation of the JAK/STAT pathway, induction of ISGs or antiviral activity of IFN (70). However, other studies showed that IFN actually downregulates PI3K/Akt pathway and that JAK/STAT activity is necessary for

induction of apoptosis (71). Therefore the mechanisms of IFN induced cell death still remain to be understood. We believe that ISG54 protein and other members of ISG54 family can shed new light on this problem. They could be a functional link between anti-viral and anti-cancer effects of IFN.

Interferon Stimulated Gene 54 family

ISG54 also known as IFIT2 (IFN inducible protein with tetratricopeptide repeats 2) is strongly induced during IFN stimulation, viral infection or dsRNA stimulation. It codes for a 472 aa-long protein with molecular weight of 54kDa, and it belongs to family encompassing four members in humans: ISG54, ISG56, ISG58 and ISG60 alternatively known as IFIT2, IFIT1, IFIT5 and IFIT3 respectively. Human ISG56 is 478-aa protein, ISG60 is 490-aa long molecule and ISG58 is 482-aa long. In mice there are only three members of ISG54 family: ISG54, ISG56 and ISG49 also referred to as IFIT2, IFIT1 and IFIT3. Those genes are located in cluster on chromosome 10 in humans and on chromosome 19 in mice. The coding sequence in humans is divided between two exons: a very short first exon with the initiating ATG and the second exon that contains remaining part of the gene. Murine ISG54 has an extra upstream exon that does not code for any protein sequence. Both coding exons are separated by an intron a few kilobases in length. The promoter of both human and murine ISG54 contains two regulatory elements the ISRE1 and ISRE2 that are localized adjacent to each other and about 200bp upstream of a TATA box (72,73), (see Figure 4). Other members of the family share the same promoter organization except ISG58 that has three ISRE elements (73).

Proteins coded by the family of genes share partial homology: there's 42% conservation between human ISG54 and ISG56 (74) and 62.8% homology between human and murine ISG54 (75). ISG58 is the most evolutionary distant member of the family, it shares 46% identity with ISG54 and 57% identity with ISG56. A characteristic feature of all proteins in the family is the presence of tetratricopeptide repeat (TPR) motifs. The TPR motif is a sequence of 34 moderately conserved amino acids that form a structure composed of two antiparallel helices separated by a short coil. Multiple TPR motifs are arranged at regular angles creating right-handed superhelix with a hydrophobic groove for possible anchoring place for ligands (76). Proteins containing multiple TPR domains such as HSP90, HSP70, HOP or mitochondrial transporter TOM70

usually participate in multiple protein-protein interaction and often form oligomeric structures (77-79). Because the sequence of the TPR domain is poorly conserved, different software algorithms predict different numbers of TPR motifs based on protein sequence. For our studies we used TPRPred algorithm designed specifically for identification and analysis of TPR domains (80). In the case of ISG54 TPRPred predicted the presence of 9 TPR repeats distributed evenly along sequence of the molecule. ISG56 and ISG60 were predicted to have 10 and 7 TPR domains respectively (80). The schematic depiction of ISG54 molecule is presented in Figure 5.

Induction of ISG54 by distinct pathways

Members of ISG54 family can be induced by signals from both inside and outside the cell. The external signal comes from binding type-I or type-III IFN molecule to their receptors. As a result STAT1/STAT2 proteins become phosphorylated and bind to IRF9 forming ISGF3 complex that moves to nucleus to stimulate expression of ISG genes. However, even in the cells with disrupted JAK/STAT signaling, activation of ISG54 is still possible (81). Intracellular signals come from recognition of Pathogen Associated Molecular Patterns (PAMPs) by specific receptors and result in activation of IRF3. IRF3 binds to ISRE elements in the promoter of ISG54 gene localized about 200bp upstream of TATA box. After recognition of ISRE GGGAAANNGAAATC sequence it recruits CREB Binding Protein (CBP)/p300 coactivator that stimulates assembly of transcriptional machinery (82-85).

While ISG54 and ISG56 have a similar promoter organization with respect to ISRE, the induction pattern of their mRNA expression can be different depending on the organ and stimulatory factor (86). Although IFNβ stimulates similar expression of both proteins in all organs, IFNα causes much higher expression of ISG56 in the colon and small intestine. Moreover, IFN had been reported to induce expression of ISG56 in myeloid dendritic cells but not in B cells or plasmacytoid dendritic cells (87). Infection with VSV leads to much higher induction of ISG56 in the liver comparing to ISG54 while stimulation with dsRNA boosts expression of ISG54 in heart with no effect on ISG56 (86). In the brains of mice infected with LCMV different ISGs are induced in different regions: pyramidal cells mainly produce ISG56, olfactory bulb is enriched in ISG54 and deep cerebellum neurons expressed all three ISGs at the

same level (88). These observations may suggest distinct response of the ISGs in particular cell types.

Furthermore molecular aspects of ISGs induction seem to be different. Interesting data on ISG54 induction come from the studies of West Nile virus infection. Experiments showed that WNV dependent ISG54 induction is strongly dependent on the presence of IkappaB kinase-epsilon (IKKε) while ISG56 and ISG60 can be expressed without IKKε (89). Lack of IKKε also impaired synthesis of ISG54 in response to IFN stimulation but had no effect on induction of ISG56 or ISG60.All these results suggest the presence of precise mechanisms that regulate expression of individual ISGs instead of being aimed at a whole protein family.

Prior studies of ISG54 function

There are a number of biological responses that have been reported with the expression of ISG/IFIT family. The different studies and observations are described below. Some of them can be due to our finding that ISG54 promotes cellular apoptosis (90).

Effects on mRNA

Members of the ISG54 family seem to be involved in multiple functions. Initially, ISG54 and its cousin ISG56 were linked to the inhibition of cellular translation. Studies performed by Ganes Sen's group showed that ISG54 and ISG56 interfere with the initiation stage of translation by binding to the eukaryotic initiation factor 3 (eIF3), multisubunit protein complex (74). Human ISG54 could bind to "e" and "c" subunits of eIF3 while ISG56 interacted only with "e" subunit. Therefore human ISG54 worked in a two-step manner, blocking two different steps of ribosome assembly while ISG56 blocked only the first step (74). On the other hand in mice ISG54 and ISG56 were found to interact only with the "c" subunit of eIF3. Association with eIF3 was mapped to the N-terminus of both ISGs encompassing two TPR motifs in ISG56 and one TPR motif in ISG54. Moreover, studies in mice showed that also ISG49 could interact with eIF3 but with no influence on on translation (87).

The effects of ISG56 on translation seem to be dependent on the type of RNA. Some data show that ISG56 inhibits translation of capped mRNA while it does not have an effect on IRES bearing RNA from encephalomyocarditis virus (EMCV) (91). On the other hand there are data

showing that ISG56 can inhibit translation of RNA containing Hepatitis C Virus (HCV) IRES but does not have an effect on cap-mediated translation (92). Other studies revealed that anti-RNA activity of ISGs may be dependent on the absence of 2'-O-methylation in the cap of viral RNA (93). 2'-O-methylation of the penultimate 5' ribose in eukaryotic mRNA takes place in the nucleus. Some viruses such as West Nile Virus (WNV), Vaccinia (VACV) or Mouse Hepatitis Virus (MHV) developed their own methyltransferases able to perform 2'-O'-methylation. Overexpression of ISG54 had no effect on replication of wild-type MHV and VACV but effectively blocked replication of viral mutants lacking 2'-O-methylase activity (93). On the other hand, animal studies showed that mutant lacking 2'-O-methylase activity is highly virulent in ISG56 knockout mice (93). These data suggest that 2'-O-Methylation of RNA plays important role in ISGs function but the exact mechanism remains unknown.

A recent study found that the inhibitory effect of ISG56 on translation may be more due to its ability to bind triphosphorylated RNA (PPP-RNA) and not to translation machinery (94). PPP-RNA is present in transcript of many viruses and it is recognized by the cytoplasmic receptor RIG-I that induces production of IFN. Experiments using beads coupled to PPP-RNA showed that ISG56 can potently bind to triphosphorylated RNA but not to RNA lacking triphosphate group. Interestingly this property was shared by ISG58 but not by ISG54 or ISG60 (94). Database analysis and computer modeling suggested that RNA binding may be dependent on the presence of a positively charged groove along the axis of ISG56. Mutation of arginine 187 to histidine (R187H) within that groove abolished interaction of ISG56 with PPP-RNA. Therefore, ISG56 was proposed to be an interceptor of viral PPP-RNA that sequesters them from ribosomes and prevents expression (94).

Some data suggest that ISG54 may also be involved in regulating the stability of specific host RNAs. Data from RAW cells stimulated with LPS showed that overexpression of ISG54 strongly inhibits synthesis of TNF-α, IL-6 and MIP-2 (95). However, ISG54 had no effect on expression of other LPS-induced proteins such as VEGF or ISG56 and did not cause any alterations to LPS induced signaling pathways. It was found that ISG54 affects mRNA stability of target genes and that this process is dependent on the composition of 3'UTRs of those genes (95). For instance study of TNFα mRNA identified a constitutive decoy element (CDE) in 3'UTR that is necessary for the inhibitory effects of ISG54. Cloning 3'UTR sequences of TNFα, MIP-2 and Il-6 into EGFP vector caused a dramatic decrease in production of EGFP in the

presence of ISG54 (95). It's possible then that ISG54 in addition to its anti-viral functions may help in regulation of cellular mRNAs.

Additional Effects of ISGs/IFITs

Recent data suggest that ISGs may play an important role in the initial induction of IFN genes by interaction with STING/MAVS/TBK1 complex. STING as described previously is ER bound adapter protein necessary for triggering IFN response to cytoplasmic DNA. MAVS integrates signals coming from RNA sensors such as RIG-I and MDA-5. Together with a set of adapter proteins they form multisubunit complex responsible for activation of TBK1, and recruitment of IRF3 (see Figure 3). As a result IRF3 becomes phosphorylated and may initiate transcription of IFN genes.

A study showed that both ISG54 and ISG56 could interact with STING but not with TBK1 or IRF3 (96). Binding of ISGs disrupted interaction between STING and MAVS and between STING and TBK1 leading to impaired induction of IFN genes. Both ISG54 and ISG56 were found to inhibit IRF3 dimerization and phosphorylation (96). Moreover, ISG56 has been reported to inhibit activation of NF-kB by blocking degradation of IkBα. Knockdown of ISG56 resulted in significantly enhanced activation of IFNβ promoter and stronger inhibition of viral replication. It's possible then that ISG54 and ISG56 negatively regulate IFN induction by controlling activation ofIRF3 and NF-kB. ISG56 appears to be the main negative regulator while ISG54 may play an auxiliary role in this process. They may provide a negative feedback regulatory loop preventing too aggressive anti-viral response that could be deleterious to the host.

The third member of family, ISG60, was found to be a positive regulator of the IFN response. Recent data suggest that ISG60 serves as an adapter protein responsible for linking MAVS with TBK1 (97). Without ISG60 expression of both IRF3 and NF-κB dependent genes is potently decreased. Immunoprecipitation experiments showed that ISG60 can bind both MAVS and TBK1 and that its association stabilizes interaction between MAVS and TBK1. Moreover, ISG60 could interact with wide range of adapter proteins including TRAF2, TRAF3, TRAF6 and TRADD. It also displayed weak binding to IKKε and RIG-I (97). Transfection of ISG60 increased IFNβ production in SeV infected HEK293 cells while ISG60 knockdown drastically impaired expression of IFNβ. Cells lacking ISG60 showed increased susceptibility to SeV

infection resulting in much higher viral replication (97). Other studies reported that ISG60 plays important role in inhibition of VSV and EMCV replication. Cells with knocked down expression of ISG60 were unable to resolve VSV infection even when treated with IFN (98). Together those findings depict ISG60 as a part of positive-feedback regulation of IFN response that puts it in the opposition of ISG56. Since both these proteins are induced at the same time it is probably the balance between them that regulates the intensity of anti-viral response in an infected cell

Studies with ISG56 show that it inhibits replication of human papilloma virus (HPV) by direct interaction with viral E1 protein (99). E1 is a crucial HPV protein with ATP-ase/helicase properties that together with E2 is responsible for replication of viral DNA. Binding of ISG56 disrupted helicase activity of E1, blocked its ability to interact with E2 protein and disabled recognition of viral *ori* sequence. Interestingly that interaction was dependent on the single aminoacid in E1 that was dispensable for its biological function (99). In case of ISG54 no direct interaction with viral proteins has been so far reported but it's possible that this highly expressed protein may as well bind to some viral targets.

Recent data showed that ISG54 may play important role in the regulation of anti-viral response in the brain (100). ISG54 knockout mice when infected intranasally with VSV, developed severe infection leading to the death of all animals within a week. In contrast only mild symptoms developed among wild type mice or among ISG56 knockout animals (100). Infection of other organs did not show any differences between ISG54 knockout and control mice. In the brains ISG54 and ISG56 are induced in the same regions and at similar levels (100). This would suggest that ISG54 stimulates rather than inhibits anti-viral response and that its function in neurons is distinct from ISG56. However, no molecular details of this mechanism have been so far discovered.

Differentiation, proliferation and migration

Besides its anti-viral effects, ISG54 has been reported to influence cell migration, division and differentiation (101,102). Studies in NIH3T3 and B16 melanoma cells showed that ISG54 colocalizes with microtubules and accumulates in the mitotic spindle (101). Other study in oral squamous cell carcinoma (OSCC) showed that ISG54 acts as an inhibitor of cell migration and motility. Migration assays using Boyden chambers revealed that shRNA knock down of ISG54 increases migration of cancer cells even without treatment with interferon while

ectopic expression of ISG54 significantly reduces migration (102). Interestingly in this study ISG54 was found to form fibrillar patterns in the cytosol and interact with cytokeratins, especially cytokeratin 18 (102). OSCC patients expressing high levels of ISG54 had more differentiated tumors with lower lymph node stage comparing to the tumors lacking ISG54. Moreover, expression of ISG54 correlated positively with survival and postsurgery lifespan of the patients (102).

Recent reports suggest that ISG60 is also involved in the control of cell proliferation and differentiation. Both ISG60 and ISG58 were discovered as the proteins induced by all-trans retinoic acid (103), compound known to stimulate cell differentiation (104,105). A study by Xiao et al. (106) showed that ISG60 associates with JAB1, member of COP-9 signalosome. COP-9 is a protein complex involved in many functions including ubiquitination, protein degradation and cell signaling (107). JAB1 functions as an isopeptidase participating in deneddylation of target proteins. It also works independently as a cofactor in Myc-regulated transcription of "wound healing" genes and as a cytoplasmic shuttle for p27 protein (107). P27 is a suppressor of the cell cycle located in the nucleus and it is degraded after being transported to the cytosol by JAB1. ISG60 binds JAB1 and sequesters it in cytoplasm preventing it from the interaction with p27. Moreover, by an unknown mechanism, it decreases the level of c-Myc protein resulting in increased expression of p21, another cell cycle suppressor (106).

Expression of ISG60 is strongly induced in patients with systemic lupus erythematosus (SLE) (108). Higher levels of ISG60 correspond to increased leucopenia and thrombocytopenia and may be explained by an anti-proliferative character of that protein. Also ISG60 expression in monocytes stimulates their differentiation into dendritic cells (108).

The role of ISG58 in biological processes is the least characterized. It is cytoplasmic, 482-aa long protein with 46% identity with ISG54 and 57% identity with ISG56. While it was reported to display some anti-viral effects and cause translation inhibition in vitro (93,94), very little is known about its functions and binding partners. It was found to be involved in myeloid differentiation and be induced via all transretinoic acid (103) (104) but mechanisms of its action remain unknown.

Together the ISG/IFIT family appears to be involved in multiple aspects of cell functioning. While primarily induced by IFN and pathogen infection their functions are not

limited to the anti-viral response. Therefore more studies are required to fully characterize members of ISG54 family and to determine their functions in cellular processes.

My studies demonstrate that the expression of ISG54 promotes cellular apoptosis (90). It is possible that many of the biological effects reported for ISG54 expression or loss of expression are a result of its ability to stimulate cell death.

Apoptosis and other forms of cell death

In this work we postulate that ISG54 can induce apoptosis and may be a part of mechanism by which IFN induces cell death. Apoptosis is the most ubiquitous form of programmed cell death. Its biological relevance is to eliminate cells during tissue/organ development become a potential threat to the organism due to DNA damage or pathogen infection. In response to DNA lesions, thermal or oxidative stress, or signals from the external environment, cells execute a precise mechanism of self-destruction. Apoptosis is characterized by chromatin DNA fragmentation, loss of cell membrane asymmetry, membrane blebbing and cell shrinkage (109). Integrity of cell membrane is retained at early stage of apoptosis. In contrast necrosis is a form of death mainly as a result of traumatic injury. It is accompanied by cell membrane disruption and often triggers reaction of the immune system. While apoptosis leads to shrinkage of dying cells, necrosis often causes cell swelling and karyolysis. Ongoing apoptosis can convert into necrosis if there is low levels of ATP and limited activity of caspases (110,111). Apoptosis usually does not induce an inflammatory response since it does not lead to release of cell contents and apoptotic cells are cleared by macrophages or engulfed by the neighboring cells (112).

The essence of the apoptotic process is activation of caspases – cysteine-aspartate proteases that when activated cleave cellular proteins such as nuclear lamins, cytokeratins or spectrins. There are two types of caspases. Initiator caspases such as CASP 2,8,9 or 10 are responsible for receiving pro-apoptotic signals either coming indirectly from extracellular stimulation or from internal cellular mechanisms. They activate effector caspases such as CASP 3,6,7 that are responsible for cleaving the primary cellular targets (102). Caspase-3 is a main executioner caspase. It can be activated by any of initiator caspases and its major target is

gelsolin, a protein responsible for organization of actin cytoskeleton. CASP3 is also the main activator of endonuclease CAD (caspase-activated DN-ase) that degrades DNA in the nucleus of dying cells.

There are two main pathways of apoptosis initiation. An intrinsic pathway is initiated by DNA damage or other types of severe cellular stress like hypoxia, heat shock, viral infection or loss of growth factors. DNA damage activates p53 that induces expression of PUMA and Noxa proteins (113). These factors activate Bax and Bak proteins that insert into mitochondrial membrane forming a pore and enabling release of mitochondrial content (114). Leakage of cytochrome c and other mitochondrial components like SMAC and Diablo initiates the apoptotic process. Cytochrome c binds the adaptor apoptotic protease activating factor-1 (APAF1), forming a large multi-protein complex known as the apoptosome (115). The apoptosome binds and activates pro-caspase-9 that subsequently activates effector caspases 3,6,7 (116,117). Other proteins released from mitochondria: AIF (apoptosis inducing factor), endonuclease G and CAD translocate to the nucleus where they cooperate in degradation of cellular DNA. Activation of the intrinsic pathway depends on the balance between pro-apoptotic factors such as Puma, Noxa, Bim, Bik, Bid and Bad and anti-apoptotic factors such as Bcl, Bcl-xL or Mcl. The latter anti-apoptotic proteins bind Bax and Bak preventing them from insertion into mitochondrial membrane. Another group of cytosolic proteins: IAP (inhibitors of apoptotic proteins) is responsible for blocking activation of caspases. SMAC and Diablo inactivate members of IAP family after being released from mitochondria allowing initiation of the cascade of caspases (118).

In contrast, the external pathway is independent of p53 activity and is linked to signaling through cell surface death receptors such as Fas, DR4 or DR5 (119). It is used by cytotoxic T lymphocytes and NK cells for killing cells infected with virus or displaying a cancerous phenotype. When the ligand binds to the death receptors, intracellular domains of the receptors associate with adaptor FADD protein (Fas-associated death domain). This stimulates formation of DISC (death-inducing signaling complex) and recruitment of inactive pro-caspases 8 and 10 that become activated by binding with DISC. This subsequently leads to activation of downstream caspases 3,6 and 7 that execute the apoptotic process (119).

Apoptosis can be also triggered in other ways. For instance T cells use a mechanism involving perforins and granzymes. Perforins form pores in the membrane of target cell while

granzyme B activates caspase 10 and caspase 3 by proteolytic cleavage (120). Granzyme B can also cleave the precursor of the pro-apoptotic protein Bid and release Bid to stimulate release of cytochrome c by activating Bax and Bad. Granzyme A stimulates apoptosis in an alternative way by entering the mitochondria, cleaving electron transporter proteins and inducing oxidative shock (121). Another specific form of apoptosis called anoikis takes place in the cells that have lost contact with surrounding extracellular matrix. Its mechanism still remains unclear but is linked to absence of survival signals coming from integrins bound to extracellular matrix (122,123). Detachment of integrins results in disruption of Ras/Raf/PI3K/Akt signaling and release of pro-apoptotic proteins Bim and Bmf that normally remain bound to the cytoskeleton. Bim stimulates Bax/Bak oligomerization, release of cytochrome c and caspase activation (122,123).

Excessive and uncontrolled apoptosis takes place in many diseases such as ischemia, Parkinson's or Alzheimer's disease (124). On the other hand many tumors have dysfunctional apoptotic mechanisms due to mutations in p53 or overexpression of caspase inhibitors (113,125). Also viruses can affect the apoptotic machinery preventing apoptosis of an infected cell (126). Their proteins either mimic apoptosis inhibitors of the host (e.g. adenoviral E1B-19K – analog of Bcl2) or eliminate cellular pro-apoptotic proteins (e.g E6AP protein from HPV that mediates p53 degradation) (127,128). Despite those numerous anti-apoptotic mechanisms, cells are still able to kill themselves. This is due to alternative ways of cell death that involve different pathways and still are not completely understood. In necroptosis signals from tumor necrosis factor α (TNF-α) receptors cause cell death and necrotic morphology but no caspase activity is required for that process (129). Oncosis is a cell death resulting from excessive swelling caused by the failure of ionic pumps that can be initiated by toxins and often takes place during ischemia (130,131). Pyroptosis is another alternative form of cell death often observed during inflammation and executed by capase-1. In pyroptosis caspase-1 stimulates membrane rupture and release of cellular content but no cytochrome c release or activation of downstream caspases takes place during that process (132). Entosis is a cell death that involves cell dying as a consequence of being engulfed by a neighboring cell of the same or different type. Interestingly engulfed cells often survive inside the host cell they can be released from the host cell or even kill the host cell. Entosis was observed in multiple cell types, mainly in tumors but also between tumors and leukocytes and in mammary acinar cells (133,134). A specific form of cell death is autophagy. Autophagy is a degradation of the cell's own components through the vesicular

structure called autophagosome. It is induced by starvation but can be also activated during pathogen infection, cellular stress, or in the cancer transformation (135). It is a complex process that depends on the action of multiple proteins and regulatory factors such as family of Atg proteins, type III phosphatidylinositol kinase (PI3K) and mTOR kinase (136). Moderate autophagy is considered to be pro-survival mechanisms but persistent autophagy can lead to the cell death (137). Cells dying as a result of autophagy do not show activation of caspases or the loss of mitochondrial potential (138-140). However, depending on the conditions autophagy may also facilitate conventional apoptosis (137,140).

All these alternative pathways seem to play important role in cell functioning yet still remain enigmatic. Therefore studying those new pathways leading to cell death may be essential for establishing novel cancer and viral therapies.

Mouse Gamma Herpesvirus 68

In our experiments we used mouse gamma herpesvirus 68 (MHV68) as a model pathogen to study the role of ISG54 proteins in viral infections. MHV68 is a large double-stranded DNA virus with ~118kB long genome containing about 80 putative open reading frames (ORFs) and 8 possible tRNAs (141). It's closely related to human gamma herpesviruses such as Kaposi's Sarcoma Herpes Virus (KSHV) and Epstein-Barr Virus (EBV). It was first isolated from bank voles in Slovakia but its main reservoir seems to be the population of wood mice (142). It infects laboratory mice as well as certain types of human cells *in vitro* but no infection of human individuals has ever been reported. Similar to other gamma herpesviruses MHV68 is known to establish life-long infection of the host through the state of latency. During latent infection the viral DNA remains as an episome in the infected cells but no cytopathic effect or immune reaction is observed. During latent infection there is very limited viral protein expression. The MHV68 genome stays in the nucleus of infected cells as a circularly closed episome and rarely integrates into chromosomes of the host (142). However, under certain circumstances, in response to particular signals, viral gene expression increases and progeny viral particles are released. This process is called reactivation and it's characteristic for all the herpesviruses. The exact mechanism of reactivation still remains unknown.

Gamma herpesviruses are known to preferentially develop latency in B lymphocytes while alpha herpesviruses develop chronic infections in neurons and beta herpesviruses develop chronic infections in myeloid cells. In nature MHV68 is believed to infect mice through the respiratory route although no cases of horizontal transfer have been observed under laboratory conditions (143,144). In the laboratory, animals are usually infected through an intranasal or intraperitoneal route. Intranasal inoculation results in the acute infection in the lungs that is characterized by production of viral particles in the lung epithelium. After 10 days the lung infection is usually cleared and the virus establishes chronic infection in B cells in the spleen. Acute replication in the spleen ends about 16-18 days post infection and the virus enters the stage of latency (145,146). At that time about 1% of splenocytes is estimated to be infected with latent form of MHV68 and about 0.01% of them are able to spontaneously reactivate the virus. However, with time frequency of spontaneous reactivation decreases and at 6 weeks post infection only very small fraction of splenocytes is able to reactivate (142). This process can be enhanced by certain stimuli such as LPS, flagellin or CpG DNA suggesting that pathogen-induced stress facilitates reactivation (147).

MHV68 codes for several proteins that influence proliferation and survival of the host cell. One of them is v-cyclin, a viral oncogene that can bind and activate CDK1 and CDK2. It works similar to cellular cyclin A but it's resistant to inhibition by the p27 tumor suppressor. V-cyclin deregulates cell cycle and was found to induce T-cell cancers in mice (142,148). Another protein is vBcl-2 (M11), a viral homolog of anti-apoptotic Bcl-2 protein. It contains BH1 domain homolog present in human Bcl-2 but no BH2 domain. vBcl-2 can efficiently inhibit apoptosis caused by Fas stimulation or TNF-α and it also blocks induction of autophagy by interaction with pro-autophagy protein Beclin-1. M11 isn't required for the acute infection but seems to play an important role in establishing of latency (142). Another anti-apoptotic protein expressed by MHV68 is vMAP (viral Mitochondrial Antiapoptotic Protein) that can interact both with Bcl-2 and with Voltage Dependent Anion Chanel (VDAC1) (149). vMAP brings Bcl-2 into the mitochondrial surface and increases its avidity for pro-apoptotic proteins such as Bid or Bad. Simultaneously by binding VDAC1 it decreases mitochondrial permeability and release of cytochrome c (149). Despite those mechanisms most MHV68 infected cells are killed by pro-apoptotic machinery. It was found that in the cells lacking Bax and Bak viral titer was increased up to 100 times (149).

The interferon system plays an important role in MHV68 infection. Animals lacking IFNAR1 experience much more severe symptoms of acute infection, display increased viral titer in lungs, and often die within 16 days. They also show significant increase in the levels of spleen reactivation but no difference in establishment of latency or in viral clearance after acute phase (150). It's still unknown though how interferon is responsible for those effects. Mice lacking PKR and RNA-se L react normally to acute replication and don't show any increase in reactivation (142). Therefore it is highly possible that other ISGs may be crucial for host response to MHV68 infection. In the following thesis I'm exploring the role of ISG54 may have in the anti-viral response and investigating how it affects different stages of MHV68 cycle.

Chapter 2. Materials and Methods

Cell culture- Human cell lines were obtained from American Type Culture Collection and cultured in DMEM with 8% FBS. Wild-type baby mouse kidney (BMK) cells and *bax-/-*, *bak -/-* double knockout BMK cells (151) were a kind gift of Dr. Wei-Xing Zong (Stony Brook University). NIH 3T12 cells and wild-type C57Bl/6 Mouse Embryo Fibroblasts (MEFs) were a kind gift from dr Laurie Krug (Stony Brook University). MEF cell lines were cultured in DMEM supplied with 10% FBS

Plasmids and transfections- Full-length human ISG54 cDNA was cloned using PCR into the following vectors: pcDNA3 (Invitrogen) with an N-terminal T7 tag, pCGN with an N-terminal HA tag (Addgene), pEF-1V5-HisB with an C-terminal V5 tag (Invitrogen), and pEGFP-N1 with a C-terminal monomeric GFP tag (Clontech). The pEGFP-N1 plasmid was modified to introduce mutations A206K, L221K, F223R to ensure a monomeric GFP (mGFP) (152). ISG54-mGFP was subcloned into the tetracycline-inducible vector pREvTRE (Clontech). pRev-ISG54-mGFP expression was induced with pLib-rtTAm2-iresTRSID-iresPuro, a gift of Dr. Michael J. Ausserlechner (Medical University Innsbruck) (153). Truncated forms of ISG54 encompassing 1-4TPR domains (aa 1-208), 2-9TPR domains (aa 94-472) 3-9 TPR domains (aa 138-472) and 4-9 TPR domains (aa 172-472) were cloned into pEF-1V5-HisB. Human ISG56, ISG58 and ISG60 genes were similarly cloned. cDNAs for human STING, PRDX5, eEF1α, DLC1, eIF3e, eIF3c were obtained from Open Biosystems and cloned into pEF1-V-HisB and pCGN vectors. pcDNA3-Bcl-xL plasmid was a gift from Dr. Colin Duckett (University of Michigan). pSpLuc-polyA plasmid containing firefly luciferase gene with 60 adenine bases at 3' terminus was a gift from Dr. Philip Marsden (University of Toronto) (154). The pSPLuc-polyA luciferase gene was cloned into pcDNA3 to generate pcDNA3-luc-polyA with a T7 promoter site. IRES-luc-polyA plasmid was constructed by cloning hepatitis C virus internal ribosome entry site (IRES) from H4325Wt (gift from Dr. Eckard Wimmer, Stony Brook University) into pcDNA3-lucPolyA. The dominant negative p53 plasmid (aa 320-393) was a kind gift from Dr. Ute Moll (Stony Brook University) (155). Plasmid encoding adenoviral E1B-19K was a kind gift of Dr. Lynne Vales (UMDNJ) (156). Plasmids encoding adenoviral E1B-55K and E4-Orf6 were kind gifts of Dr.

Patrick Hearing (Stony Brook University). Plasmids encoding murine GFP-Bax, GFP-Bak, human constitutive active Akt, and p110 and p85 subunits of PI3K were kind gifts of Dr Wei-Xing Zong (Stony Brook University). Plasmid encoding human H-Ras-V12 was a gift from dr Linda van Aelst (Cold Spring Harbor Laboratory). Plasmids encoding KSHV v-Bcl-2 protein and MHV68 M11 protein were a kind gift from Dr. Beth Levine (University of Texas-Southwestern).

TransIT LT1 reagent (Mirus) was used for DNA transfections. We used 2ul of TransIT reagent per 1ug of DNA. For transfections of 6 well plates we used 1ug of ISG54mGFP, or both 0.25ug of mGFP plasmid with 0.75ug of empty pCGN vector as a control. Since mGFP was expressed at much higher levels than ISG54mGFP we used a lower amount of mGFP plasmid to keep similar levels of ectopically expressed proteins. For the experiments where ISG54mGFP was cotransfected with another gene we used 1ug of ISG54mGFP and 1.5ug of plasmid coding for the respective gene per well. For the experiments where ISG54mGFP was cotransfected with two different genes we used 1ug of ISG54mGFP and 1ug of each of respective plasmids. DNA and transfection reagent were resuspended in 250ul of serum free DMEM, incubated for 15 minutes at the room temperature and added dropwise to the cell media. 6hs after transfection, media were aspirated, cells were washed with fresh DMEM to remove transfection reagent and supplied with fresh complete DMEM.

TransMessenger Transfection Reagent (Qiagen) was used for RNA transfections. RNA transfection was performed using 2ul of Enhancer R and 2ul of TransMessenger Transfection Reagent per 1ug of RNA according to manufacturer's protocol (Qiagen). We used 3ug of luciferase mRNA per 10cm plate of HeLa cells.

Western-blot, immunoprecipitation and antibodies- For Western blots, cell lysates were prepared in 0.5% NP-40 buffer and proteins separated by SDS-PAGE (157). Protein concentration was determined with the colorimetric assay (Bio-Rad) using bovine serum albumin as the standard. Proteins were transferred to nitrocellulose membrane (Thermo Scientific) and reactive signals were detected with the Odyssey Imager (Li-COR Biosciences). For immunoprecipitation 400-500μg of protein were incubated with antibody overnight at 4ºC and immunocomplexes were collected on protein G agarose beads (Invitrogen). Polyclonal rabbit anti-C-terminal ISG54 antibodies were generated against GST-ISG54 (381-473a.a.). Commercial antibodies used included monoclonal anti-V5 (Invitrogen), polyclonal rabbit anti-HA (Santa

Cruz Biotechnology), monoclonal anti-FLAG (Sigma), monoclonal anti GRP78/BIP (BD Transduction Laboratories), anti-active caspase-3 (Cell Signaling), secondary antibody conjugated to TRITC (Jackson Laboratory), normal IgG (Santa Cruz Biotechnology), and secondary antibodies for Odyssey Imager anti-mouse (Rockland) and anti-rabbit (Invitrogen). Cells positive for GFP expression were isolated by fluorescence activated cell sorting (FACS) with a Becton-Dickinson FACS Vantage cell sorter.

Cell death- For the cell death assay cells were plated on 6 well plates and each experiment was represented by three independent triplicates. Cells were transfected with ISG54mGFP and empty PCGN plasmid or ISG54mGFP with the plasmid containing a particular gene of interest. As a negative control we used plasmid coding for mGFP. At 24, 48 and 72hs after transfection cells were trypsinized from plates, washed with PBS, and stained with propidium iodide (PI) according to manufacturer instructions (Invitrogen). For annexin V staining, cells were resuspended in staining buffer (BD Pharmingen) and allophycocyanin (158) conjugated annexin V (APC-V) was added according to manufacturer instructions (BD Pharmingen). Cells were analyzed with FACS Calibur flow cytometer (Becton Dickinson) and the gate was set for cells positive for GFP expression to collect 10,000 counts. Distribution of PI and annexin V staining was visualized as a histogram and analyzed with BD CellQuest software to determine percentage of the cells positive for propidium iodide and annexin V.

Microscopy and Immunofluorescence- Immunofluorescence was performed following cell fixation with 4% paraformaldehyde and permeabilization in 0.2% TritonX-100. Cells were incubated with primary antibodies followed by the incubation with secondary antibody conjugated to TRITC. Unless stated otherwise, all the incubations with antibodies were performed in a humid chamber at 37°C. For ER visualization we used primary monoclonal mouse anti-calnexin antibody (BD Transduction Laboratories) at 1:100 dilution and incubation period of 2h. For detection of active caspases-3 we used anti-active caspase-3 from Cell Signaling (1:100 dilution, incubation for 8hs at 4°C) and for detection of ISG54v5 we used Santa Cruz anti-v5 antibody (1:100 dilution, 2h incubation). Secondary TRITC-conjugated antibodies were used at 1:200 dilution with incubation time of 1.5h. Cells were visualized with Zeiss Axiovert 200M and Axiovision v.4.5. Live cell imaging was performed with cells seeded on glass bottom plates (Mattek Corporation). Mitochondria were visualized by incubation with 500nM MitoTracker Orange CMTMRos prior to imaging (Invitrogen). The Zeiss Tempcontrol

37-2 Digital and CTI Controller 3700 was used with the Zeiss LSM 510 laser scanning microscope system (Zeiss) and an alpha Plan-FLUAR100x/1.45 objective. Live cell images were captured using Zeiss LSM 5 Pascal imaging software.

Study of mitochondrial potential- HeLa cells plated on 6 well plates were transfected with mGFP or ISG54mGFP. 24h and 48h after transfection cells were stained with 200nM MitoTracker Orange (Invitrogen) obtained by dilution of 1mM DMSO stock in serum free DMEM. After 25 min of incubation at 37°C cells were washed with fresh medium, trypsynized and analyzed by flow cytometry. Signal from MitoTracker was detected in PI channel and its distribution was visualized by a histogram. Cells positive for mGFP or ISG54mGFP were evaluated for the intensity of MitoTracker staining focusing on the size of population with low signal intensity.

Translation analysis- 3ug of mRNAs encoding the luciferase gene were transfected into cells expressing ISG54 and evaluated for translation. *In vitro* transcription was performed with Ambion mMessagem Machine T7 Kit. Luciferase RNA was synthesized from a T7 promoter in pcDNA3-luc-polyA, and a 5'-7-methyl guanosine (m^7G) cap was added to the mRNA *in vitro*. IRES-luc-polyA was used to prepare 5'-IRES-regulated luciferase mRNA. Following reactions, DNA templates were degraded with DNAase and mRNA was precipitated with LiCl. Integrity and amount of transcribed RNA were evaluated with electrophoresis and spectrophotometry. Cells were transfected with ISG54-mGFP or mGFP, and the following day they were transfected with the 5'-cap luciferase mRNA or IRES luciferase mRNA. Five hours following RNA transfection the cells were sorted for GFP fluorescence (Becton-Dickinson FACS Vantage cell sorter) and then tested for luciferase activity with Promega Dual-Luciferase Reporter Assay and Lumat LB9507 Luminometer (EG G Berthold).

Mass spectrometry analysis- HeLa cells were transfected with plasmids T7-ISG54 pcDNA3 or T7-pcDNA3, and were subsequently treated with 1,000 U/ml IFN-α (gift from Roche, Nutley, NJ) overnight. Cell lysates were prepared and incubated with anti-T7 antibodies conjugated to agarose beads (Novagen). Proteins were eluted with Novagen elution buffer, neutralized, and treated with iodoacetamide. Proteins were separated by SDS-PAGE and stained with SilverQuest (Invitrogen). Protein samples were analyzed by mass spectrometry by ProtTech Inc. (Norristown, PA).

Glycerol gradient sedimentation- Cell lysates were prepared with isotonic buffer

(140mM NaCl, 50mMTris-pH8.2, 5mM EDTA, 0.5%NP40) and clarified by centrifugation at 18,000g for 15 min. Samples were concentrated with Amicon Ultra4 Filter columns, and 700µg of protein were applied to the top of 25-40% glycerol gradients (159). One gradient was prepared with molecular mass references corresponding to 50µg of bovine serum albumin (66kDa), alcohol dehydrogenase (150kDa), catalase (250kDa), and apoferritin (448kDa). Samples were centrifuged in Beckman SW60Ti rotor for 40h at 40,000rpm at 4°C, and 150µl fractions were collected from the top of each gradient for analysis. Mass marker references were visualized with Coomassie R250 staining.

shRNA knockdown- Four double stranded oligonucleotides targeting human ISG54 cDNA were designed for use in the AmbionpSilencerTm system and were cloned into pSilencer 2.1-U6-puro vector. The oligonucleotides corresponded to nt136 (5'-GATCCGCTTCATAAGATGCGTGAATTCAAGAGATTCACGCATCTTATGAAGCTTTTT TGGAAA-3'), nt652 (5'-GATCCGGAATTCAGTAAAGAGCTTCTCAAGAGAAAGCTCTTT ACTGAATTCCTTTTTTGGAAA-3'), nt1075 (5'-GATCCGGAATTCAGTAAAGAGCTTCTC AAGAGAAAGCTCTTTACTGAATTCCTTTTTTGGAAA-3'), and nt1203 (5'-GATCCACC AGAAATCAAGGGAGAATTCAAGAGATTCTCCCTTGATTTCTGGTTTTTTTGGAAA-3'). HeLa cells were transfected with one of the pSilencer ISG54 shRNA plasmids or with a pSilencer control containing a random shRNA sequence (Ambion). Stable cell lines were selected for resistance to 660ng/ml puromycin. ISG54 knockdown efficiency was evaluated by Western-blot and Image J software (NIH).

ISG54 KO mice- ISG54 KO mice were obtained from Knock Out Mouse Project (KOMP) Consortium Repository. Knockout was performed in C57BL/6 mice by replacement of 4162bp fragment of mouse chromosome 19 (position 34644839-34648964) with an insert consisting of lacZ gene and loxP flanked neo cassette. Deletion encompassed promoter of ISG54 gene and the first exon that contained 5'UTR. However, coding sequence of the protein remained intact. To verify the knockout on genomic level we used PCR with primers: REG-10236F (5'CTGACCCTGAAAGGCTTGGCTCT3') that bound to5' end of ISG54 gene, 5'Universal Laz-Rev (5'GCTGGCTTGGTCTGTCTGTCCTA3') that bound to 5' end on LacZ insert and 5'WT Fwd1 (5'GGACTTACCTCATGACTGCTGTGTAAC 3') that bound to the region of ISG54 gene deleted by the mutation. Genotyping was performed both on mouse tails and on the DNA of the isolated splenocytes. To verify knockout on a transcriptional level RT-PCR reaction

was performed. RNA from splenocytes was extracted using Trizol reagent (Invitrogen) and 2μg of isolated RNA was reversely transcribed using Moloney Murine Leukemia Virus (MMLV) reverse transcriptase (Promega) according to the company's protocol. For the PCR reaction forward primer was designed to bind nucleotides 115-140 of exon2 in ISG54 gene while reverse primer bound nucleotides 445-422 of exon3. 1μl of reverse transcription product was used as a template and GAPDH primers were used in a control reaction. To evaluate ISG54 protein level in the knockout animals, freshly isolated splenocytes were incubated overnight with 2000U of murine IFNβ (Biogen). Spleens were harvested from animals euthanized by CO_2 inhalation and disrupted between frosted glass slides. Red blood cells were lysed using ACK Lysing Buffer (0.15M NH_4Cl, 10mM $KHCO_3$, 0.1mM EDTA) for 5 minutes at room temperature. ACK buffer was neutralized with complete DMEM, splenocytes were spin down at 1600rpm for 5 minutes, resuspended in complete DMEM and filtered through 100uM cell strainer. Isolated splenocytes were seeded on 10cm plates and 6hs after plating they were stimulated with 2000U IFNβ (Biogen). Next day they they were lysed and the presence of ISG54 was verified by Western-blot with anti-N terminal ISG54 antibodies.

Isolation of splenocytes from infected animals- Mice were euthanized by inhalation of isofluorane. Spleens were removed and placed in cold PBS on ice. Homogenization of the spleens was performed in dounce homogenizer and the cells were filtered through 100μM Nytex filter. Cells were collected by centrifugation at 1600 rpm for 10 minutes and resuspended in TAC (Tris ammonium chloride- Red blood cell lysing buffer) (Sigma R7757) 2ml per spleen. After 5 min of lysis at room temperature TAC was inactivated by adding complete DMEM and splenocytes were spin down at 1600rpm for 10 minutes. In case of incomplete lysis of erythrocytes, incubation with TAC was repeated. Pellets containing B-cells were resuspended in 10ml cold DMEM, filtered again through Nytex 100uM filter and the cells were counted with hemocytometer and kept on ice for further experiments. Fresh splenoctyes from each combined pool were plated on MEF monolayer for Limited Dilution Assay (LDA) while $5x10^6$ splenocytes were frozen at -70℃ to be later used for Limited Dilution PCR (LD-PCR) analysis.

Isolation of Mouse Embryo Fibroblasts (MEFs)-Female mice at 12-15 days of pregnancy were euthanized by CO_2 inhalation and the embryos were isolated from the uterus and placed in a cold PBS. Heads and innards were removed and the bodies were minced with sterile razor blades and incubated in trypsin for 1h at 37℃. Trypsin was quenched by adding complete

DMEM, and digested embryonic tissue was pipetted 20x to release more cells. Cellular suspension was then plated on 10cm plates and incubated for 72h to let MEFs attach to the plate and become confluent. After 72h cells were split at 1:2 ratio (passage 1) and then when they became confluent split again (passage 2). At passage 2 they were harvested and frozen at -70°C in 10% DMSO, 40% FBS DMEM to be used for further experiments.

Infection of MEFs with MHV68– For the infection we used MEFs at passage five from initial harvest. Wild-type Murine gammaherpesvirus 68 (MHV68), coding for YFP protein and MHV68 deficient in M11 protein were kind gifts from Dr Laurie Krug (Stony Brook University). One day prior to infection MEFs were seeded on 6-well plates at $2x10^5$ cells/well and the next day they were infected with MHV68 at multiplicities of infection (MOI) 1 and 0.01. Each experimental point was performed in triplicates. Serial dilutions of primary viral stocks were prepared in DMEM. Media from the cells were removed and 200µl of appropriate virus dilution was added per well (10^6Pfu/ml for MOI 1 and 10^4Pfu/ml for MOI 0.01). Cells were incubated for 1h at 37°C rocked every 15 min, then washed once with PBS and supplemented with complete DMEM. MEFs infected with MOI 1 were collected at 6h, 12h, 24h and 36h after infection while the MEFs infected with MOI 0.01 were collected at 12h, 24h, 36h and 48h after infection. Additionally we evaluated MHV68 infection in the cells that were pretreated overnight with 100U/ml IFNβ (Biogen). Those cells were collected at 24hs and 36hs. Harvest was performed by freezing the whole plate with cells at-70°C. To disrupt the cells and release the virus, a series of four consecutive freeze-thaw cycles was performed. Six consecutive ten-fold dilutions from 10^{-1} to 10^{-6} were prepared from the lysates and used for the plaque assay. To study progress of MHV68 infection, MEFs were infected with YFP-MHV68 at MOI 0.01. At 24,48 and 72hs after infection cells were collected by trypsinization resuspended in PBS and analyzed with FACS Calibur Cytometer. Gate was set for the population positive for GFP, 50000 cells were collected, and the percentage of cells expressing viral encoded YFP was compared between wild-type and ISG54KO MEFs. Spreading of the infection was also visualized using fluorescence microscopy by comparing areas infected with YFP MHV68 that emitted yellow fluorescence.

Plaque assay- For the plaque assay we used NIH 3T12 mouse fibroblasts. Day prior to infection 3T12 cells were seeded on 6 well plates $1.8x10^5$ cells per well where each well represented one of six constitutive dilutions of a single sample (from 10^{-1} to 10^{-6}). On the day of infection media were removed and 200ul of each viral dilution was added to the cells. Cells were

incubated for 1hs, rocked every 15min and then covered with 2ml of DMEM media containing 1.5% methylcellulose and 7% FBS. After 1 week of cell culture media were removed, cells were washed 3x with PBS, fixed for 5 min with methanol and stained with Crystal Violet 0.1% solution in 20% methanol). Plaques were counted on each plate and the numbers from the wells that gave 5-120 colonies were averaged to calculate the viral titer for a single sample.

Study of acute MHV68 infection in mice- For the experiments we used mice that were 8-12 weeks old wild type and ISG54/IFIT2 knockout matched in terms of sex and age. Mice were anaesthetized with isofluorane and infected intranasaly with 1000Pfu of MHV68 in 20µl of infection medium (DMEM). 4 or 9 days after infection mice were euthanized by inhalation of isofluorane and their left and right lungs were removed. To determine viral titer we used the plaque assay. Lungs tissue was subjected to four rounds of mechanical disruption of 1 min each using 1.0-mm zirconia/silica beads (Biospec Products, Bartsville, OK) in a Mini-Beadbeater-8 (Biospec Products). Serial 10-fold dilutions of organ homogenates were plated on NIH 3T12 monolayers in a 200-µl volume. Infections were performed for 1 h at 37°C with rocking every 15 min and the cells were covered with 1.5% methylcellulose DMEM. After one week plaque assay was read as described previously.

Limited Dilution PCR (LD-PCR) – LD-PCR with a double nested single copy-sensitive reaction was used to determine the number of latent viral genomes in the spleen by amplifying ORF50 of MHV68. For LD-PCR we used $5x10^6$ splenocytes from combined pools of wild-type or ISG54 knockout spleens isolated at day 16 after infection and frozen at -70°C. Reaction was performed according to protocol developed by Dr Samuel Speck (160) and modified by laboratory of Dr Laurie Krug (161). Frozen samples were thawed, counted, resuspended in isotonic buffer, and plated in serial threefold dilutions with 10^4 uninfected NIH 3T12 cells in 96-well plates (Eppendorf Scientific, Westbury, NY). All the subsequent reactions were performed using Eppendorf Mastercycler Pro S. Cells were disrupted by lysis with proteinase K and incubated for 6 h at 56°C on the plates covered with PCR foil (Eppendorf). Ten microliters of round 1 PCR mix was added to each well with micropipetter by foil puncture and the plates were covered with fresh PCR foil. After the first-round of PCR, 10 µl of round 2 PCR mix was added to each well and the samples were subjected to a second round of PCR. The sequences of the first outer PCR primers used were 5′-AACTGGAACTCTTCTGTGGC-3′ and 5′-

GGCCGCAGACATTTAATGAC-3′, which amplify a 586-bp product. The sequences of the second inner PCR primers used were 5′-CCCCAATGGTTCATAAGTGG-3′ and 5′-ATCAGCACGCCATCAACATC-3′, which amplify a 382-bp product. Each PCR mixture contained 50 mM KCl, 10 mMTris-HCl (pH 8.5), 0.1% Triton X-100, 1.5 mM $MgCl_2$, 0.2 mM nucleotides, 1 ng of each primer per μl, and 1 U of *Taq* polymerase (Promega). Products were separated on 2% agarose gels and visualized by ethidium bromide staining. Twelve PCRs were performed for each sample dilution, and a total of six dilutions were performed per sample. Every PCR plate contained control reactions (uninfected cells and 10 copies, 1 copy, and 0.1 copy of plasmid DNA in a background of 10^4 cells). Percentage of wells positive for viral genome was calculated for each dilution and analyzed with GraphPad Prism Software. Based on the Poisson distribution, the frequencies of viral genome-positive cells were obtained from the nonlinear regression fit of the data where the regression line intersected 63.2%.

Limited Dilution (LDA) Assay- LDA assay was used to measure reactivation of MHV68 in the splenocytes according to the protocol used by laboratory of Dr Laurie Krug. Freshly isolated splenocytes were resuspended in complete DMEM and plated in serial twofold dilutions (starting with 10^5 cells) onto MEF monolayers in 96-well tissue culture plates. Twelve dilutions were plated per sample, and 24 wells were plated per dilution. Wells were evaluated for cytopathic effect (CPE) 2 weeks after plating by microscopic examination. To detect preformed infectious virus, parallel samples of mechanically disrupted cells were plated onto MEF monolayers. This process kills >99% of live cells, which allows preformed infectious virus to be discerned from virus reactivating from latently infected cells. Percentage of wells positive for cytopathic effect was calculated for each dilution and analyzed with GraphPad Prism software. The frequency of reactivating cells was obtained using non-linear regression fit of the data with regression line intersected at 63.2%.

Statistical Analysis- Unless stated otherwise we used independent two sample t-test with equal variance to evaluate statistical significance of our data. In most of the experiments one-tailed t-test was used. A two-tailed t-test was used for cotransfections of ISG54 with other ISGs. The p values were calculated using Microsoft Excel software. The p values < 0.05 were considered to be statistically significant.

Chapter 3. Results

ISG54 and apoptosis

Expression of ISG54 promotes cell death

To study the cellular effects of ISG54 we created a monomeric GFP (mGFP)-tagged derivative of human ISG54 and expressed it in HeLa cells by transient transfection. Surprisingly ISG54-mGFP seemed to have a negative effect on the cell survival and proliferation. While at 24hs after transfection most of the HeLa cells expressing ISG54 looked healthy and ISG54-mGFP was evenly distributed in the cytosol, at 48hs this phenotype dramatically changed. First of all there was a dramatic decrease in the number of cells positive for ISG54-mGFP from 24hrs to 72hrs (see Figure 6). This did not occur with mGFP expression (data not shown). The cells that retained expression of ISG54, displayed a weak green fluorescence, only slightly more intensive than the background. Secondly, the morphology of the cells expressing ISG54 changed. Many of them detached from the substrate, some become excessively elongated or appeared very small with ISG54 in the nucleus (Figure 6). Together those observations suggested that expression of ISG54 may be detrimental to the cells and probably causes their death.

To evaluate this hypothesis we performed propidium iodide (PI) staining of the HeLa cells expressing ISG54-mGFP. PI is excluded from living cells with an intact membrane but after membrane perforation it enters the nuclei of the dead cells and binds to DNA. Such binding results in an 100-fold increase in PI fluorescence that can be monitored with flow cytometry. We transfected HeLa cells with ISG54-mGFP or mGFP as a control and at 24, 48 and 72hs after transfection we stained them with PI before analysis with flow cytometry. We evaluated the distribution of PI signal in the cells that were GFP positive in mGFP or ISG54-mGFP transfected population. At 24hs cells expressing ISG54mGFP showed a slight increase in the cell death in comparison to mGFP controls (Figure 7). However, at 48h there was a dramatic increase in the PI signal from the cells expressing ISG54. At 72hs over 70% of the cells expressing ISG54mGFP were dead as assessed by PI staining. Analysis of the cells that did not express detectable ISG54mGFP in the same population showed that they displayed only a slight increase in cell death by 72hs (Figure 8). Those data suggested that expression of ISG54 is specifically responsible for induction of death in the cells transfected with ISG54mGFP.

Inducible ISG54 promotes cell death

To further study effects of ISG54 on cell death we tested an inducible system of ISG54 expression. We used two sets of vectors: pRevTre containing a tetracycline response element in the promoter and pLib-rtTAm2-iresTRSID-iresPuro (gifts from dr Wei-Xing Zong) that coded for both tetracycline sensible repressor and activator. In the absence of tetracycline the repressor was bound to tetracycline response element on pRevTre while activator remained inactive. Adding tetracycline should trigger the activator and remove the repressor leading to the strong expression of the gene of interest. We cloned ISG54mGFP into pRevTre placing it under control of the tetracycline responsive promoter and observed efficient induction of ISG54 by tetracycline stimulation. Unfortunately we were unable to establish a stable cell line expressing ISG54.This appeared to be due to a very low level of ISG54 production in uninduced cells. The pro-apoptotic functions of ISG54 with uninduced promoter leakage probably eliminated the cells with time. On the other hand we were successful in obtaining effective induction of ISG54 during a transient transfection. In this case inducible ISG54 caused the same cell death in HeLa cells as the protein that was constitutively expressed (Figure 9).

ISG54 induces cell death by way of apoptosis

To evaluate whether ISG54 expressing cells die by apoptosis we performed annexinV staining. AnnexinV binds to phosphatidylserine that is exposed on the outer leaflet of the plasma membrane in apoptotic cells. HeLa cells were transfected with ISG54-mGFP or mGFP as a control and at 24h, 48h and 72hs after transfection they were stained with allophycocyanin-annexinV (APC-V) and analyzed by flow cytometry. Similar to PI staining there was not much difference between control and ISG54 expressing cells at 24hs, but at later timepoints we observed a dramatic increase in apoptosis among the cells that expressed ISG54-mGFP (Figure 10). At 72hs over 80% of the cells positive for ISG54-mGFP were also positive for annexin V. In the same population, cells that did not express ISG54 showed only a slight increase in annexin V staining. This data suggested that cells death caused by ISG54 is executed by apoptosis

ISG54 induces apoptosis in different cell lines

Our primary data on ISG54 promoted cell death was generated with HeLa cells. To check whether the pro-apoptotic effect of ISG54 could be observed in other cell lines we evaluated effects of ISG54 expression in human cancer cell lines: HT1080 and HEC1B. HT1080 is human fibrosarcoma line and HEC1B is derived from endometrial adenocarcinoma. Both those cells

lines were transfected with ISG54mGFP or mGFP control and stained with annexinV at 24h, 48h and 72hs. ISG54 induced apoptosis in both HT1080 and HEC1B cells (Figure 11). The pro-apoptotic effect did not appear as dramatic as seen in HeLa cells but cell death was still significant. Again it was specific to the cells expressing ISG54. These results suggested that ISG54 induces cell death in multiple types of cancer and therefore may work through common pro-apoptotic mechanisms. Differences in effectiveness of ISG54 to promote apoptosis in particular cell lines could be due to their diverse genetic background and versatile pro-survival mechanisms.

Levels of ISG54mGFP expression are similar to endogenous ISG54

While apoptosis induced by ISG54 was evident, it was still possible that this phenomenon was simply an effect of protein overexpression. To address this issue we used FACS sorting to isolate the cells expressing ISG54mGFP and compare ISG54 levels to cells treated with IFN. HeLa cells were transfected with ISG54mGFP and at 24 and 48hs after transfection we isolated the population positive for GFP. Next, by using Western-blotting with specific anti-ISG54 antibodies we compared the levels of ISG54mGFP with the levels of endogenous ISG54 that was induced in HeLa culture by IFN stimulation. We found that the amount of ISG54 produced in response to IFN signal was similar to the amount of transiently expressed ISG54mGFP (Figure 12). These results suggested that the observed ISG54 induced apoptosis is caused by the specific effect of that protein, not just by overexpression.

ISG54mGFP does not induce an Unfolded Protein Response and ER stress

It was still possible that transiently expressed ISG54mGFP even at physiological levels could be folded improperly and therefore causes ER stress and apoptosis. An Unfolded Protein Response (UPR) often results in a cell death (162). To address this issue we decided to evaluate the levels of Bip protein in the cells expressing ISG54. Bip is an ER chaperone that is strongly upregulated during ER stress. We transfected Hela cells with ISG54-mGFP or control mGFP and 24hs and 48hs after transfection we isolated the population of GFP positive cells. Next, we lysed the cells and by Western blotting we evaluated the level of Bip protein (Figure 13). As a positive control we used lysates from the cells treated with tunicamycin, a strong ER stress inducer that is known to upregulate Bip. The same amount of protein from each sample as determined with the protein assay reagent (Biorad) was evaluated by Western blot (40ug). The experiment showed that both at 24hs when the amount of ISG54mGFP was at peak and at 48hs when apoptosis

started to be dominant, levels of Bip remained unchanged. It should be noted that expression of a control protein such as alpha tubulin was not tested in this experiment. However the results suggest that ISG54 folds properly in the cells and does not induce UPR.

To determine whether ISG54 accumulates in the ER we used confocal microscopy combined with immunofluorescence. Cells were transfected with ISG54mGFP, fixed with paraformaldehyde and ER membranes were visualized by staining with anti-calnexin antibody. Calnexin, an abundant ER protein, is often used as a marker of ER in immunofluorescence experiments. Confocal imaging showed that ISG54mGFP is present in ER but not at higher levels than in the cytosol (Figure 14). Analysis of green fluorescence distribution showed that there is no accumulation of ISG54mGFP in the ER in comparison to calnexin that localizes preferentially in that compartment (Figure 14). Finally, we wanted to check whether inhibition of ER stress has any effect on ISG54 induced apoptosis. Six hours after transfection with ISG54mGFP we treated the cells with Salubrinal, a commercially available ER stress inhibitor. Salubrinal blocks the action of phosphatases that dephosphorylate eukaryotic translation initiation factor 2, subunit α (eIF2α) and halts protein synthesis allowing for recovery from ER stress (25). It was shown to be efficient against apoptosis induced by tunicamycin treatment (25). However, in the case of ISG54 expression, treatment with Salubrinal had no effect on apoptosis (Figure 15). These results suggest that ISG54 does not induce ER stress and it is not retained in the ER. Therefore apoptosis that is observed during ISG54 expression is not simply due to accumulation of unfolded protein.

ISG54 knockdown decreases sensitivity to IFN-induced apoptosis

IFN is known to induce apoptosis in several types of cancer. ISG54 is strongly upregulated by IFN and therefore its pro-apoptotic properties are likely to be a part of IFN killing mechanism. If ISG54 plays a significant role in IFN-induced apoptosis, knocking down ISG54 should make cells more resistant to IFN cytotoxicity. To test this we designed four shRNAs aimed at different regions of ISG54 mRNA (Figure 16). We transfected HeLa cells separately with those shRNAs and by antibiotic selection we established four stable cell lines expressing each shRNA. Western blot showed that upon IFN stimulation anti-ISG54 shRNA described as sh1075 had a significant knockdown effect compared to the other anti-ISG54shRNAs and to the control unspecific shRNA (Figure 16). Analysis of band intensity displayed that levels of ISG54 were reduced over 60% in 1075sh cell line. Next, we evaluated how ISG54 knockdown

influences the pro-apoptotic effect of IFN. We stimulated cells for 72hs with IFN and then by flow cytometry we analyzed apoptosis in each line. We found that cells expressing the 1075 shRNA showed a significant decrease in IFN induced apoptosis compared to the control cells that expressed either scrambled non-specific sh RNA or 136 shRNA that had no influence on ISG54 level (see Figure 17). These results suggest that ISG54 is involved in the IFN-induced apoptosis and is a part of mechanism by which IFN exerts cell death.

ISG54-induced apoptosis proceeds through activation of caspases

Caspases are the main executors of the apoptotic process. They can be induced either via external (caspase-8) or internal (caspase-9) pathways of apoptosis initiating a signaling cascade that activates executor caspases. The final step of that process is activation of caspase-3, a main executor enzyme that cleaves crucial cellular components. To evaluate whether caspase-3 is activated in ISG54 expressing cells we used immunofluorescence combined with fluorescent microscopy. HeLa cells were transfected with ISG54mGFP or mGFP and at 24hs and 48hs after transfection they were fixed, permeabilized and stained with anti-active caspase-3 antibody. Examination under fluorescent microscopy enabled us to calculate the percentage of GFP expressing cells is also positive for active caspase-3 (Figure 18). We found that activation of caspase-3 was over three times higher in the cells expressing ISG54mGFP comparing to the control. It was particularly visible in those cells that showed morphological changes such as shrinkage or substrate detachment. Together at 48hs over 30% of the ISG54 positive cells displayed caspase-3 activation (Figure 18).

To evaluate the effect of caspase inhibition on ISG54 induced apoptosis we used two kinds of caspase inhibitors: ZVAD-FMK that blocks all the members of caspase family and ZIETD-FMK that targets specifically caspase-8. Cells were transfected with ISG54mGFP and 6 hours after transfection the media were changed and the inhibitors were added. Flow cytometry analysis showed that ZVAD-FMK caused a significant decrease of ISG54-induced apoptosis, however ZIETD-FMK had practically no effect (Figure 19). These results may indicate that while ISG54-induced cell death proceeds through caspases, the external pathway initiated by caspase-8 plays a minor role in this process. Consequently ISG54-induced apoptosis is likely dependent on the intrinsic pathway and therefore linked to the mitochondria.

ISG54-promoted apoptosis is executed via a mitochondrial pathway

The most common apoptotic pathway proceeds through mitochondria and is controlled by the Bcl protein family members. To evaluate whether ISG54 works through the mitochondrial apoptotic pathway we examined the effect of Bcl-xL or Bcl-2 that are known potent inhibitors of mitochondrial apoptosis (163). HeLa cells expressing ISG54-mGFP with ot without Bcl-xL or Bcl2 were stained with PI and analyzed with flow cytometry. We found that both Bcl-2 and Bcl-xL dramatically inhibited pro-apoptotic effect of ISG54 with Bcl-xL slightly more effective (Figure 20). Next we determined whether Bax and Bak, two main initiators of mitochondrial apoptosis are required for ISG54-induced cell death. We used Baby Mouse Kidney (Bmk) cells that lack Bax/Bak (gift from Dr Wei-Xing Zong), transfected them with ISG54mGFP and monitored cell death at 24, 48 and 72h using flow cytometry. ISG54 induced significant apoptosis in wt Bmk cells, but the cell line lacking Bax/Bak was completely resistant to ISG54 promoted cell death even at 72hs (Figure 21). These results indicated that ISG54 causes cell death by triggering mitochondrial pathway of apoptosis.

Viral proteins are able to block ISG54-promoted apoptosis

DNA viruses can express proteins that block the apoptotic cellular defense. For this reason we tested whether viral proteins that block the mitochondrial apoptotic pathway can counteract the effect of ISG54. Since ISG54 is induced in response to viral infection, pathogens could have evolved mechanisms inhibiting its action. We evaluated the effect of three anti-apoptotic viral proteins: adenoviral protein E1B-19K, Kaposi's Sarcoma Herpes Virus(KSHV) v-Bcl2 protein and Mouse GammaHerpesvirus 68 (MHV68) M11 protein. Those molecules are homologues of human Bcl-2 proteins and are known to enhance survival of infected cells (164). All the three viral proteins effectively inhibited ISG54-induced apoptosis although not as effective as original Bcl-xL protein (Figure 22). Interestingly v-Bcl2 was the only one that stabilized the levels of ISG54 protein (data not shown). These data suggested that viruses are able to block ISG54 action and during infection with certain types of pathogens ISG54-induced apoptosis can be effectively neutralized.

ISG54 does not localize to the mitochondria

Since apoptosis induced by ISG54 proceeds through the mitochondrial pathway we wanted to determine whether ISG54 localizes inside the mitochondria. To address that issue we transfected cells with ISG54mGFP and stained them with fluorescent dye MitoTracker Orange that is permeable to living cells. MitoTracker binds to the metabolically active mitochondria and

allows precise visualization of mitochondrial compartment with fluorescent microscopy. Live cell imaging performed 24h post transfection with confocal microscope showed ISG54 throughout the cytoplasm but excluded from mitochondria (Figure 23). This result indicates that although ISG54 exerts its pro-apoptotic effect through mitochondrial pathway it does not enter mitochondria itself. Nevertheless it's still possible that ISG54 can be bound or interacts with external mitochondrial membrane.

ISG54 promotes Bax translocation to mitochondria

Since ISG54 required the presence of Bax and Bak for its pro-apoptotic effect we decided to test whether it causes mitochondrial translocation of Bax protein. During apoptosis Bax inserts into the outer mitochondrial membrane and forms a pore that enables release of pro-apoptoptic factors such a cytochrome c, Smac or Diablo (165). A common method to study this process is to visualize Bax translocation with a fluorescent marker (166).Under normal conditions Bax is evenly distributed throughout the cells but during apoptosis it moves to mitochondria and is seen in a characteristic puncta pattern. For our experiments we cotransfected HeLa cells with ISG54v5 and Bax-GFP and at 24, 48 and 72h we observed them under confocal microscope. ISG54v5 was visualized by immunofluorescence with use of primary anti-v5 antibodies and secondary antibodies labeled with TRITC. At 24hs ISG54 retained cytoplasmic localization while Bax could be present both in cytosol and nucleus (Figure 24). At 72h signal from ISG54 significantly decreased, cells expressing ISG54 displayed morphological changes and Bax-GFP formed characteristic green puncta indicating on mitochondrial localization. These observations suggest that expression of ISG54 facilitates translocation of Bax into mitochondria

ISG54 expression leads to the loss of mitochondrial potential

One of the features of apoptotic cell death is depolarization of the mitochondrial membrane and loss of mitochondrial potential. To study whether ISG54 can cause a decrease of mitochondrial potential we used staining with Mitotracker a dye that specifically binds to mitochondria. In active mitochondria Mitotracker gets oxidized and produces much stronger fluorescence than in its reduced form. Therefore dying cells with inactive mitochondria give weaker signal coming from Mitotracker fluorescence when comparing to the living cells and such a difference can be detected and analyzed with flow cytometry. We transfected HeLa cells with ISG54mGFP or mGFP as a control and at 24 and 48hs we stained them with Mitotracker Orange and analyzed with flow cytometry. Cells with decreased mitochondrial potential formed

a characteristic peak on the left side of histogram representing the distribution of Mitotracker fluorescence (Figure 25). We found that expression of ISG54 increased over two-fold amount of cells with low mitochondrial potential. That finding is consistent with earlier observations that ISG54 induces apoptosis and that proceeds through mitochondria.

ISG54 promoted apoptosis is p53 independent

The tumor suppressor protein p53 plays important role in the induction of apoptosis in response to DNA damage and intracellular stress. In order to evaluate whether ISG54-induced apoptosis depends on the presence of p53 we cotransfected cells with ISG54mGFP and a dominant negative mutant of p53. Dominant negative mutant encodes for carboxyl-terminal part of p53 that oligomerizes with wild-type p53 therefore preventing formation of functional tetramers (155,167). We found that expression of dominant negative mutant of p53 had no influence on ISG54-induced apoptosis (Figure 26). By immunofluorescence we determined that mutated p53 was successfully transfected into the cells and coexpressed well with ISG54mGFP (Figure 24) yet it showed no inhibitory effect. We also tested the effect of two adenoviral proteins E1B-55K and eORF6 that are known to bind p53 and inhibit its functions (168). Cotransfection of ISG54mGFP with either of those proteins did not alter observed apoptosis (Figure 27). We could not verify the expression levels of viral proteins due to lack of specific antibodies, however both plasmids (gift from Dr Patrick Hearing, Stony Brook) were reported to give good protein expression (169). Therefore these results suggest that ISG54-promoted apoptosis is independent of p53.

ISG54 expression does not inhibit translation

Previous reports linked ISG54 to translation inhibition and negative regulation of protein synthesis (74,170). Since protein synthesis is necessary for cell survival, it was possible that ISG54 expressing cells die because of a translation block. To determine this possibility we transfected the cells with mRNA of a reporter luciferase gene and evaluated how the presence of ISG54 will influence its translation. HeLa cells were transfected with ISG54-v5 or an empty pEF1-v5 vector and 12hs after transfection they were transfected with capped and polyadenylated luciferase mRNA generated by *in vitro* transcription. After 6hs the cells were lysed and translation efficiency was determined by luciferase assay. As a positive control for a translation block cells expressing empty pEF1-v5 vector and capped polyadenylated luciferase mRNA were treated either with 10 ug/ml cycloheximide or 1000U/ml IFN prior to mRNA

transfection. ISG54 showed no effect on translation inhibition while both cycloheximide and IFN treatment abolished translation of reporter mRNA (Figure 28, upper panel).

Next we evaluated how ISG54 influences translation of different types of mRNA. As ISG54 was reported to have different effects on translation depending on the regulatory features of the mRNA (91), in the next experiment we used both capped mRNA and uncapped mRNA expressing an internal ribosome entry site (IRES). One mRNA encoded firefly luciferase mRNA bearing a conventional 5'-7-methylguanosine (5'-m7G) cap. The second one was the same luciferase reporter but regulated by the HCV IRES sequence on its 5' terminus. Both types of mRNA were generated by *in vitro* transcription. In order to isolate the population of cells that actively express ISG54, HeLa cells were first transfected with mGFP or ISG54mGFP plasmids and 24hs after transfection they were transfected with capped or IRES regulated mRNA. 6hs after transfection with reporter mRNA we used FACS to collect GFP positive cells, lysed them and determined efficiency of mRNA translation by a luciferase assay. Again, we did not observe any influence of ISG54 expression either on capped or IRES-bearing mRNA (Figure 28, lower panel).

In a previous study ISG54 was reported to inhibit translation by binding to "e" and "c" subunits of eukaryotic translation initiation factor 3 (eIF3) and sequestering them from mRNA (74). If this was the cause of apoptosis, then ectopic expression of those translation factors would possibly overcome translation inhibition and reduce cell death caused by ISG54. We obtained cDNAs encoding eIF3c and eIF3e and cloned them into expression plasmids tagged with the V5 epitope. Transfection analyses and Western blot verified their expression (Figure 29 top). We cotransfected HeLa cells with ISG54mGFP in combination with either eIF3c, eIF3e, or eIF3c and eIF3e together (Figure 29). However, we could observe no effect on ISG54-induced apoptosis even in the presence of combined expression of eIF3c and eIF3e. Therefore while it is possible that ISG54 has some influence on protein synthesis, it does not appear to be a notable factor in ISG54 induced apoptosis.

Ras, Akt and PI3K partially inhibit ISG54-induced apoptosis

Cancer cells have mutations in many pro-survival pathways that give them resistance to apoptotic stimuli. To evaluate whether known proliferative signaling molecules can influence ISG54 induced apoptosis, we tested several oncogenes that are known to protect tumors from cell death. We cotransfected HeLa cells with ISG54mGFP with a particular oncogene and by

using flow cytometry we measured apoptosis at 24hs, 48hs and 72hs after transfection. We found that H-Ras V12, an activated mutant form of human Ras oncogene, can partially inhibit ISG54-induced apoptosis (Figure 30). In the presence of Ras we observed about 60% reduction in cell death at 48hs and 30% reduction at 72hs. H-Ras is GTP-ase that plays role in signal transduction from receptor tyrosine kinases such as epidermal growth factor receptor (EGFR) to downstream effector kinases such as phosphatidylinositol-3-kinase (PI3K) or Akt (171). We cotransfected cells with ISG54mGFP and constitutive active forms of Akt and PI3K to test how they influence ISG54 induced cell death. Both Akt and PI3K showed some inhibitory effect although less than Ras (Figure 30). Other tested oncogenes such as c-Myc, v-Src, Brk and c-Abl displayed no influence on ISG54 mediated cell death, however due to lack of specific antibodies we were unable to evaluate their protein expression (data not shown). These results suggest that mutations in Ras/PI3K/Akt pathway may play an important role in protection against ISG54 and consequently IFN-induced cell death.

ISG54 interacts with ISG56, ISG60 and with itself

To elucidate the molecular mechanism of ISG54 action we investigated potential interacting proteins. Studies with a yeast-two hybrid assay performed previously in our lab indicated that ISG54 interacts with ISG56 and ISG60, two other members of its family. To verify these results in mammalian cells we transfected HeLa cells with T7-ISG54 or with empty T7 epitope vector as a control and stimulated them overnight with IFN. The purpose of IFN was to induce proteins that might bind ISG54, or to generate potential posttranslational modifications in ISG54 that could enhance its interactions with partners. The next day cells were lysed and proteins were collected on agarose beads coupled with anti-T7 antibodies. Eluted proteins were separated by SDS-PAGE and stained with silver (Figure 31). Distinct protein bands were apparent in the immunocomplexes from the cells expressing T7-ISG54. Those bands were excised from the gel and analyzed by mass-spectrometry (ProTech). They were identified as members of ISG54 family: ISG54, ISG56 and ISG60. This result confirmed our initial finding from the yeast two-hybrid assay.

To further confirm binding of ISG54 to its putative binding partners we performed a series of reciprocal immunoprecipitations. HeLa cells were cotransfected with plasmids coding for ISG54-v5 and either FLAG-ISG54, FLAG-ISG56, FLAG-ISG58, FLAG-ISG60 or empty FLAG epitope plasmid. ISG54 was immunoprecipitated with anti-v5 antibodies and the

associated proteins were detected by Western-blotting with anti-FLAG antibodies. We found that ISG54 associated with itself, ISG56 and ISG60 but not efficiently with ISG58 (Figure 32). Input analysis showed that all the proteins were expressed (Figure 32). In a reverse experiment the FLAG-tagged ISGs were precipitated using anti-FLAG antibodies while ISG54 was detected with anti-ISG54 serum. Again we could see strong interaction with ISG60 and ISG54, weaker with ISG56 and no binding to ISG58 (Figure 33). We performed an analogous immunoprecipitation experiment for ISG56 and interestingly we found that it can also bind ISG60 (Figure 34). Together those results confirmed an interaction of ISG54 with ISG56 and ISG60 and suggested that they may be involved in the formation of a multimeric complex.

Analysis of ISG54 TPR domain interactions with ISGs

ISG54 is predicted to have nine TPR motifs distributed evenly along the molecule (80). We focused on determining which fragments of ISG54 are necessary for interaction with its binding partners. We created a series of V5-tagged truncations of ISG54. The 1-4TPR construct encodes the first four TPR domains and the N-terminus whereas 2-9TPR, 3-9TPR and 4-9TPR contain noted TPR motifs and an intact C-terminus (Figure 35). We cotransfected HeLa cells with those truncations and HA-ISG54 or HA-ISG56 or HA-ISG60. ISG proteins were immunoprecipitated using anti-HA serum and truncations were detected by Western-blot with anti-v5 antibodies. All of the constructs expressed well and could be detected Western-blotting (Figure 36). We found that the first TPR domain of ISG54 is necessary for its interaction with ISG60. Without this fragment we were unable to detect any binding between ISG54 and ISG60 (Figure 37). On the other hand all of the TPR truncations were able to interact with ISG56 and ISG54 (Figure 38, 39). Their binding was weaker than the binding of full length protein but still detectable. These results indicate that the interface of ISG54 association with itself or with ISG56 is distinct from the interface of association with ISG60.

ISG54, ISG56 and ISG60 form oligomeric complex at ~150-250kDa molecular weight

Since the coimmunoprecipitation experiments showed reciprocal interaction between ISG54 ISG56 and ISG60, it was possible that all these proteins form multimeric complex. To determine the molecular mass of this putative aggregate we used glycerol gradient sedimentation. In this technique cell lysates are applied to the top of glycerol gradient that is centrifuged for 40hs at 215000g. Proteins separate according to their molecular mass which is estimated by comparison to known molecular weight markers in a separate gradient. As markers

we used a mixture of bovine serum albumin, catalase, alcohol dehydrogenase and apoferritin (Figure 40). HeLa cells were cotransfected with ISG54-V5, FLAG-ISG56 and FLAG-ISG60 and stimulated overnight with IFN-α. Detergent lysates were sedimented through 25-40% glycerol gradient and fractions containing the proteins were identified by Western-blot. ISG54-V5 localized in the fractions corresponding to 150-250kDa (Figure 41) and endogenous ISG54 induced by IFN sedimented in the same fractions. Western blot with anti-FLAG antibodies showed that ISG56 and ISG60 colocalize in the same fractions at 150-250kDa. To check the influence of IFN on ISG complex formation we performed a comparable experiment without IFN stimulation. We obtained the same results with ISG54, ISG56 and ISG60, they all sedimented in fractions between 150 and 250kDa. Interestingly, no monomeric form of ISG54 was detected. These results suggest that ISG54, ISG56 and ISG60 form a multimeric complex and very likely they cooperate together during the IFN response.

ISG60 modulates ISG54 apoptotic effect

Since our data suggested that ISG54 binds both ISG56 and ISG60, we evaluated how other ISGs would influence the pro-apoptotic effect of ISG54. We cotransfected HeLa cells with ISG54mGFP and ISG56-v5 or ISG60-v5 and analyzed cell death with PI and annexinV staining. While ISG56 had minimal influence on ISG54 induced apoptosis, ISG60 showed a potent inhibitory effect. In the presence of ISG60, apoptosis induced by ISG54 was reduced by approximately 50% (Figure 42). It was possible that ISG60 binding could reduce ISG54 protein stability and promote cell survival by simply reducing levels of ISG54. However, analysis by Western-blotting showed that ISG60 maintained the amount of ISG54mGFP ISG54 was actually expressed at higher levels (Figure 43). Also, analysis with flow cytometry revealed that the number of cells expressing ISG54mGFP increases in the presence of ISG60. Normally the population of cells expressing ISG54mGFP decreases significantly at 48hs, but with ISG60 coexpression this decline proceeds significantly more slowly (Figure 43). Consequently these results indicate that ISG60 does not reduce pro-apoptotic effect of ISG54 by ISG54 protein degradation. To determine whether a direct interaction with ISG54 is necessary for the modulatory effect of ISG60, we evaluated the ISG54 truncation that lacks the first TPR domain and cannot bind to ISG60. The 2-9TPR construct was well expressed and could induce cell death at similar levels to full-length protein; however this response could not be suppressed by ISG60 (Figure 44).Although ISG60 could suppress apoptosis induced by full-length ISG54, it could not

inhibit apoptosis byISG54 lacking the first TPR. This result indicates that ISG60 must bind to ISG54 to have a suppressive effect.

Since ISG60 is potently induced by IFN, we speculated that IFN stimulation should also have modulatory effect on ISG54-induced apoptosis. Therefore we transfected HeLa cells with ISG54mGFP and stimulated them with IFN to induce ISG60 and other proteins that might regulate functions of ISG54. We found that in the presence of IFN, ISG54-induced cell death is substantially reduced and the number of cells expressing ISG54mGFP is sustained in the culture (Figure 45). IFN stimulation had no effect on apoptosis caused by 2-9TPR ISG54 truncation that lacked first TPR domain necessary for the interaction with ISG60 (Figure 45). Together those results suggest that during IFN response pro-apoptotic effect of ISG54 is modulated through interactions with N-terminal part of the protein. Also ISG60 seems to be a significant modulator of ISG54-induced apoptosis.

TPR domains of ISG54 and their role in apoptosis

In order to determine which region of ISG54 is responsible for induction of apoptosis we created series of mGFP-tagged truncations of ISG54 protein (Figure 46). HeLa cells were subsequently transfected with each of those truncations and the levels of apoptosis among GFP positive cells was evaluated by flow cytometry and compared to full-length protein (Figures 47). While expression of the N-terminal part of ISG54, devoid of any TPR domains, caused only limited cell death, adding just the first TPR domain induced apoptosis similar to the full length protein. On the other hand the C-terminal fragment encompassing the last 9^{th} TPR did not induce cell death. Other truncations caused moderate to high levels of apoptosis that increased with the number of TPR motifs. These data indicate that the presence of the set of TPR domains is involved in the pro-apoptotic action of ISG54 with the first TPR domain having the most dramatic effect. This may also explain why the binding of first TPR motif by ISG60 effectively decreases ISG54 induced cell death.

ISG54 interacts with STING, eEF1, PRDX5 and DLC1

Besides the members of ISG54 family our yeast-two hybrid screen revealed other proteins that potentially interact with ISG54. Among them there was translation eukaryotic elongation factor 1α (eEF-1α), peroxiredoxin 5 (PRDX5), and dynein light chain 1 (DLC1). All of those proteins seemed interesting with regard to the apoptotic function of ISG54. Besides

eEF-1α role in translation, it is known to be involved in cytoskeleton organization, viral propagation, and modulation of cell death (172). PRDX5 is a strong anti-oxidant enzyme that participates in elimination of reactive oxygen species (ROS) and protects the cells from apoptosis (173,174). DLC1 is a protein participating in intracellular transport and binds and sequesters Bim, a potent inducer of mitochondrial apoptosis (175,176). In *Drosophila* DLC1 was found to be necessary for autophagy and autophagy mediated cell death (177). Therefore ISG54 interaction with each of those factors could be important for anti-viral and pro-apoptotic functions of ISG54. Additionally, previous reports indicated that ISG54 can associate with STING (63), a mitochondria bound adapter protein and that ISG54 binding downregulates STING mediated anti-viral response (96). To verify those interactions we transfected cells with v5-tagged STING, eEF-1α, DLC1 and PRDX5. Cells were stimulated overnight with IFNα and ISG54 was immunoprecipitated with anti-ISG54 serum. Visualization of bound proteins with Western-blot showed that ISG54 associates with STING, eEF1α, PRDX5 and DLC1 (Figures 48,49). Next, we evaluated the effect of each of those proteins on ISG54-induced apoptosis by cotransfecting them with ISG54mGFP and measuring cell death by flow cytometry analysis following annexinV and PI staining. However, none of those proteins displayed inhibitory effects on ISG54-promoted apoptosis (data not shown). This result suggested that pro-apoptotic function of ISG54 cannot be inhibited by overexpression of these proteins.

ISG54 in anti-viral defense

ISG54 has an inhibitory effect on MHV68 replication in vitro

In order to study the role of ISG54 in anti-viral defense we obtained C57BL/6 mice with a targeted deletion in ISG54 gene from the Knock-Out Mouse Project (KOMP) consortium. The deletion removed the promoter and the first exon of ISG54 gene (Figure 50) and knock-out efficiency was confirmed at both mRNA and protein level using RT-PCR and the Western-blotting (Figure 51). While heterozygous mice had decreased level of mRNA for ISG54 they displayed the same level of the protein. For this reason we compared wild-type and knockout animals. For *in vitro* studies we obtained mouse embryo fibroblasts (MEFs) from the embryos at days 12-15 and cultivated them in culture until passage 5. As a control we used MEFS from wild

type C57BL/6 animals. At passage 5 we infected both MEF lines with MHV68 at two multiplicities of infection (MOIs): 1 and 0.01. MEFs infected with MOI 1 were harvested at 6h, 12, 24h and 36h after infection and the MEFs infected with MOI 0.01 were harvested at 12h, 24h, 36h and 48h. Cells were disrupted using multiple freeze-thaw cycle and a viral titer was determined using plaque assay on mouse 3T12 cells. We found that MHV68 replicates significantly better (more than ten times) in the ISG54KO cells as compared to the wild type cells. In the absence of ISG54 viral titer was more than five times higher with MOI 1 and more than ten times higher with MOI 0.01 (Figure 52). At early timepoints there was no difference between wild type and knockout cells but with time the difference in viral replication became evident. To study the progress of MHV68 infection, we infected MEFs with a virus coding for YFP protein and evaluated the number of YFP positive cells with fluorescent microscopy and flow cytometry. At 24hs cells expressing MHV68 YFP were present at very low levels and practically undetectable under the microscope. However, at 48hs there was significant increase in the number of infected cells. Cultures of ISG54KO cells displayed wide clusters of cells positive for the virus with strong yellow fluorescence, while the infected areas in wild-type cells were much smaller with weaker intensity of fluorescence (Figure 53). Analysis with flow cytometry showed that at 48hs there is more than two times infected cells in ISG54KO MEFs comparing to the wild-type MEFs (Figure 54).

We also analyzed viral replication in the cells that were pretreated overnight with 100U IFNβ. As expected IFN decreased substantially MHV68 titer; however there was no significant difference in titer between wild type and ISG54KO cells (Figure 55). These results suggest that ISG54 plays inhibitory role in MHV68 replication but its effects can be substituted by action other genes induced during IFN stimulation of MEFs in vitro.

Since the anti-apoptotic M11 (v-Bcl2) protein from MHV68 was found to inhibit ISG54-induced apoptosis (Figure 27), we evaluated replication of the virus lacking M11 in wild-type (wt) vs. ISG54KO cells. MEFs from the ISG54 KO animal were expected to have less apoptosis in response to infection and therefore we predicted that the M11 deficient virus would replicate better in ISG54 KO cells than wt MEFs. We infected MEFs at MOI 0.01 and determined viral titer with plaque assay at different time points. MHV68 lacking M11 replicated significantly better in ISG54KO cells with a viral titer more than a log greater (Figure 56).

Next we evaluated the replication of M11 mutant virus in wt MEFs and ISG54 KO MEFs in comparison to wt MHV68 virus. It was possible that in wt MEFs with expression of pro-apoptotic ISG54, M11 mutant virus would produce a lower viral titer compared to wt MHV68 virus. However, in the wild-type MEFs, the M11 mutant virus and wt MHV68 replicated to similar titers (Figure 57). This result is consistent with a previous study demonstrating M11 is not required for MHV68 lytic infection even though it is required for efficient latency establishment in mice (178). On the other hand in the MEFs lacking ISG54 (KO), the M11 mutant virus produced two times lower titer compared to wt MHV68 (Figure 57). This suggested that anti-apoptotic properties of M11 expressed in wt MHV68 could be revealed in the absence of ISG54. Therefore in wt cells, ISG54 nullified the function of M11 and M11 could not counteract action of ISG54. This was unexpected considering that ectopic expression of M11 was found to inhibit ISG54-induced apoptosis (Figure 27). However, during infection ISG54 is expressed with other ISGs, and it's possible that together those proteins effectively neutralize the action of M11.

ISG54 and its influence on MHV68 replication in mice

After we saw anti-viral effect of ISG54 during in vitro experiments, we evaluated how it affects MHV68 replication in living mice. First we studied influence of ISG54 knockout on the acute phase of MHV68 replication during intranasal infection. Acute phase takes place in the lungs and results in the peak of viral titer between days 4 and 9 after infection. We infected mice intranasally with 1000Pfu and 4 and 9 days after infection, animals were sacrificed. Their lungs were isolated and homogenized and the viral titer was determined by plaque assay. We could observe that that the viral titer in the ISG54 knockout animals was slightly elevated (Figure 58). Western blot from lung tissue detected ISG54 protein in the wild type animals but not in knockout mice (Figure 59). Together those data suggested that ISG54 is present during MHV68 infection and plays role in anti-viral defense.

ISG54 influences splenic latency and reactivation of MHV68

Gammaherpesviruses can establish chronic infection and latency in the spleen. We evaluated the effect of ISG54 on establishment of latency by MHV68. Latency is measured about two weeks after infection when viral DNA persists B cells as an episome. In our approach we evaluated both the number of latent genomes and the rate of viral reactivation. Wild-type and knockout mice were infected intranasally with 1000Pfu of MHV68 and 16 days after infection

we sacrificed the animals and collected the spleens. Isolated splenocytes from 5 similarly infected animals were combined and used in two types of assays. In Limited Dilution Assay (LDA) intact splenocytes were seeded on the monolayer of mouse embryo fibroblasts (MEFs) to evaluate virus reactivation. The reactivation was measured by observation of cytopathic effect. Together twelve two-fold dilutions of the intact splenocytes were plated on MEFs. Since reactivating virus causes total lysis of mouse fibroblasts in the well, the cytopathic effect identifies reactivation. By calculating the number of reactivation positive wells for each dilution and fitting non-linear regression curve we could estimate minimal number of splenocytes required to observe reactivation. We found that mice lacking ISG54 showed significantly higher reactivation of MHV68 comparing to wild type (Figure 60). There was about ten times more reactivating virus in ISG54KO suggesting that ISG54 could be involved in suppressing reactivation of MHV68. In a parallel control we evaluated how many viral particles were already preformed in splenocytes before reactivation.Splenocytes were mechanically disrupted and seeded in eight two-fold dilutions on monolayer of MEFs. In this case we observed only very limited cytopathic effect indicating that the amount of pre-formed virus is much lower than the amount formed on the way of reactivation (Figure 60)

To evaluate splenic latency in wild type vs. knockout animals we used Limited Dilutions PCR (LD-PCR). In this technique splenocytes are diluted in a series of five three-fold dilutions. After disrupting cells with proteinase K treatment, double-nested PCR is performed using primers complementary to MHV68 genome. Similarly to reactivation assay, this assay is carried out in 96-well plates with single dilutions being represented by 12-wells. Wells that contain splenocytes bearing MHV68 episome, react positively giving a PCR product that can be detected on the gel. The relationship between percentage of positive reactions and the number of splenocytes used for each dilution can be plotted and illustrated by non-linear regression curve that enables to estimate minimal number of splenocytes required to find a single latent virus. We found that ISG54 knockout animals displayed increased splenic latency resulting in about 10 times more copies of viral DNA in the spleen (Figure 61). We verified expression of ISG54 in splenocytes of infected mice by Western-blotting and found that it was produced in wild-type but not in knockout animals (Figure 62). Together those results pointed that ISG54 is involved in anti-MHV68 response in the murine spleen and is likely involved in the inhibition of latency and reactivation.

Chapter 4. Discussion

IFNs are unique among the cytokines for their ability to confer cellular resistance to viral infections and for their ability to inhibit the growth of cancer cells. In this thesis I am presenting my research on IFN stimulated gene 54 (ISG54) that appears to play a role in both these aspects of IFN response. To date several IFN induced genes have been recognized for their role in viral defense (2,179), but the mechanisms by which IFNs are effective in the treatment of cancer have not been determined. Type I IFN has been reported to induce gene products that can lead to growth arrest or apoptotic signaling in cancer cells, but also to increase growth and proliferation in normal cells (13,180-183). Therefore it is possible that the cell fate during IFN response is determined by the prevalence of a particular group of genes. We propose ISG54 as one of the genes that may contribute to IFN-induced cell death. It is already known that this gene is robustly induced by type I IFNs (73,184), viral infection (185), or DNA damage (186), and that apoptosis can occur coordinately in reaction to each stimulus.

Our study demonstrates that expression of ISG54 promotes cell death via apoptosis in different types of cancer cell lines. Flow cytometry analysis using both PI and annexin V staining indicate that cells expressing ectopic ISG54 die at a significantly higher rate than control cells. The pro-apoptotic effect of ISG54 starts to be apparent at about 48h after transfection. Since caspase activation is central to the execution phase of apoptosis, we evaluated the activation of caspase-3 by immunofluorescence. It was found that caspase-3 is strongly activated in the cells expressing ISG54, especially as apoptosis is morphologically evident. Furthermore the pan-caspase inhibitor ZVAD-FMK significantly reduced ISG54 promoted apoptosis. Next, we studied which of apoptotic pathways is involved in ISG54 induced cell death. Pathways that lead to caspase activation are often designated as either extrinsic or intrinsic (114,187-189). The extrinsic pathway is initiated outside the cell by ligation of transmembrane death receptors and the subsequent activation of caspases. The intrinsic pathway, also called the mitochondrial pathway, is dependent on pro-apoptotic proteins such as Bax or Bak that induce permeability of mitochondrial outer membrane, release of apoptogenic molecules, and activation of caspases. These designations are not completely accurate as the receptor-mediated extrinsic pathway can also trigger the intrinsic pathway. We have found that overexpression of the anti-apoptotic Bcl-xl and Bcl-2 proteins dramatically decreases cell death induced by ISG54 (190). Moreover, viral

anti-apoptotic proteins E1B-19K, v-Bcl2 and M11 that are known to block mitochondrial apoptotic pathway effectively counteract ISG54-induced apoptosis. In addition, cells that lack expression of pro-apoptotic Bax and Bak proteins are resistant to the apoptotic effects of ISG54. Bax and Bak are cytosolic proteins but they translocate into the mitochondrial membrane during apoptosis and this can be observed as a dramatic change in their cellular distribution. By using confocal microscopy imaging we reported that in the presence of ISG54 Bax forms characteristic puncta that indicate its mitochondrial translocation. We also observed that mitochondrial potential of the cells expressing ISG54mGFP decreases with time in comparison to the cells expressing mGFP. These data indicate that ISG54 functions to trigger a mitochondrial pathway of apoptosis. Live cell imaging show that ISG54 does not localize in mitochondria, but it's still possible that it can interact with the outer mitochondrial membrane or the proteins that can enter mitochondria.

Since the p53 tumor suppressor induces transcription of pro-apoptotic Bcl-2 proteins NOXA and PUMA, we evaluated the possible contribution of p53 using a dominant negative mutant (155,167,191-194). ISG54-induced apoptosis was found to continue unabated in the presence of the p53 interfering mutant. Therefore while ISG54 uses similar downstream components of apoptotic pathway as p53, its mechanisms seems to be p53 independent. On the other hand components of Ras signaling pathway are able to at least partially inhibit ISG54-induced apoptosis. H-Ras V12 has the strongest inhibitory effect while the effect of PI3K and Akt kinases is weaker but still significant. IFN has been reported to downregulate PI3/Akt pathway, therefore it is possible that ISG54 may be involved in disrupting signals coming from growth factor receptors (71). However, this effect probably plays only a minor role in ISG54 induced apoptosis.

IFNs are commonly used cytokines in therapy of specific cancers. Their therapeutic effect is often linked to inhibition of cancer growth and induction of apoptosis. Our data suggest that ISG54 may be an important part of the mechanism leading to IFN-stimulated cell death. By using shRNA knockdown we evaluated whether decreased expression of ISG54 makes cells less susceptible to the pro-apoptotic effects of IFN. We found that cells with reduced expression of ISG54 display less apoptosis in response to IFN treatment. These findings indicate that ISG54 may be at least partially responsible for pro-apoptotic actions of IFN.

This is the first description of the pro-apoptotic function of ISG54. Previous studies

linked ISG54 and ISG56 to the inhibition of translation, particularly translation initiated via an IRES. This effect was explained by ability of ISG54 to bind eukaryotic translation initiation factors: eIF3c and eIF3e.(74,75,91,92,195). However, in our system ISG54 did not decrease cap-dependent or IRES-dependent translation. Also overexpression of eIF3e, eIF3c or both this translation factors together had no inhibitory effect on ISG54-induced apoptosis. Therefore although ISG54-induced cell death may be connected to inhibition of protein synthesis, it appears to be triggered by other cellular pathways.

Looking at the biological significance of ISG54-induced apoptosis it's possible that ISG54 levels are coordinated to the progress of anti-viral response. If the pathogen is eliminated, the levels of ISG54 decrease and the cell survives. If, however, infection continues, ISG54 keeps accumulating in the cell leading to its death.

The pathways that lead to ISG54-induced apoptosis remain to be established. There are multiple possible mechanisms that could be considered. The observation that expression of ISG54 causes drop of mitochondrial potential may suggest a direct influence of ISG54 on that organelle. Our imaging experiments did not detect ISG54 inside the mitochondria but it's possible that a fraction of ISG54 associates with outer mitochondrial membrane. With time as the protein accumulates it may disrupt functioning of complexes present in the mitochondrial membrane such as chaperones, or transmembrane transporters. Many chaperones such as Heat Shock Protein (HSP) 90 and HSP70 as well as mitochondrial transporter proteins such as Translocase of Outer Membrane 70 (TOM70) contain TPR domains that can possibly interact with ISG54. It's also possible that with time some fraction of ISG54 enters mitochondria and disrupts their functioning. Therefore it would be interesting to tag ISG54 with mitochondrial targeting sequence and evaluate whether it increases the level of apoptosis. Another approach is to study cellular localization of ISG54mGFP at later timepoints after transfection, for instance at 72h. This may be a challenge since levels of ISG54 drop significantly with time and many cells expressing ISG54 display altered morphology. On the other hand effective visualization of ISG54 in dying cells could tell us a lot about the way by which it induces apoptosis.

Cells expressing ISG54 starting after about 48h suggesting that mechanism of ISG54 induced apoptosis takes time to be executed. Among characterized forms of cell death autophagy is the one that is prolonged in time. Therefore it is possible that ISG54 causes apoptosis by the mechanism of autophagy. Autophagy is often induced during viral infection helping to eliminate

the pathogen so it's possible that ISG54, as a protein induced by viruses, is involved in that process. To study this hypothesis we could evaluate the influence of autophagy inhibitors such as wortmannin or 3-methyladenine (3-MA) on ISG54-induced apoptosis. Those compounds have been reported to effectively block autophagy, so if ISG54 causes this process, inhibitors should decrease ISG54-induced cell death (196). Our preliminary data indicate that 3-MA treatment has partially inhibitory effect on ISG54-induced apoptosis. Another approach is to evaluate whether expression of ISG54 causes formation of puncta by Microtuble-associated protein light chain 3 (LC3), a phenomenon that is considered a hallmark of autophagy (197). Cells could be transfected with RFP-tagged LC3 protein and ISG54mGFP or mGFP as a control and observe formation of red LC3 puncta at different times after transfection. If ISG54 stimulates autophagy, we should see emerging pattern of LC3II puncta in ISG54 expressing cells.

To investigate the means by which ISG54 performs its biological function we explored protein-protein interactions first by yeast two-hybrid assay and then by affinity tag purification and mass spectrometry. This approach identified interactions with two other TPR-containing family members, ISG56 and ISG60, but not with the fourth member of this family, ISG58. The interactions were verified with co-immunoprecipitation methods, and revealed that ISG54 also forms complexes with itself. The protein-protein interface of ISG54 with ISG60 is distinct from that of ISG54 with ISG56 or itself. The first TPR domain of ISG54 is essential for binding to ISG60, but it is not required for binding ISG54 or ISG56. We have also determined that ISG56 can bind to ISG60, and that both ISG54 and ISG60 are able to form homomeric complexes (data not shown).

The numerous possibilities for protein-protein interactions among these three ISGs led us to estimate the mass of the complex. Glycerol gradient sedimentation indicated the presence of ISG54, ISG56, and ISG60 in multimeric complexes of approximately 150-200kDa. Considering the molecular weight of these ISG proteins, they may form trimeric or tetrameric complexes. The exact stoichiometry and composition of the complex remain to be established, and the range of possible protein interactions evokes many theoretical combinations. Interestingly we were unable to detect monomeric fraction of ISG54 suggesting that all the pool of that protein remains bound in multimeric aggregates. Considering the fact that TPR motifs are known to play a role in formation of multiprotein complexes, the concept that these ISGs create a scaffold for docking target proteins is intriguing.

We also studied the influence of ISG54 family members on ISG54-induced cell death. While ISG56 did not affect pro-apoptotic effect of ISG54, ISG60 significantly reduced apoptosis in ISG54-expressing cells. This effect was strictly dependent on the direct interaction between ISG60 and the first TPR domain of ISG54. Interestingly although ISG60 decreased the cytotoxic influence of ISG54 it did not show a negative effect on ISG54 expression. In fact in the presence of ISG60, levels of ISG54 were stabilized and ISG60 seemed to protect ISG54 from degradation. These data suggest that ISG60 may play a modulatory role, stabilizing ISG54 on one hand but on the other hand precisely controlling its apoptotic functions. It's likely that ISG54, ISG60 and other ISGs form an intricate well regulated system that depending on the conditions determines cell survival or apoptosis. Association of ISG54 with ISG60 promotes survival while the binding of proteins that release ISG54 from ISG60 could lead to cell death. Proteins regulating ISG54-ISG60 interaction, however, remain to be identified.

To determine which part of the ISG54 molecule is responsible for its pro-apoptotic effect we created a series of truncations eliminating different TPR motifs from ISG54 protein. Generally we found that the cell death promoted by ISG54 is proportional to the number of TPR motifs present in the molecule. This is not the case for the first TPR domain which was able to induce the same level of apoptosis as a full-length protein. Interestingly, it is the same TPR motif that is bound by ISG60, a potent inhibitor of ISG54-induced cell death. The mechanisms by which structural properties of TPR motif may induce apoptosis remain to be determined. It is possible that TPR domains of ISG54 interact with other proteins containing TPR motifs and disrupt their functioning leading to cell death. It was reported that overexpression of a small glutamine rich TPR containing protein SGT leads to apoptosis (198). Also a short TPR peptide was found to effectively induce death of cancer cells by disrupting the interaction between Hsp90 and Hop (199). Future studies could be designed to test recombinant peptides containing sequence of N-terminal part of ISG54 regarding their ability to kill cancer cells. Such peptides used in an appropriate delivery system could be applied as cancer therapeutics. Moreover, solving three-dimensional structure of N-terminal domain could help in creating small molecular weight compounds that mimic structural features of ISG54 and also induce apoptosis. Such novel compounds could become useful drugs in cancer therapy. Consequently, solving the crystal structure of ISG54 or at least its N-terminal part appears to be worth consideration.

ISG54 was reported to interact with STING (63), an ER bound adapter protein and to

participate in downregulation of IFN signaling (96). By immunoprecipitation we positively verified interaction between ISG54 and STING, however we did not observe any effect of STING on the ISG54 induced apoptosis. It is possible that interaction of ISG54 and STING has a function independent of apoptosis.

We also verified interactions of ISG54 with other proteins that were first identified in a yeast two-hybrid screen. We found that ISG54 is able to bind dynein light chain 1 (DLC1), eukaryotic elongation factor-1α (eEF-1α) and peroxiredoxin 5 (PRDX5). Biological significance of those interactions remains to be determined. Since each of these binding targets is somehow involved in cell survival and regulation of apoptosis elucidating the mechanism of their interactions can shed new light on ISG54-induced cell death.

In the future in depth details of interactions between ISG54 and its novel binding partners need to be pursued. Truncated versions of ISG54 can be used to determine which fragments of the ISG54 molecule are responsible for the interactions with its partners. We should also evaluate how expression of ISG54 changes cellular localization of those proteins. For instance, PRDX5 is mitochondrial protein while STING associates with ER membranes. Would the expression of ISG54 which is a cytoplasmic protein change this localization? A particularly interesting binding partner is DLC1 that is known to bind pro-apoptotic protein Bim and sequester it within cytoskeleton (176). Release of Bim from DLC1 leads to the permeabilization of mitochondria and induction of apoptosis. It's possible that ISG54 by its interaction with DLC1 stimulates release of Bim and causes cell death. Therefore cellular localization of Bim in the presence and absence of ISG54 using immunofluorescence and live-cell imaging needs to be evaluated. Also direct interaction between ISG54 and Bim should be examined by immunoprecipitation.

Future studies can focus more on the other potential binding targets that were identified in yeast two-hybrid screen. Such partners among many include Interferon-induced transmembrane protein 1 (IFITM1), Superoxide Dismutase 2 (SOD2) or Apoptosis-Linked Gene 2 (ALG2) protein. They are involved in anti-viral response, antioxidative protection and regulation of apoptosis. Each of these candidates might be an important binding partner responsible for biological functions of ISG54.

In our studies we also evaluated the role of ISG54 in anti-viral defense. By using ISG54 knockout mice and mouse gammaherpesvirus 68 (MHV68) as a model pathogen we explored the

role of ISG54 in regulation of viral replication, latency and reactivation. *In vitro* experiments with isolated mouse embryo fibroblasts showed that cells lacking ISG54 produced significantly higher amounts of virus comparing to the wild-type. The difference started to be apparent as early as 12-24hs after infection and persisted throughout course of infection. Microscopic studies of cells infected with YFP-expressing MHV68 showed that viral infection spreaded faster in ISG54 deficient cells. Interestingly, lack of ISG54 was more visible in the cells infected with lower multiplicities of infection (MOIs). While infection at MOI 1 yielded over five times higher viral titer in the cells lacking ISG54, infection at MOI 0.01 produced over tenfold difference. The shape of growth curves indicated that ISG54 delayed initiation of infection while at later timepoints rates of viral replication were similar between wild-type and KO cells. In MEFs that were pretreated with IFN overnight prior to infection we could not detect significant differences in viral titer between wild-type and ISG54KO cells. Therefore it is possible that ISG54 plays the most important role at the early stages of the infection when the amount of virus is low, the IFN response is just beginning and the cells have not triggered all the anti-viral mechanisms. For instance, ISG54 may be present before other proteins such as 2'-5' oligoadenylate synthase or PKR become activated and therefore it works as a first line of cellular anti-viral defense. Also, ISG54 may be induced by lower amounts of pathogens in comparison to 2'-5' OAS or PKR. Consequently during infection with high MOIs, observed effects of ISG54 knockout are less severe, since high dose of suddenly administered MHV68 quickly turns on the variety of antiviral genes. When the cells are stimulated with interferon, over 300 genes become strongly upregulated and the other induced ISGs such as ISG56 compensate the effect of ISG54 knockout.

In our experiments with cancer cell lines ISG54 displayed strong pro-apoptotic properties. Therefore it was possible that its antiviral effect may be a consequence of the induction of apoptosis in MHV68 infected cells. MHV68 genome codes for M11 protein that mimics Bcl2 protein and can inhibit ISG54-induced apoptosis. To evaluate whether M11 has effect on ISG54 we studied replication of M11 deficient virus in wild type vs. ISG54KO cells. Similarly to what was previously observed for wild-type virus, replication was significantly higher in ISG54 deficient MEFs. However, in the absence of ISG54 wild-type virus produced twofold higher titer comparing to M11 mutant. Therefore M11 still supported viral replication even in the absence of ISG54. This could be explained by the inhibitory effect of M11 on the

other pro-apoptotic mechanisms triggered during infection and independent of ISG54. In the presence of ISG54 the difference between wild-type virus and M11 mutant virus was insignificant suggesting that ISG54 could somehow nullify the effect of M11. Therefore induction of cell death seems to be involved in anti-viral functions of ISG54, although it probably plays only a minor role in the inhibition of viral replication. It should be noted that MHV68 codes for another anti-apoptotic protein vMAP that likely can compensate for the functions of M11 (149). In order to better understand the pro-apoptotic role of ISG54 during MHV68 infection it would be recommended to use viral mutant that lacks both M11 and vMAP.

In addition to *in vitro* experiments we also studied the role of ISG54 *in vivo* by direct infection of ISG54 knockout mice. We found that ISG54 deficient animals show slightly elevated viral titer in the lungs during acute phase of infection but that difference was not statistically significant. On the other hand we could observe a significant increase in both splenic latency and reactivation in ISG54 knockout animals. Limited dilution PCR (LD-PCR) showed about tenfold higher number of latent viral genomes in ISG54 deficient spleens. Also the number of reactivating viral particles detected in LDA assay was tenfold higher in ISG54 knockout mice. However, not all of our experiments showed such significant differences. Although we are trying to use age and sex matched animals it is possible that scale of latency and reactivation depends also on the other factors such as conditions the animals were kept under, accidental contact with other pathogens or amount of stress they experienced. As we are not able to fully control all these issues, more experiments should be performed to study more in depth role of ISG54 in latency and reactivation. Since the exact molecular details of splenic latency and reactivation remain unknown, it is difficult to propose a convincing mechanism of ISG54 action. Our data suggest that ISG54 has an inhibitory effect on MHV68 reactivation and latency. Both those phenomena are sporadic events that are performed by single viral particles. Since ISG54 seems to be particularly important in response to low levels of virus it is possible that ISG54 knockout cells are more prone to such single events and display more latency and reactivation.

Further experiments should be performed to fully characterize the role of ISG54 in antiviral defense. One possibility is to characterize how ISG54 influences viral latency and reactivation depending on the dose of virus. It is possible that we would observe a more significant difference for the low infection doses as observed in MEFs. Another approach is to study how ISG54KO affects different types of splenic cells in response to viral infection. Using

specific fluorescent-tagged antibodies we could label different subsets of splenocytes such as B or T cells and by flow cytometry compare their profile in wild-type vs. knockout animals. By using YFP-expressing MHV68 we can also visualize infected cells and compare their numbers and profiles. It's possible that elimination of ISG54 makes some of splenocytes more prone to infection. Another challenge would be to characterize the effect of ISG54 knockout in the mice that were pretreated with IFN prior to infection. In the cell culture IFN pretreatment nullifies the effect of ISG54 knockout but it does not have to be the same in the animal system. Different organs may respond differently to IFN stimulation. Moreover, in the spleen where MHV68 establishes chronic infection, low levels of IFN are constitutively present even in the absence of pathogens (200).

Elucidation of the molecular mechanisms that allow ISG54 to participate in anti-viral defense is another future challenge. Our data show that ISG54-induced apoptosis probably plays only a minor role in blocking viral replication. Therefore anti-viral activity of ISG54 is likely linked to another mechanism. Previously ISG54 was reported to interact with STING and this interaction was also confirmed in our experiments. Since STING is a part of multiprotein complex involved in activation of IRF3 and ISG54 itself forms complex with ISG56 and ISG60, it is possible that both these protein complexes interact with each other. Together they could be responsible for effective induction of IFN response during viral infection. Therefore it is worth to evaluate interactions of ISG54,56 and 60 with other members of STING complex such as TBK1 or MAVS. Another approach would be to measure induction of IFN genes in Wild-type vs. ISG54KO MEFs using RT-PCR. Since signaling through STING leads to production of IFN, ISG54KO MEFs should display impaired expression of IFN genes.

ISG54 is robustly induced following virus infection or IFN treatment, so it's possible that its effects are not limited to influence on STING signaling and causing apoptosis. Interaction with other binding partners can also contribute to anti-viral activity. For instance, binding to eEF-1α and DLC1 that are involved in functioning of cytoskeleton may disrupt transport of viral particles or assembly of viral capsids. Binding to PRDX5 may result in increased levels of reactive oxygen species that play important role in immune defense and possible interaction with IFITM1 can activate other signaling pathways. All these interactions are worth studying and may broaden our knowledge about functions of ISG54 in fighting off viral infections.

Together our data show that ISG54 is an important element in the interferon response. By

promoting apoptosis it plays a substantial role in the cytotoxic effect of IFN and contributes to anti-viral defense. The sacrifice of a transformed or infected cell can ensure survival of the host, evident by the fact that many cancers and viruses have evolved mechanisms to block the cellular apoptotic defense (113,125,126,201). Moreover, ISG54 has a significant effect on viral latency and reactivation, phenomena that are intricate parts of chronic infection by herpesviruses. It forms an oligomeric complex with other members of ISG54 family and binds the proteins that are crucial in defense against intracellular pathogens and oxidative stress. In the future more studies in our lab would be performed to fully explore all the functions of ISG54. Deciphering the mechanism by which it promotes apoptosis can improve existing IFN-based cancer therapies as well as define new therapeutic targets. Elucidating its effect on reactivation and latency can open new possibilities in therapy of diseases caused by herpesviruses.

Chapter 5. References

1. Schultz, U., Kaspers, B., and Staeheli, P. (2004) *Developmental and comparative immunology* **28**, 499-508
2. Sadler, A. J., and Williams, B. R. (2008) *Nature reviews. Immunology* **8**, 559-568
3. Ghoreschi, K., Laurence, A., and O'Shea, J. J. (2009) *Immunological reviews* **228**, 273-287
4. Platanias, L. C. (2005) *Nature reviews. Immunology* **5**, 375-386
5. Borden, E. C., Sen, G. C., Uze, G., Silverman, R. H., Ransohoff, R. M., Foster, G. R., and Stark, G. R. (2007) *Nature reviews. Drug discovery* **6**, 975-990
6. de Weerd, N. A., Samarajiwa, S. A., and Hertzog, P. J. (2007) *The Journal of biological chemistry* **282**, 20053-20057
7. Jaks, E., Gavutis, M., Uze, G., Martal, J., and Piehler, J. (2007) *Journal of molecular biology* **366**, 525-539
8. Yamaoka, K., Saharinen, P., Pesu, M., Holt, V. E., 3rd, Silvennoinen, O., and O'Shea, J. J. (2004) *Genome biology* **5**, 253
9. Reich, N. C., and Liu, L. (2006) *Nature reviews. Immunology* **6**, 602-612
10. Decker, T., Muller, M., and Stockinger, S. (2005) *Nature reviews. Immunology* **5**, 675-687
11. Kisseleva, T., Bhattacharya, S., Braunstein, J., and Schindler, C. W. (2002) *Gene* **285**, 1-24
12. Banninger, G., and Reich, N. C. (2004) *The Journal of biological chemistry* **279**, 39199-39206
13. de Veer, M. J., Holko, M., Frevel, M., Walker, E., Der, S., Paranjape, J. M., Silverman, R. H., and Williams, B. R. (2001) *Journal of leukocyte biology* **69**, 912-920
14. Ning, S., Pagano, J. S., and Barber, G. N. (2011) *Genes and immunity* **12**, 399-414
15. Marie, I., Durbin, J. E., and Levy, D. E. (1998) *The EMBO journal* **17**, 6660-6669
16. Hiscott, J. (2007) *Cytokine & growth factor reviews* **18**, 483-490
17. Hanna, R. A., Quinsay, M. N., Orogo, A. M., Giang, K., Rikka, S., and Gustafsson, A. B. (2012) *The Journal of biological chemistry* **287**, 19094-19104
18. Hacker, H., and Karin, M. (2006) *Science's STKE : signal transduction knowledge environment* **2006**, re13
19. Fitzgerald, K. A., McWhirter, S. M., Faia, K. L., Rowe, D. C., Latz, E., Golenbock, D. T., Coyle, A. J., Liao, S. M., and Maniatis, T. (2003) *Nature immunology* **4**, 491-496
20. Belgnaoui, S. M., Paz, S., and Hiscott, J. (2011) *Current opinion in immunology* **23**, 564-572
21. Randall, R. E., and Goodbourn, S. (2008) *The Journal of general virology* **89**, 1-47
22. Carroll, J. F., Fulda, K. G., Chiapa, A. L., Rodriquez, M., Phelps, D. R., Cardarelli, K. M., Vishwanatha, J. K., and Cardarelli, R. (2009) *Obesity (Silver Spring)* **17**, 1420-1427
23. Kumar, H., Kawai, T., and Akira, S. (2011) *International reviews of immunology* **30**, 16-34
24. Uematsu, S., and Akira, S. (2007) *The Journal of biological chemistry* **282**, 15319-15323
25. Boyce, M., Bryant, K. F., Jousse, C., Long, K., Harding, H. P., Scheuner, D., Kaufman, R. J., Ma, D., Coen, D. M., Ron, D., and Yuan, J. (2005) *Science* **307**, 935-939

26. Sarkar, S. N., Peters, K. L., Elco, C. P., Sakamoto, S., Pal, S., and Sen, G. C. (2004) *Nature structural & molecular biology* **11**, 1060-1067
27. Loo, Y. M., and Gale, M., Jr. (2011) *Immunity* **34**, 680-692
28. Ishikawa, H., and Barber, G. N. (2011) *Cellular and molecular life sciences : CMLS* **68**, 1157-1165
29. Nakhaei, P., Hiscott, J., and Lin, R. (2010) *Journal of molecular cell biology* **2**, 110-112
30. Zhong, B., Yang, Y., Li, S., Wang, Y. Y., Li, Y., Diao, F., Lei, C., He, X., Zhang, L., Tien, P., and Shu, H. B. (2008) *Immunity* **29**, 538-550
31. Ishikawa, H., Ma, Z., and Barber, G. N. (2009) *Nature* **461**, 788-792
32. Watanabe, T., Asano, N., Kitani, A., Fuss, I. J., Chiba, T., and Strober, W. (2011) *Gut microbes* **2**, 61-65
33. Murray, P. J. (2009) *Nature immunology* **10**, 1053-1054
34. Sabbah, A., Chang, T. H., Harnack, R., Frohlich, V., Tominaga, K., Dube, P. H., Xiang, Y., and Bose, S. (2009) *Nature immunology* **10**, 1073-1080
35. Strober, W., Murray, P. J., Kitani, A., and Watanabe, T. (2006) *Nature reviews. Immunology* **6**, 9-20
36. Deonarain, R., Alcami, A., Alexiou, M., Dallman, M. J., Gewert, D. R., and Porter, A. C. (2000) *Journal of virology* **74**, 3404-3409
37. Ida-Hosonuma, M., Iwasaki, T., Yoshikawa, T., Nagata, N., Sato, Y., Sata, T., Yoneyama, M., Fujita, T., Taya, C., Yonekawa, H., and Koike, S. (2005) *Journal of virology* **79**, 4460-4469
38. Muller, U., Steinhoff, U., Reis, L. F., Hemmi, S., Pavlovic, J., Zinkernagel, R. M., and Aguet, M. (1994) *Science* **264**, 1918-1921
39. Chakrabarti, A., Jha, B. K., and Silverman, R. H. (2011) *Journal of interferon & cytokine research : the official journal of the International Society for Interferon and Cytokine Research* **31**, 49-57
40. Rebouillat, D., and Hovanessian, A. G. (1999) *Journal of interferon & cytokine research : the official journal of the International Society for Interferon and Cytokine Research* **19**, 295-308
41. Li, X. L., Blackford, J. A., and Hassel, B. A. (1998) *Journal of virology* **72**, 2752-2759
42. Silverman, R. H. (2007) *Journal of virology* **81**, 12720-12729
43. Jayan, G. C., and Casey, J. L. (2002) *Journal of virology* **76**, 3819-3827
44. Zahn, R. C., Schelp, I., Utermohlen, O., and von Laer, D. (2007) *Journal of virology* **81**, 457-464
45. Taylor, D. R., Puig, M., Darnell, M. E., Mihalik, K., and Feinstone, S. M. (2005) *Journal of virology* **79**, 6291-6298
46. Gelinas, J. F., Clerzius, G., Shaw, E., and Gatignol, A. (2011) *Journal of virology* **85**, 8460-8466
47. Spadaro, F., Lapenta, C., Donati, S., Abalsamo, L., Barnaba, V., Belardelli, F., Santini, S. M., and Ferrantini, M. (2011) *Blood*
48. Sadler, A. J., and Williams, B. R. (2007) *Current topics in microbiology and immunology* **316**, 253-292
49. Haller, O., and Kochs, G. (2002) *Traffic* **3**, 710-717
50. Zhou, A., Paranjape, J. M., Der, S. D., Williams, B. R., and Silverman, R. H. (1999) *Virology* **258**, 435-440

51. Belardelli, F., Ferrantini, M., Proietti, E., and Kirkwood, J. M. (2002) *Cytokine & growth factor reviews* **13**, 119-134
52. Pace, L., Vitale, S., Dettori, B., Palombi, C., La Sorsa, V., Belardelli, F., Proietti, E., and Doria, G. (2010) *J Immunol* **184**, 5969-5979
53. Le Bon, A., Schiavoni, G., D'Agostino, G., Gresser, I., Belardelli, F., and Tough, D. F. (2001) *Immunity* **14**, 461-470
54. Yang, J., Pu, Y. G., Zeng, Z. M., Yu, Z. J., Huang, N., and Deng, Q. W. (2009) *BMC infectious diseases* **9**, 156
55. ElHefnawi, M. M., Zada, S., and El-Azab, I. A. (2010) *Virology journal* **7**, 130
56. Asselah, T., Lada, O., Moucari, R., Martinot, M., Boyer, N., and Marcellin, P. (2007) *Clinics in liver disease* **11**, 839-849, viii
57. Bracci, L., La Sorsa, V., Belardelli, F., and Proietti, E. (2008) *Expert review of vaccines* **7**, 373-381
58. Samuel, C. E. (2001) *Clinical microbiology reviews* **14**, 778-809, table of contents
59. Ferrantini, M., Capone, I., and Belardelli, F. (2007) *Biochimie* **89**, 884-893
60. Sangfelt, O., Erickson, S., Castro, J., Heiden, T., Gustafsson, A., Einhorn, S., and Grander, D. (1999) *Oncogene* **18**, 2798-2810
61. Tiefenbrun, N., Melamed, D., Levy, N., Resnitzky, D., Hoffman, I., Reed, S. I., and Kimchi, A. (1996) *Molecular and cellular biology* **16**, 3934-3944
62. Chawla-Sarkar, M., Lindner, D. J., Liu, Y. F., Williams, B. R., Sen, G. C., Silverman, R. H., and Borden, E. C. (2003) *Apoptosis : an international journal on programmed cell death* **8**, 237-249
63. Hosono, T., Tanaka, T., Tanji, K., Nakatani, T., and Kamitani, T. (2010) *British journal of cancer* **102**, 873-882
64. Thyrell, L., Erickson, S., Zhivotovsky, B., Pokrovskaja, K., Sangfelt, O., Castro, J., Einhorn, S., and Grander, D. (2002) *Oncogene* **21**, 1251-1262
65. Leaman, D. W., Chawla-Sarkar, M., Vyas, K., Reheman, M., Tamai, K., Toji, S., and Borden, E. C. (2002) *The Journal of biological chemistry* **277**, 28504-28511
66. Chawla-Sarkar, M., Leaman, D. W., and Borden, E. C. (2001) *Clinical cancer research : an official journal of the American Association for Cancer Research* **7**, 1821-1831
67. Selleri, C., Sato, T., Del Vecchio, L., Luciano, L., Barrett, A. J., Rotoli, B., Young, N. S., and Maciejewski, J. P. (1997) *Blood* **89**, 957-964
68. Takaoka, A., Hayakawa, S., Yanai, H., Stoiber, D., Negishi, H., Kikuchi, H., Sasaki, S., Imai, K., Shibue, T., Honda, K., and Taniguchi, T. (2003) *Nature* **424**, 516-523
69. Sangfelt, O., Erickson, S., Castro, J., Heiden, T., Einhorn, S., and Grander, D. (1997) *Cell growth & differentiation : the molecular biology journal of the American Association for Cancer Research* **8**, 343-352
70. Thyrell, L., Hjortsberg, L., Arulampalam, V., Panaretakis, T., Uhles, S., Dagnell, M., Zhivotovsky, B., Leibiger, I., Grander, D., and Pokrovskaja, K. (2004) *The Journal of biological chemistry* **279**, 24152-24162
71. Dedoni, S., Olianas, M. C., and Onali, P. (2010) *Journal of neurochemistry* **115**, 1421-1433
72. Bluyssen, H. A., Vlietstra, R. J., Faber, P. W., Smit, E. M., Hagemeijer, A., and Trapman, J. (1994) *Genomics* **24**, 137-148

73. Levy, D., Larner, A., Chaudhuri, A., Babiss, L. E., and Darnell, J. E., Jr. (1986) *Proceedings of the National Academy of Sciences of the United States of America* **83**, 8929-8933
74. Terenzi, F., Hui, D. J., Merrick, W. C., and Sen, G. C. (2006) *The Journal of biological chemistry* **281**, 34064-34071
75. Terenzi, F., Pal, S., and Sen, G. C. (2005) *Virology* **340**, 116-124
76. Scheufler, C., Brinker, A., Bourenkov, G., Pegoraro, S., Moroder, L., Bartunik, H., Hartl, F. U., and Moarefi, I. (2000) *Cell* **101**, 199-210
77. Allan, R. K., and Ratajczak, T. (2011) *Cell stress & chaperones* **16**, 353-367
78. Cortajarena, A. L., and Regan, L. (2006) *Protein science : a publication of the Protein Society* **15**, 1193-1198
79. Chan, N. C., Likic, V. A., Waller, R. F., Mulhern, T. D., and Lithgow, T. (2006) *Journal of molecular biology* **358**, 1010-1022
80. Karpenahalli, M. R., Lupas, A. N., and Soding, J. (2007) *BMC bioinformatics* **8**, 2
81. Bandyopadhyay, S. K., Leonard, G. T., Jr., Bandyopadhyay, T., Stark, G. R., and Sen, G. C. (1995) *The Journal of biological chemistry* **270**, 19624-19629
82. Hiscott, J., Pitha, P., Genin, P., Nguyen, H., Heylbroeck, C., Mamane, Y., Algarte, M., and Lin, R. (1999) *Journal of interferon & cytokine research : the official journal of the International Society for Interferon and Cytokine Research* **19**, 1-13
83. Levy, D. E., Kessler, D. S., Pine, R., Reich, N., and Darnell, J. E., Jr. (1988) *Genes & development* **2**, 383-393
84. Daly, C., and Reich, N. C. (1995) *The Journal of biological chemistry* **270**, 23739-23746
85. Weaver, B. K., Kumar, K. P., and Reich, N. C. (1998) *Molecular and cellular biology* **18**, 1359-1368
86. Terenzi, F., White, C., Pal, S., Williams, B. R., and Sen, G. C. (2007) *Journal of virology* **81**, 8656-8665
87. Fensterl, V., White, C. L., Yamashita, M., and Sen, G. C. (2008) *Journal of virology* **82**, 11045-11053
88. Wacher, C., Muller, M., Hofer, M. J., Getts, D. R., Zabaras, R., Ousman, S. S., Terenzi, F., Sen, G. C., King, N. J., and Campbell, I. L. (2007) *Journal of virology* **81**, 860-871
89. Perwitasari, O., Cho, H., Diamond, M. S., and Gale, M., Jr. (2011) *The Journal of biological chemistry* **286**, 44412-44423
90. Stawowczyk, M., Van Scoy, S., Kumar, K. P., and Reich, N. C. (2011) *The Journal of biological chemistry* **286**, 7257-7266
91. Hui, D. J., Bhasker, C. R., Merrick, W. C., and Sen, G. C. (2003) *The Journal of biological chemistry* **278**, 39477-39482
92. Wang, C., Pflugheber, J., Sumpter, R., Jr., Sodora, D. L., Hui, D., Sen, G. C., and Gale, M., Jr. (2003) *J Virol* **77**, 3898-3912
93. Daffis, S., Szretter, K. J., Schriewer, J., Li, J., Youn, S., Errett, J., Lin, T. Y., Schneller, S., Zust, R., Dong, H., Thiel, V., Sen, G. C., Fensterl, V., Klimstra, W. B., Pierson, T. C., Buller, R. M., Gale, M., Jr., Shi, P. Y., and Diamond, M. S. (2010) *Nature* **468**, 452-456
94. Pichlmair, A., Lassnig, C., Eberle, C. A., Gorna, M. W., Baumann, C. L., Burkard, T. R., Burckstummer, T., Stefanovic, A., Krieger, S., Bennett, K. L., Rulicke, T., Weber, F., Colinge, J., Muller, M., and Superti-Furga, G. (2011) *Nature immunology* **12**, 624-630
95. Berchtold, S., Manncke, B., Klenk, J., Geisel, J., Autenrieth, I. B., and Bohn, E. (2008) *BMC immunology* **9**, 75

96. Li, Y., Li, C., Xue, P., Zhong, B., Mao, A. P., Ran, Y., Chen, H., Wang, Y. Y., Yang, F., and Shu, H. B. (2009) *Proceedings of the National Academy of Sciences of the United States of America* **106**, 7945-7950
97. Liu, X. Y., Chen, W., Wei, B., Shan, Y. F., and Wang, C. (2011) *J Immunol* **187**, 2559-2568
98. Schmeisser, H., Mejido, J., Balinsky, C. A., Morrow, A. N., Clark, C. R., Zhao, T., and Zoon, K. C. (2010) *Journal of virology* **84**, 10671-10680
99. Saikia, P., Fensterl, V., and Sen, G. C. (2010) *Journal of virology* **84**, 13036-13039
100. Fensterl, V., Wetzel, J. L., Ramachandran, S., Ogino, T., Stohlman, S. A., Bergmann, C. C., Diamond, M. S., Virgin, H. W., and Sen, G. C. (2012) *PLoS pathogens* **8**, e1002712
101. Saha, S., Sugumar, P., Bhandari, P., and Rangarajan, P. N. (2006) *The Journal of general virology* **87**, 3285-3289
102. Lai, K. C., Chang, K. W., Liu, C. J., Kao, S. Y., and Lee, T. C. (2008) *Molecular cancer research : MCR* **6**, 1431-1439
103. Li, Y., Batra, S., Sassano, A., Majchrzak, B., Levy, D. E., Gaestel, M., Fish, E. N., Davis, R. J., and Platanias, L. C. (2005) *The Journal of biological chemistry* **280**, 10001-10010
104. Niikura, T., Hirata, R., and Weil, S. C. (1997) *Blood cells, molecules & diseases* **23**, 337-349
105. Yu, M., Tong, J. H., Mao, M., Kan, L. X., Liu, M. M., Sun, Y. W., Fu, G., Jing, Y. K., Yu, L., Lepaslier, D., Lanotte, M., Wang, Z. Y., Chen, Z., Waxman, S., Wang, Y. X., Tan, J. Z., and Chen, S. J. (1997) *Proceedings of the National Academy of Sciences of the United States of America* **94**, 7406-7411
106. Xiao, S., Li, D., Zhu, H. Q., Song, M. G., Pan, X. R., Jia, P. M., Peng, L. L., Dou, A. X., Chen, G. Q., Chen, S. J., Chen, Z., and Tong, J. H. (2006) *Proc Natl Acad Sci U S A* **103**, 16448-16453
107. Wei, N., Serino, G., and Deng, X. W. (2008) *Trends Biochem Sci* **33**, 592-600
108. Chen, C. H., Su, C. Y., Chien, C. Y., Huang, C. C., Chuang, H. C., Fang, F. M., Huang, H. Y., Chen, C. M., and Chiou, S. J. (2008) *British journal of cancer* **99**, 1453-1461
109. Krysko, D. V., Vanden Berghe, T., D'Herde, K., and Vandenabeele, P. (2008) *Methods* **44**, 205-221
110. Leist, M., Single, B., Castoldi, A. F., Kuhnle, S., and Nicotera, P. (1997) *The Journal of experimental medicine* **185**, 1481-1486
111. Denecker, G., Vercammen, D., Declercq, W., and Vandenabeele, P. (2001) *Cellular and molecular life sciences : CMLS* **58**, 356-370
112. Peng, Y., Martin, D. A., Kenkel, J., Zhang, K., Ogden, C. A., and Elkon, K. B. (2007) *J Autoimmun* **29**, 303-309
113. Pietsch, E. C., Sykes, S. M., McMahon, S. B., and Murphy, M. E. (2008) *Oncogene* **27**, 6507-6521
114. Adams, J. M., and Cory, S. (2007) *Oncogene* **26**, 1324-1337
115. Ow, Y. P., Green, D. R., Hao, Z., and Mak, T. W. (2008) *Nat Rev Mol Cell Biol* **9**, 532-542
116. Riedl, S. J., and Salvesen, G. S. (2007) *Nat Rev Mol Cell Biol* **8**, 405-413
117. Riedl, S. J., and Shi, Y. (2004) *Nat Rev Mol Cell Biol* **5**, 897-907
118. Martinez-Ruiz, G., Maldonado, V., Ceballos-Cancino, G., Grajeda, J. P., and Melendez-Zajgla, J. (2008) *J Exp Clin Cancer Res* **27**, 48
119. Ashkenazi, A., and Herbst, R. S. (2008) *J Clin Invest* **118**, 1979-1990

120. Martinvalet, D., Thiery, J., and Chowdhury, D. (2008) *Methods in enzymology* **442**, 213-230
121. Martinvalet, D., Dykxhoorn, D. M., Ferrini, R., and Lieberman, J. (2008) *Cell* **133**, 681-692
122. Taddei, M. L., Giannoni, E., Fiaschi, T., and Chiarugi, P. (2012) *The Journal of pathology* **226**, 380-393
123. Frisch, S. M., and Screaton, R. A. (2001) *Current opinion in cell biology* **13**, 555-562
124. Elmore, S. (2007) *Toxicologic pathology* **35**, 495-516
125. Fulda, S. (2009) *International journal of cancer. Journal international du cancer* **124**, 511-515
126. Best, S. M. (2008) *Annu Rev Microbiol* **62**, 171-192
127. Talis, A. L., Huibregtse, J. M., and Howley, P. M. (1998) *The Journal of biological chemistry* **273**, 6439-6445
128. Han, J., Sabbatini, P., Perez, D., Rao, L., Modha, D., and White, E. (1996) *Genes & development* **10**, 461-477
129. Hitomi, J., Christofferson, D. E., Ng, A., Yao, J., Degterev, A., Xavier, R. J., and Yuan, J. (2008) *Cell* **135**, 1311-1323
130. Trump, B. F., Berezesky, I. K., Chang, S. H., and Phelps, P. C. (1997) *Toxicologic pathology* **25**, 82-88
131. Majno, G., and Joris, I. (1995) *The American journal of pathology* **146**, 3-15
132. Bergsbaken, T., Fink, S. L., and Cookson, B. T. (2009) *Nature reviews. Microbiology* **7**, 99-109
133. Overholtzer, M., and Brugge, J. S. (2008) *Nature reviews. Molecular cell biology* **9**, 796-809
134. Overholtzer, M., Mailleux, A. A., Mouneimne, G., Normand, G., Schnitt, S. J., King, R. W., Cibas, E. S., and Brugge, J. S. (2007) *Cell* **131**, 966-979
135. Klionsky, D. J., Cuervo, A. M., and Seglen, P. O. (2007) *Autophagy* **3**, 181-206
136. Mizushima, N., and Komatsu, M. (2011) *Cell* **147**, 728-741
137. Levine, B., and Kroemer, G. (2008) *Cell* **132**, 27-42
138. Saeki, K., Yuo, A., Okuma, E., Yazaki, Y., Susin, S. A., Kroemer, G., and Takaku, F. (2000) *Cell death and differentiation* **7**, 1263-1269
139. Kundu, M., and Thompson, C. B. (2008) *Annual review of pathology* **3**, 427-455
140. Maiuri, M. C., Zalckvar, E., Kimchi, A., and Kroemer, G. (2007) *Nature reviews. Molecular cell biology* **8**, 741-752
141. Virgin, H. W. t., Latreille, P., Wamsley, P., Hallsworth, K., Weck, K. E., Dal Canto, A. J., and Speck, S. H. (1997) *Journal of virology* **71**, 5894-5904
142. Barton, E., Mandal, P., and Speck, S. H. (2011) *Annual review of immunology* **29**, 351-397
143. Nash, A. A., Dutia, B. M., Stewart, J. P., and Davison, A. J. (2001) *Philosophical transactions of the Royal Society of London. Series B, Biological sciences* **356**, 569-579
144. Sunil-Chandra, N. P., Efstathiou, S., Arno, J., and Nash, A. A. (1992) *The Journal of general virology* **73 (Pt 9)**, 2347-2356
145. Usherwood, E. J., Stewart, J. P., Robertson, K., Allen, D. J., and Nash, A. A. (1996) *The Journal of general virology* **77 (Pt 11)**, 2819-2825
146. Sunil-Chandra, N. P., Efstathiou, S., and Nash, A. A. (1992) *The Journal of general virology* **73 (Pt 12)**, 3275-3279

147. Gargano, L. M., Forrest, J. C., and Speck, S. H. (2009) *Journal of virology* **83**, 1474-1482
148. van Dyk, L. F., Hess, J. L., Katz, J. D., Jacoby, M., Speck, S. H., and Virgin, H. I. (1999) *Journal of virology* **73**, 5110-5122
149. Feng, P., Liang, C., Shin, Y. C., Xiaofei, E., Zhang, W., Gravel, R., Wu, T. T., Sun, R., Usherwood, E., and Jung, J. U. (2007) *PLoS pathogens* **3**, e174
150. Barton, E. S., Lutzke, M. L., Rochford, R., and Virgin, H. W. t. (2005) *Journal of virology* **79**, 14149-14160
151. Degenhardt, K., Sundararajan, R., Lindsten, T., Thompson, C., and White, E. (2002) *The Journal of biological chemistry* **277**, 14127-14134
152. Shaner, N. C., Steinbach, P. A., and Tsien, R. Y. (2005) *Nat Methods* **2**, 905-909
153. Ausserlechner, M. J., Obexer, P., Deutschmann, A., Geiger, K., and Kofler, R. (2006) *Mol Cancer Ther* **5**, 1927-1934
154. Mawji, I. A., and Marsden, P. A. (2006) *Exp Biol Med (Maywood)* **231**, 704-708
155. Stommel, J. M., Marchenko, N. D., Jimenez, G. S., Moll, U. M., Hope, T. J., and Wahl, G. M. (1999) *The EMBO journal* **18**, 1660-1672
156. Vales, L. D., and Darnell, J. E., Jr. (1989) *Genes Dev* **3**, 49-59
157. Kumar, K. P., McBride, K. M., Weaver, B. K., Dingwall, C., and Reich, N. C. (2000) *Mol Cell Biol* **20**, 4159-4168
158. Ward, Y. D., Thomson, D. S., Frye, L. L., Cywin, C. L., Morwick, T., Emmanuel, M. J., Zindell, R., McNeil, D., Bekkali, Y., Girardot, M., Hrapchak, M., DeTuri, M., Crane, K., White, D., Pav, S., Wang, Y., Hao, M. H., Grygon, C. A., Labadia, M. E., Freeman, D. M., Davidson, W., Hopkins, J. L., Brown, M. L., and Spero, D. M. (2002) *Journal of medicinal chemistry* **45**, 5471-5482
159. Kotanides, H., Moczygemba, M., White, M. F., and Reich, N. C. (1995) *J Biol Chem* **270**, 19481-19486
160. Weck, K. E., Kim, S. S., Virgin, H. I., and Speck, S. H. (1999) *Journal of virology* **73**, 4651-4661
161. Krug, L. T., Collins, C. M., Gargano, L. M., and Speck, S. H. (2009) *Journal of virology* **83**, 4732-4748
162. Walter, P., and Ron, D. (2011) *Science* **334**, 1081-1086
163. Zhou, F., Yang, Y., and Xing, D. (2011) *The FEBS journal* **278**, 403-413
164. Cuconati, A., and White, E. (2002) *Genes & development* **16**, 2465-2478
165. Kroemer, G., Galluzzi, L., and Brenner, C. (2007) *Physiological reviews* **87**, 99-163
166. Wolter, K. G., Hsu, Y. T., Smith, C. L., Nechushtan, A., Xi, X. G., and Youle, R. J. (1997) *The Journal of cell biology* **139**, 1281-1292
167. Shaulian, E., Haviv, I., Shaul, Y., and Oren, M. (1995) *Oncogene* **10**, 671-680
168. Trahair, T. N., Alexander, I. E., Rowe, P. B., and Smythe, J. A. (2000) *The Journal of general virology* **81**, 2983-2991
169. Karen, K. A., and Hearing, P. (2011) *Journal of virology* **85**, 4135-4142
170. Fensterl, V., and Sen, G. C. (2011) *Journal of interferon & cytokine research : the official journal of the International Society for Interferon and Cytokine Research* **31**, 71-78
171. Castellano, E., and Downward, J. (2011) *Genes & cancer* **2**, 261-274
172. Mateyak, M. K., and Kinzy, T. G. (2010) *The Journal of biological chemistry* **285**, 21209-21213

173. Knoops, B., Goemaere, J., Van der Eecken, V., and Declercq, J. P. (2011) *Antioxidants & redox signaling* **15**, 817-829
174. Zhou, Y., Kok, K. H., Chun, A. C., Wong, C. M., Wu, H. W., Lin, M. C., Fung, P. C., Kung, H., and Jin, D. Y. (2000) *Biochemical and biophysical research communications* **268**, 921-927
175. Puthalakath, H., Huang, D. C., O'Reilly, L. A., King, S. M., and Strasser, A. (1999) *Molecular cell* **3**, 287-296
176. Day, C. L., Puthalakath, H., Skea, G., Strasser, A., Barsukov, I., Lian, L. Y., Huang, D. C., and Hinds, M. G. (2004) *The Biochemical journal* **377**, 597-605
177. Batlevi, Y., Martin, D. N., Pandey, U. B., Simon, C. R., Powers, C. M., Taylor, J. P., and Baehrecke, E. H. (2010) *Proceedings of the National Academy of Sciences of the United States of America* **107**, 742-747
178. de Lima, B. D., May, J. S., Marques, S., Simas, J. P., and Stevenson, P. G. (2005) *The Journal of general virology* **86**, 31-40
179. George, C. X., Li, Z., Okonski, K. M., Toth, A. M., Wang, Y., and Samuel, C. E. (2009) *J Interferon Cytokine Res* **29**, 477-487
180. Katsoulidis, E., Carayol, N., Woodard, J., Konieczna, I., Majchrzak-Kita, B., Jordan, A., Sassano, A., Eklund, E. A., Fish, E. N., and Platanias, L. C. (2009) *J Biol Chem* **284**, 25051-25064
181. Kayagaki, N., Yamaguchi, N., Nakayama, M., Eto, H., Okumura, K., and Yagita, H. (1999) *J Exp Med* **189**, 1451-1460
182. Gomez, D., and Reich, N. C. (2003) *J Immunol* **170**, 5373-5381
183. Clemens, M. J. (2003) *J Interferon Cytokine Res* **23**, 277-292
184. Lafage, M., Clauss, I., Couez, D., Simonetti, J., Wathelet, M. G., and Huez, G. (1992) *Genomics* **13**, 458-460
185. Andersen, J., VanScoy, S., Cheng, T. F., Gomez, D., and Reich, N. C. (2008) *Genes Immun* **9**, 168-175
186. Weaver, B. K., Ando, O., Kumar, K. P., and Reich, N. C. (2001) *FASEB J* **15**, 501-515
187. Strasser, A., O'Connor, L., and Dixit, V. M. (2000) *Annu Rev Biochem* **69**, 217-245
188. Wang, C., and Youle, R. J. (2009) *Annu Rev Genet* **43**, 95-118
189. Youle, R. J., and Strasser, A. (2008) *Nat Rev Mol Cell Biol* **9**, 47-59
190. Boise, L. H., Gonzalez-Garcia, M., Postema, C. E., Ding, L., Lindsten, T., Turka, L. A., Mao, X., Nunez, G., and Thompson, C. B. (1993) *Cell* **74**, 597-608
191. Oda, E., Ohki, R., Murasawa, H., Nemoto, J., Shibue, T., Yamashita, T., Tokino, T., Taniguchi, T., and Tanaka, N. (2000) *Science* **288**, 1053-1058
192. Nakano, K., and Vousden, K. H. (2001) *Mol Cell* **7**, 683-694
193. Yu, J., Zhang, L., Hwang, P. M., Kinzler, K. W., and Vogelstein, B. (2001) *Mol Cell* **7**, 673-682
194. Vousden, K. H., and Prives, C. (2009) *Cell* **137**, 413-431
195. Hui, D. J., Terenzi, F., Merrick, W. C., and Sen, G. C. (2005) *J Biol Chem* **280**, 3433-3440
196. Blommaart, E. F., Krause, U., Schellens, J. P., Vreeling-Sindelarova, H., and Meijer, A. J. (1997) *European journal of biochemistry / FEBS* **243**, 240-246
197. Tanida, I., Ueno, T., and Kominami, E. (2008) *Methods Mol Biol* **445**, 77-88
198. Wang, H., Shen, H., Wang, Y., Li, Z., Yin, H., Zong, H., Jiang, J., and Gu, J. (2005) *FEBS letters* **579**, 1279-1284

199. Horibe, T., Kohno, M., Haramoto, M., Ohara, K., and Kawakami, K. (2011) *Journal of translational medicine* **9**, 8
200. Taniguchi, T., and Takaoka, A. (2001) *Nature reviews. Molecular cell biology* **2**, 378-386
201. Tschopp, J., Thome, M., Hofmann, K., and Meinl, E. (1998) *Curr Opin Genet Dev* **8**, 82-87

Appendix

Figures and Illustrations

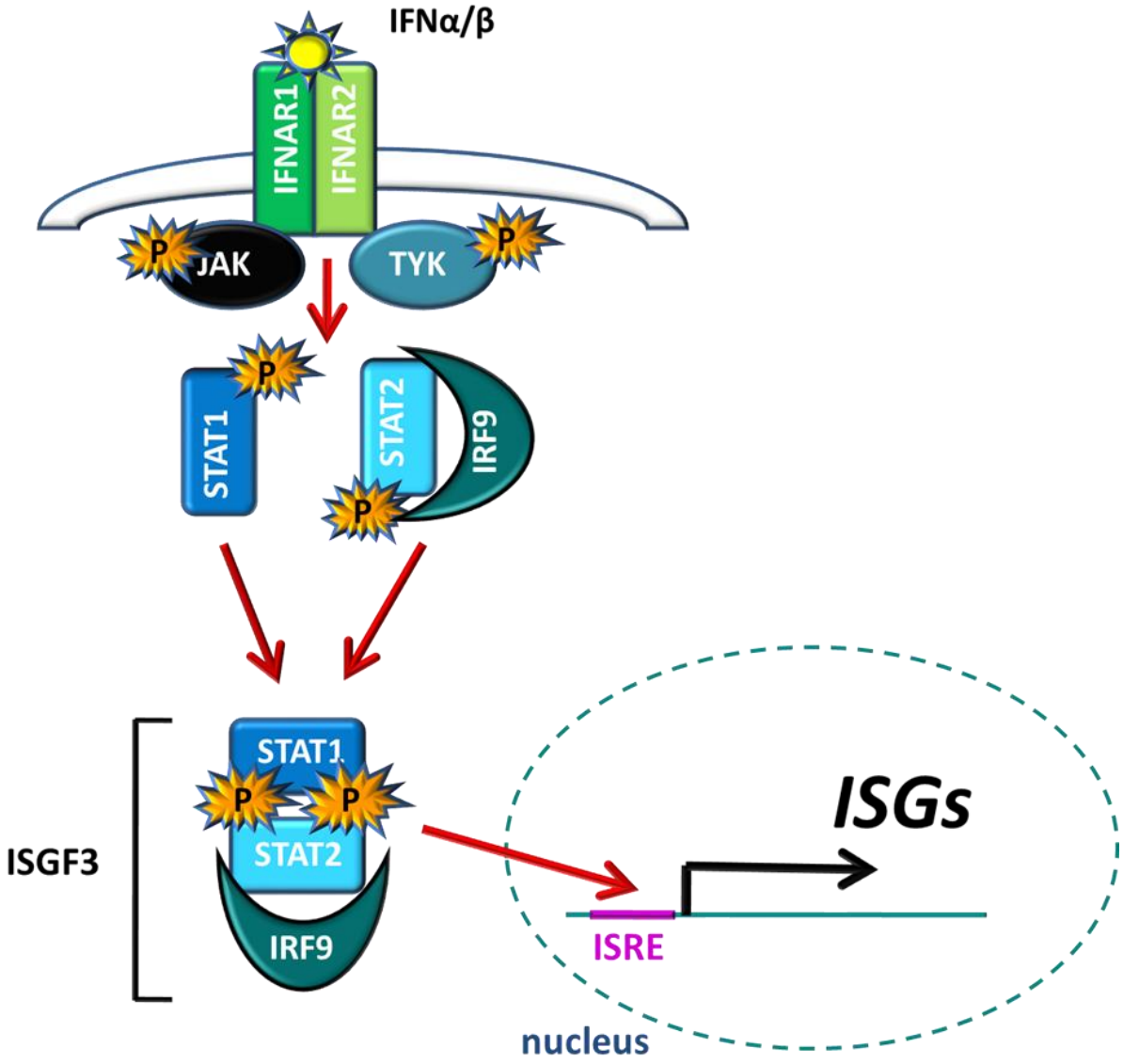

Figure 1. Activation of Interferon Stimulated Genes (ISGs). Binding of type-I IFN to type I IFN receptor composed of subunits IFNα Receptor 1 (IFNAR1) and IFNAR2 activates Janus kinases (JAK and TYK) that autophosphorylate themselves and then recruit Signal Transduction and Transactivation (STAT) proteins. STAT1 and STAT2 that remains bound to Interferon Regulatory Factor 9 (IRF9) become phosphorylated and form trimeric molecule referred to as Interferon-Stimulated Gamma Factor 3 (ISGF3). ISGF3 subsequently translocates to the nucleus where it binds to the promoter of the genes containing Interferon Stimulated Response Element (ISRE) and induces expression of ISGs

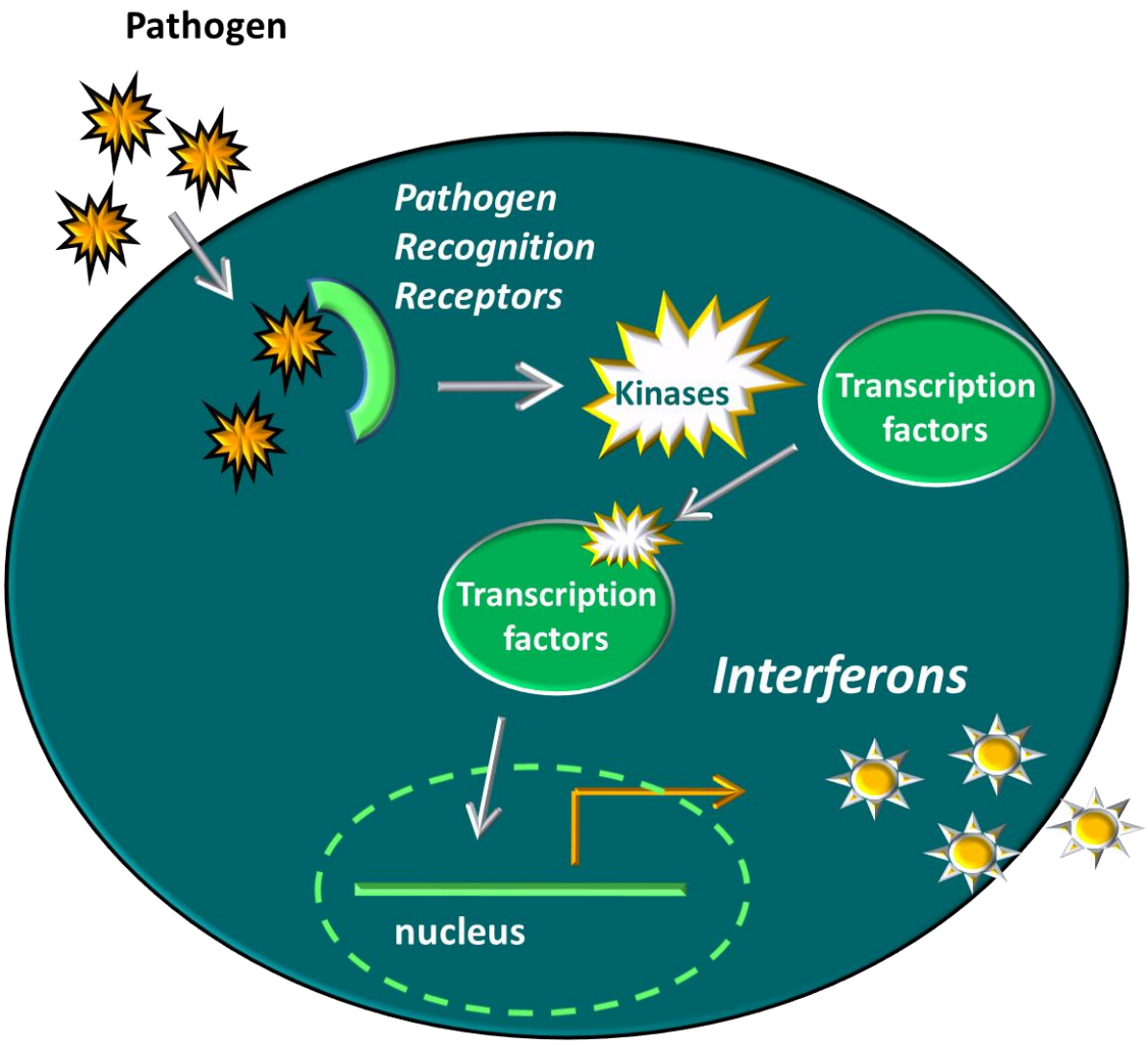

Figure 2.Mechanism of type I IFN induction. Pathogen Recognition Receptors (PRRs) recognize foreign molecules and trigger protein-protein interaction cascade leading to activation of latent kinases. Kinases phosphorylate transcription factors that become activated and initiate transcription of IFN genes. Interferons are next secreted from the cells to the extracellular milieu,

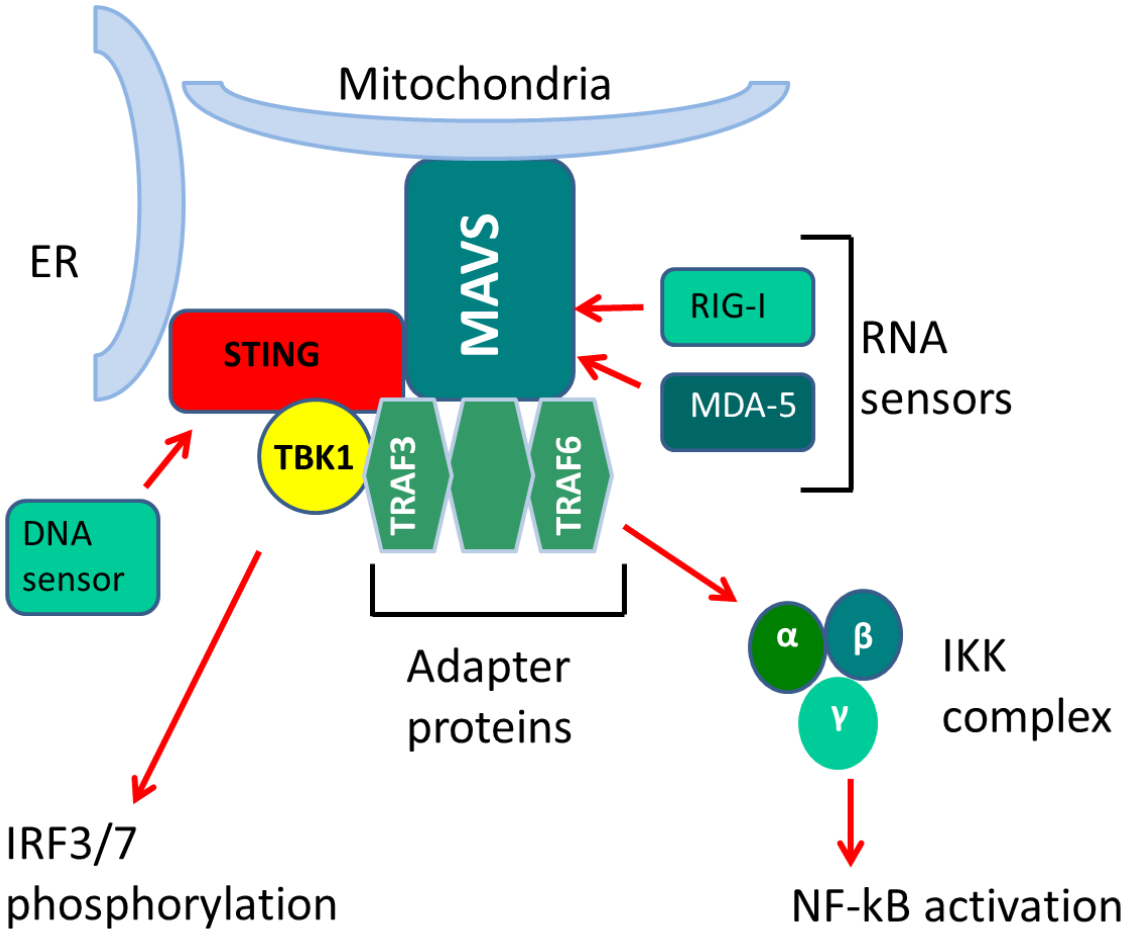

Figure 3. Role of STING and MAVS in induction of type I IFN response. Stimulator of Interferon Genes (STING) and Mitochondrial Antiviral Signaling (MAVS) are adapter proteins anchored in the ER and mitochondrial membrane respectively. Viral RNA sensors RIG-I (retinoic acid inducible gene I) and MDA-5 melanoma differentiation associated factor 5) bind MAVS after recognition of alien RNA. MAVS interacts with the complex of over 30 adapter proteins including TNF receptor associated factors 3 and 6 (TRAF3/6) that participate in activation of TBK1 (Tank-binding kinase 1) and IKK complex respectively. TBK1 phosphorylates Interferon Regulatory Factors 3 and 7 (IRF3/7) that stimulate expression of IFNα and β genes while IKK activates NF-κB (that enhances expression of IFNβ).
STING is involved activation of TBK1 in response to pathogens' DNA. It localizes in the ER membranes associated with mitochondria and interacts both with TBK1 and MAVS. It also binds TRAF3 protein and may interact directly with IRF3. It is speculated that after infection with dsDNA containing pathogen, specific DNA sensors can bind STING and induce TBK1 activation. However, so far these sensors have not been yet identified.

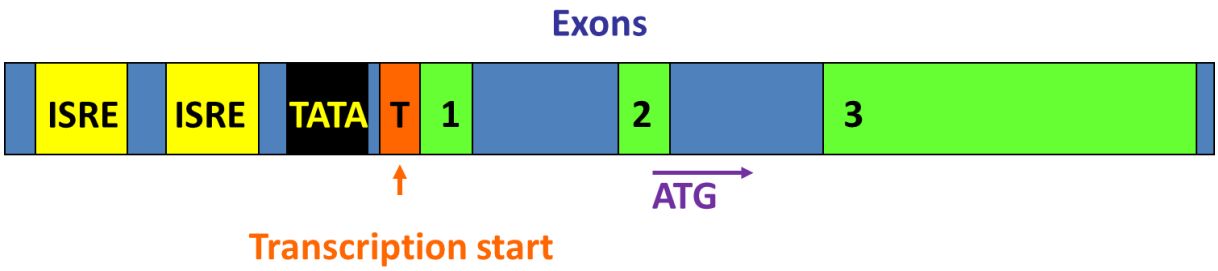

Figure 4. Schematic organization of mouse ISG54 gene. Mouse ISG54 promoter contains TATA box and two upstream IFN-stimulated response elements (ISRE). ISRE elements are the only known regulatory sequences of either murine or human ISGs. Mouse ISG54 gene consists of three exons. First exon does not code for any protein sequence, second codes only for the initiation ATG codon while the third exon codes for the rest of the protein. Human ISG54 has the same organization except it lacks the first non-coding exon.

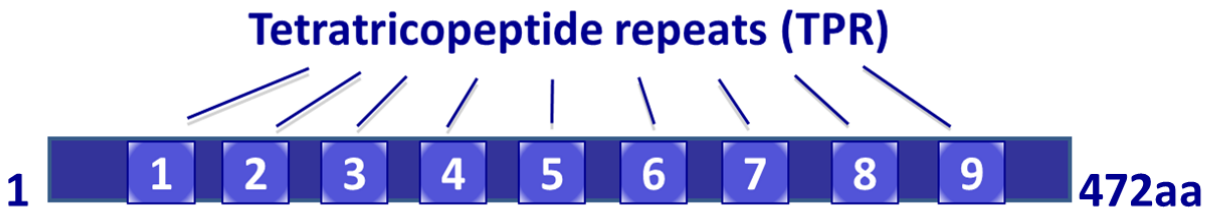

Repeat	Begin	Alignment	End	P-value
TPR	51	ATMCNLLAYLKHLKGQNEAALECLRKAEELIQQE	84	1.6e-06
TPR	94	LVTWGNYAWVYYHMGRLSDVQIYVDKVKHVCEKF	127	6.5e-07
TPR	138	LDCEEGWTRLKCGGNQNERAKVCFEKALEKKPKN	171	1.5e-05
TPR	175	TSGLAIASYRLDNWPPSQNAIDPLRQAIRLNPDN	208	3.5e-04
TPR	213	VLLALKLHKMREEGEEEGEGEKLVEEALEKAPGV	246	6.6e-03
TPR	247	TDVLRSAAKFYRRKDEPDKAIELLKKALEYIPNN	280	9.0e-10
TPR	334	FRVCSILASLHALADQYEDAEYYFQKEFSKELTP	367	2.3e-04
TPR	372	LLHLRYGNFQLYQMKCEDKAIHHFIEGVKINQKS	405	9.0e-04
TPR	430	SEALHVLAFLQELNEKMQQADEDSERGLESGSLI	463	7.8e-03

Figure 5. Schematic depiction of ISG54 protein. ISG54 is 54 kDa protein that is characterized by the presence of tetratricopeptide (TPR) motifs. Since the three-dimensional structure of ISG54 has not been solved, the exact number of TPR domains remains unknown. Presented graph is based on the calculations made with TPRPRed algorithm from Max Plack's Institute (80). Simulation predicts the presence of 9 TPR motifs distributed evenly along the protein sequence. The amino acid sequence of TPR motifs is weakly conserved and does not show significant similarities between particular domains.

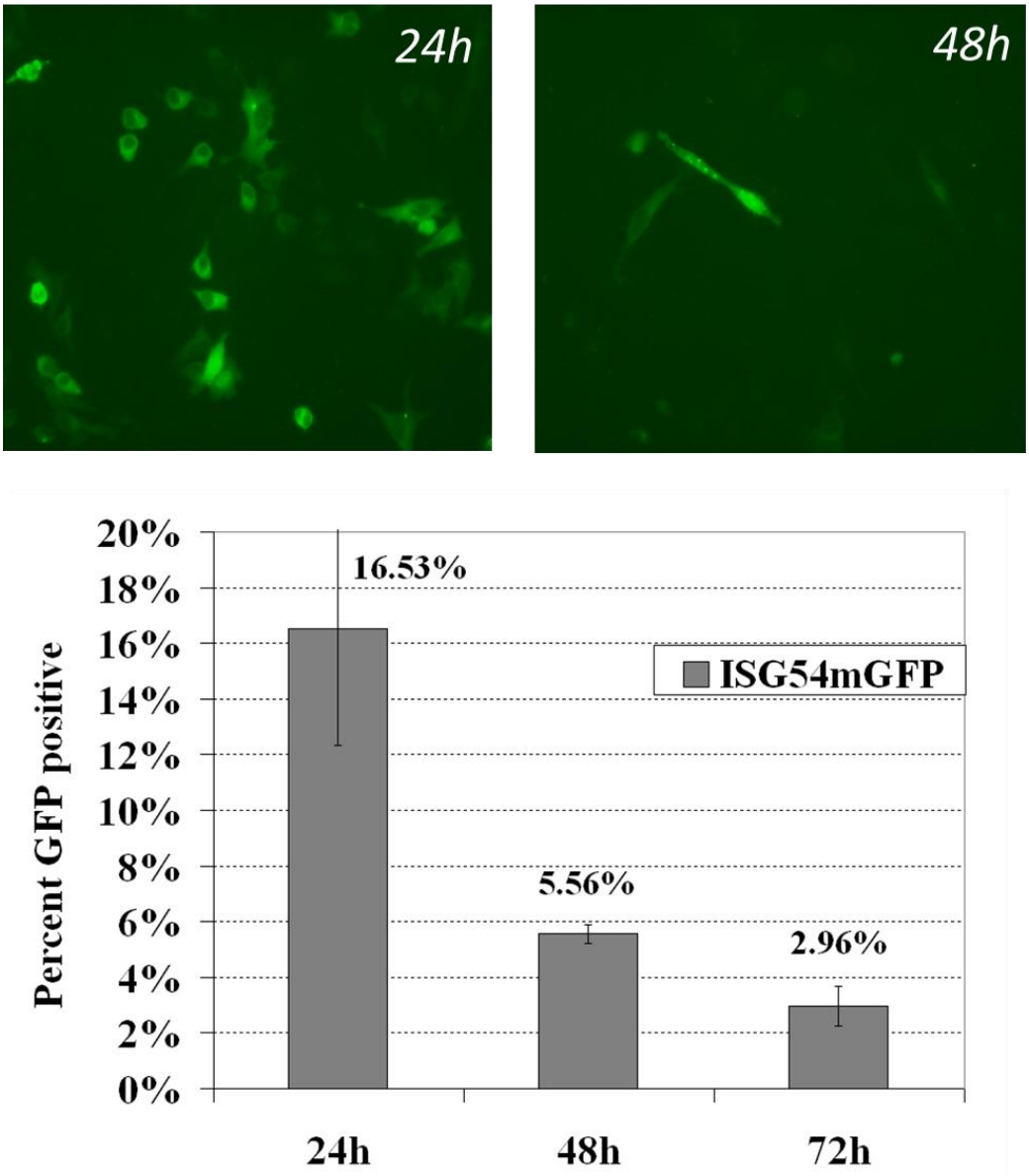

Figure 6. Expression of ISG54mGFP decreases quickly with time. HeLa cells were transfected with ISG54mGFP and the number of GFP positive cells at different timpoints after transfection was evaluated with fluorescent microscopy (*upper panel*) and with flow cytometry (lower panel). A relatively low number of cells expressed ISG54 24hs after transfection and that number decreased dramatically with time. Cells expressing ISG54 showed altered morphology indicating on the possibility of ongoing apoptosis

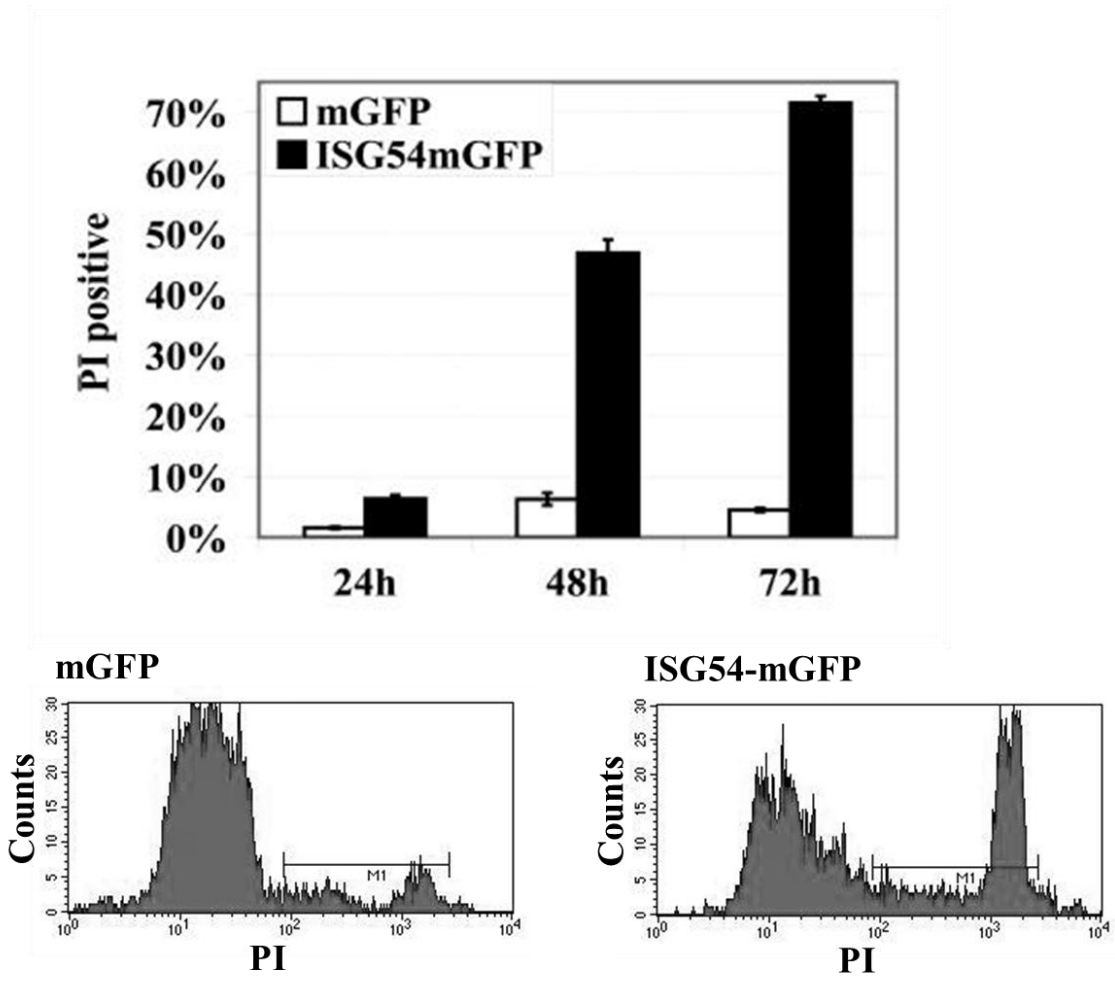

Figure 7. Expression of ISG54 induces cell death. HeLa cells were transfected with plasmid encoding ISG54mGFP or mGFP, stained with PI at 24h, 48h and 72h after transfection and analyzed with flow cytometry. The percent of cells positive for both GFP and PI was quantified. Cell expressing ISG54mGFP displayed significantly higher level of cell death comparing to mGFP control. *Lower panel:* A single dimension histograms of flow cytometry data obtained for the cells expressing mGFP or ISG54-mGFP after 48 h transfection are shown. Calculated *p* values comparing cells expressing mGFP and ISG54mGFP were <0.0001

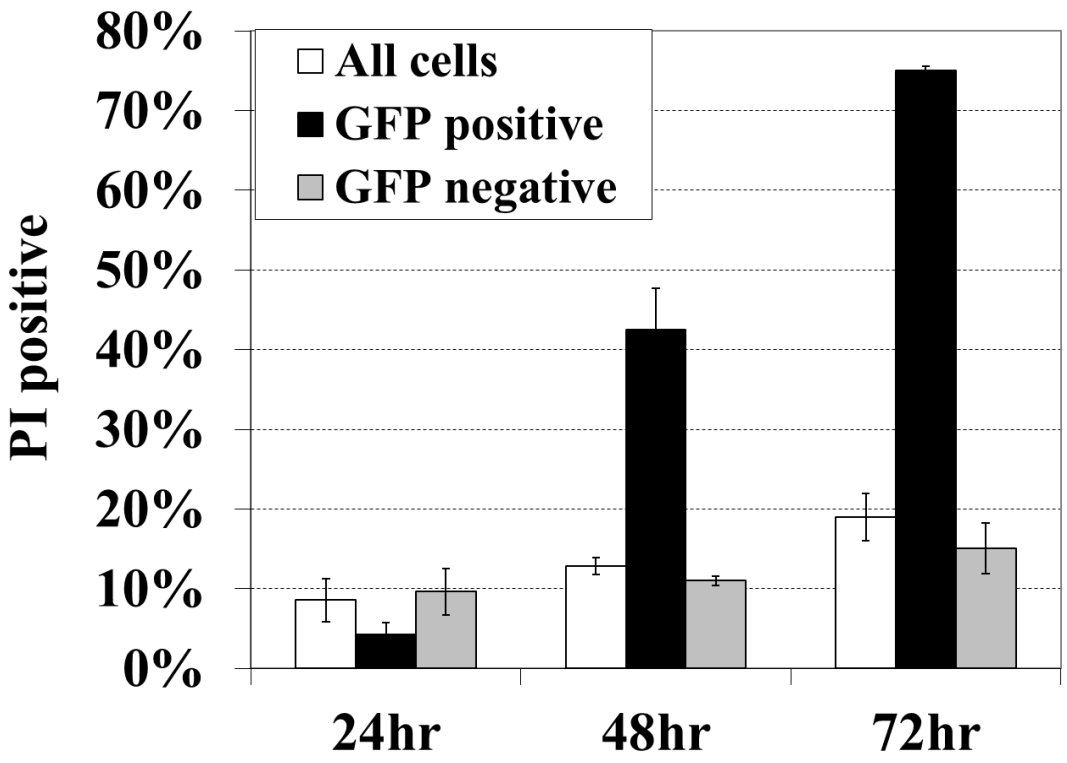

Figure 8. Cell death in cultures transfected with ISG54mGFP. HeLa cells were transfected with ISG54mGFP, stained with PI 24h, 48h and 72hs after transfection and analyzed with flow cytometry. The percent of PI positive cells was compared between the cells positive and negative for GFP. Cell death was significantly elevated in the cells that expressed ISG54mGFP. Calculated *p* values comparing cells expressing and non-expressing ISG54mGFP for 48 and 72hs timepoints were <0.001.

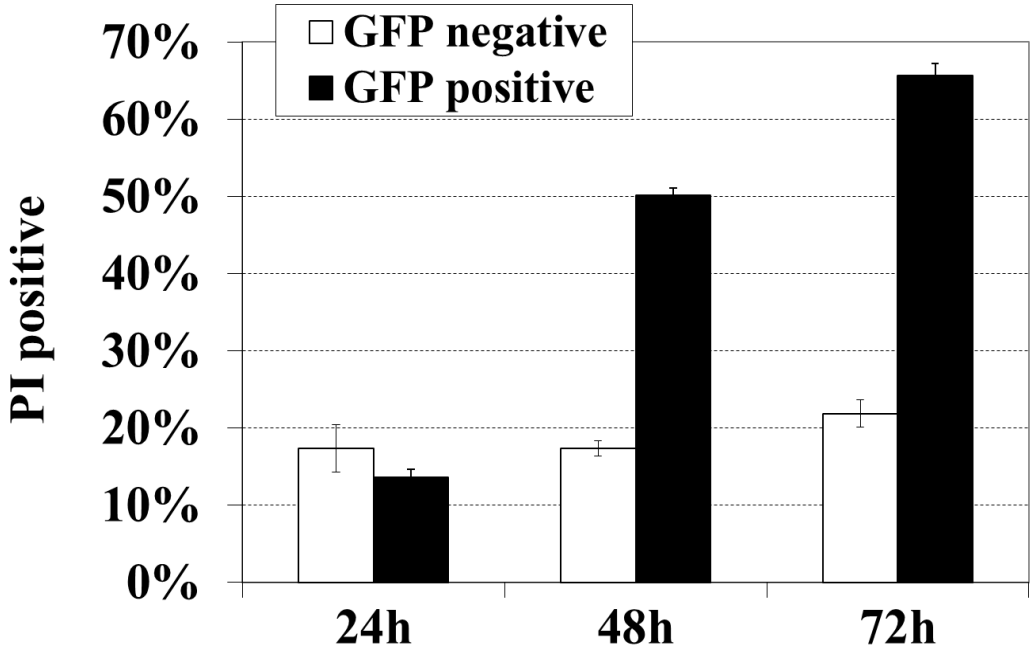

Figure 9. ISG54 promotes cell death in an inducible system. HeLa cells were co-transfected with tetracycline-inducible pRev-ISG54-mGFP and pLib-rtTAm2-iresTRSID-iresPuro coding for TetRepressor/Transactivator. Cells were stimulated with 2μg/ml doxycycline for 24, 48, and 72 hrs, stained with PI and analyzed with flow cytometry for cell death. GFP positive and negative cells in the culture were compared in terms of PI staining. Calculated *p* values comparing GFP positive and negative cells for 48 and 72hs timepoints were <0.001.

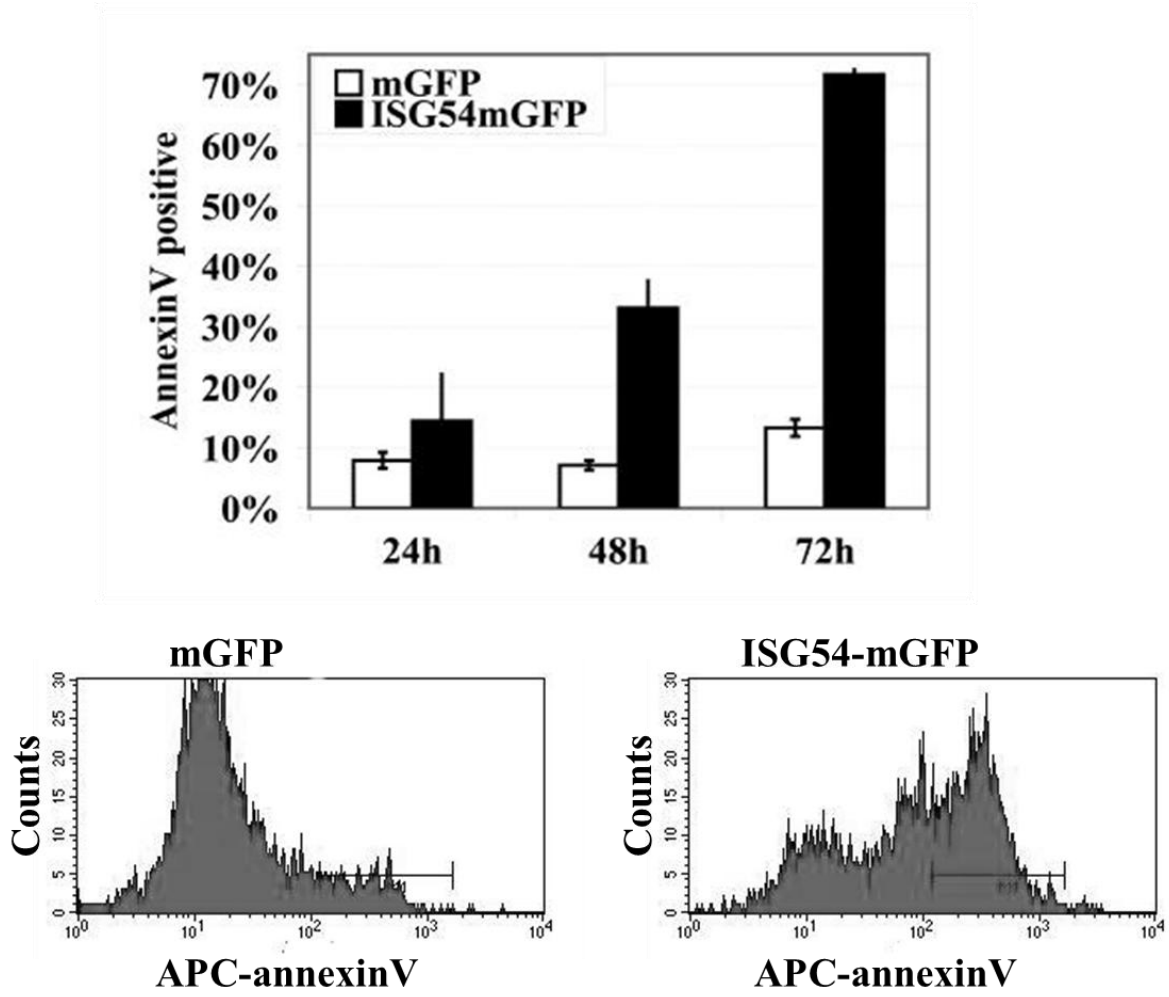

Figure 10. Expression of ISG54 induces apoptosis. HeLa cells were transfected with plasmid encoding ISG54mGFP or mGFP, stained with annexinV at 24h, 48h and 72h after transfection and analyzed with flow cytometry. The percent of cells positive for both GFP and annexinV was quantified. Cell expressing ISG54mGFP displayed significantly higher level of apoptosis comparing to mGFP control. *Lower panel:* A single dimension histograms of flow cytometry data obtained for the cells expressing mGFP or ISG54-mGFP after 48 h transfection are shown. Calculated *p* values comparing cells expressing mGFP and ISG54mGFP were <0.001.

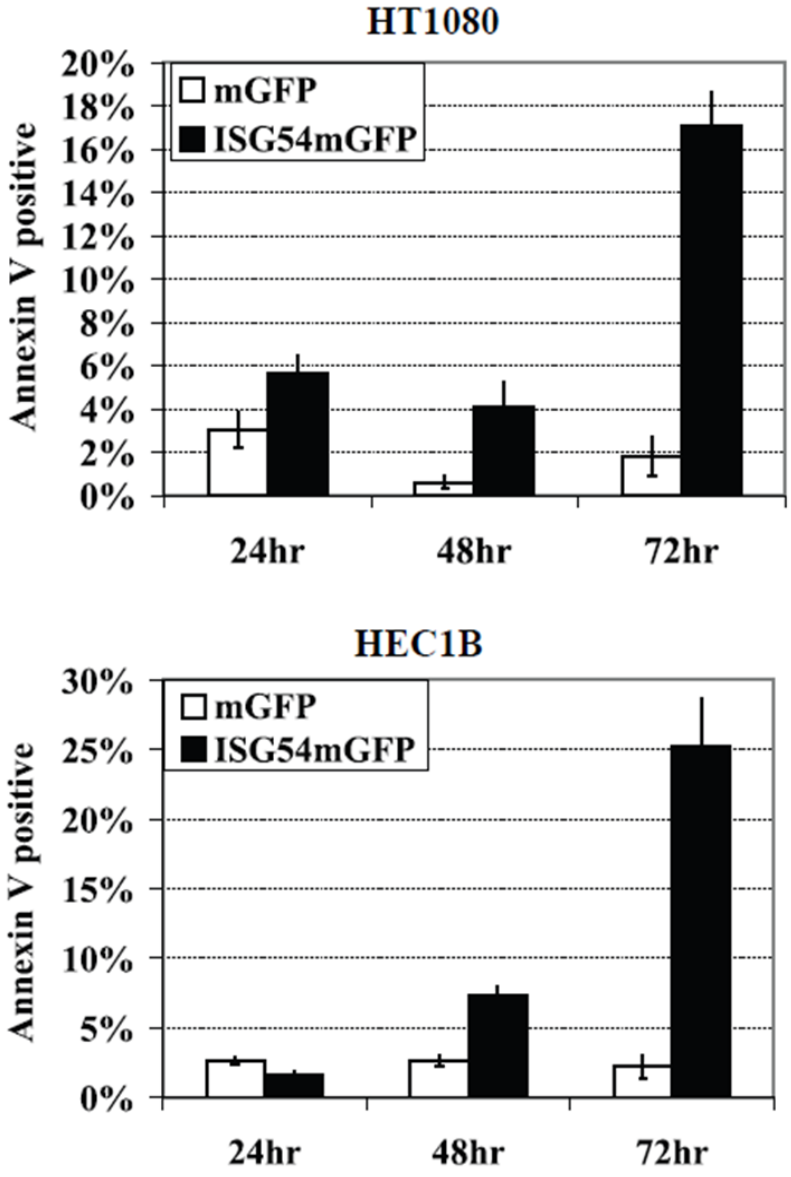

Figure 11. ISG54 promotes apoptosis in various cell lines. HT1080 cells (upper panel) and HEC1B cells (lower panel) were transfected with plasmid encoding ISG54mGFP or mGFP, stained with PI at 24h,48h and 72h after transfection and analyzed with flow cytometry. Percent of the cells positive for GFP and annexinV was quantified. Calculated *p* values for 72hs timepoint comparing cells expressing mGFP and ISG54mGFP were <0.001.

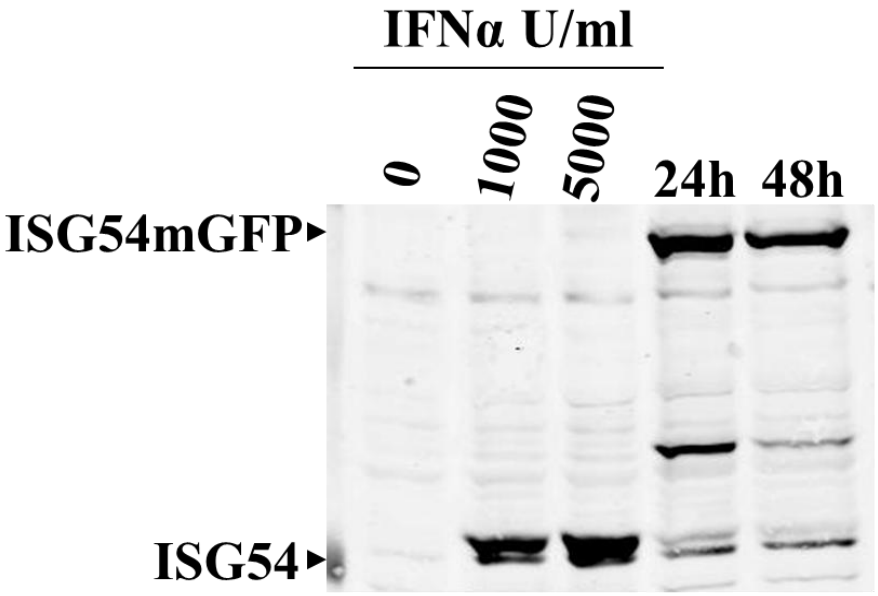

Figure 12. Levels of ISG54 protein expressed in transfected cultures compared to endogenous ISG54 induced in response to IFNα. HeLa cells were untreated, or treated with 1000 or 5000 U/mlIFNα for 48 hrs to serve as endogenous samples. HeLa cells were transfected with ISG54-mGFP plasmid for 24 or 48 hrs, and cells expression ISG54-GFP were isolated by FACS. Lysates were prepared from the respective cells and the same amount of protein was evaluated by Western blot with polyclonal antibody to human ISG54. A representative experiment is shown, and the protein levels were compared with Image J software. Results indicated that ISG54-mGFP expression was equivalent to 98% of endogenous ISG54 induced by 5000 U/ml IFNα at 24 hrs, and 91% of endogenous ISG54 induced at 48hrs.

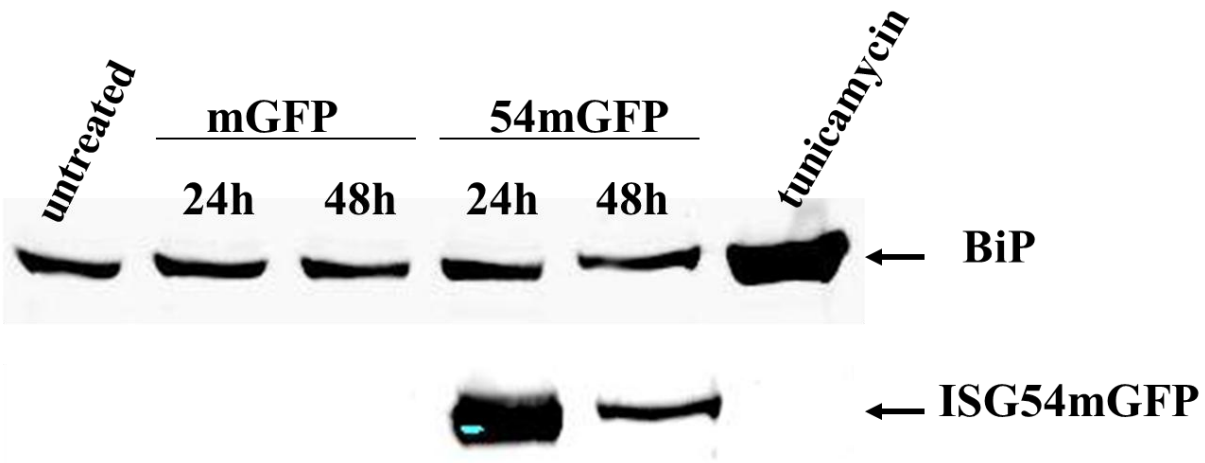

Figure 13. ISG54 does not induce an Unfolded Protein Response. HeLa cells were transfected with ISG54mGFP or mGFP as a control. At 24h and 48h after transfection GFP positive cells were isolatedby FACS. These cells were lysed and evaluated with Western-Blotting for the induction of BiP protein. Untransfected cells and cells treated overnight with 10ug/ml tunicamycin were used as a positive and negative control respectively. No induction of BiP was observed in ISG54 positive cells.

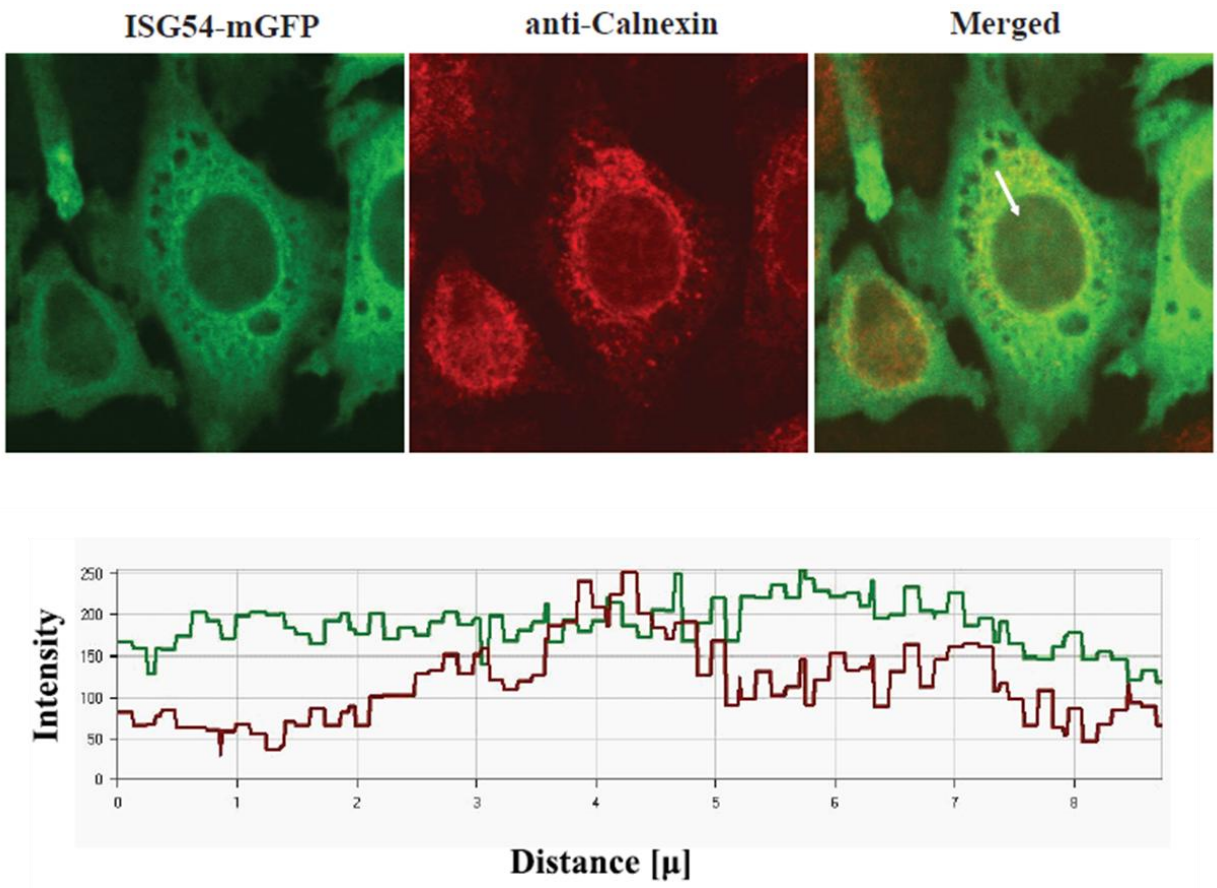

Figure 14. ISG54mGFP does not display increased accumulation in the ER. *Upper panel:* HeLa cells expressing ISG54mGFP were stained by immunofluorescence with antibodies to calnexin, an ER marker, and secondary TRITC-conjugated anti-mouse antibodies. Colocalization of ISG54mGFP (green) and calnexin (red) was calculated with ImageJ software. Pearson's coefficient values of colocalization were calculated between 0.05-0.12 indicating only a weak positive correlation. *Lower panel:* Image of the cell from upper panel (arrow in merged image) was analyzed with LSM5 Pascal software to evaluate the correlation between red and green fluorescence. Graph presents the profile of fluorescence along the white arrow. Red fluorescence peaks crossing into the ER region, but fluorescence of ISG54mGFP remains the same.

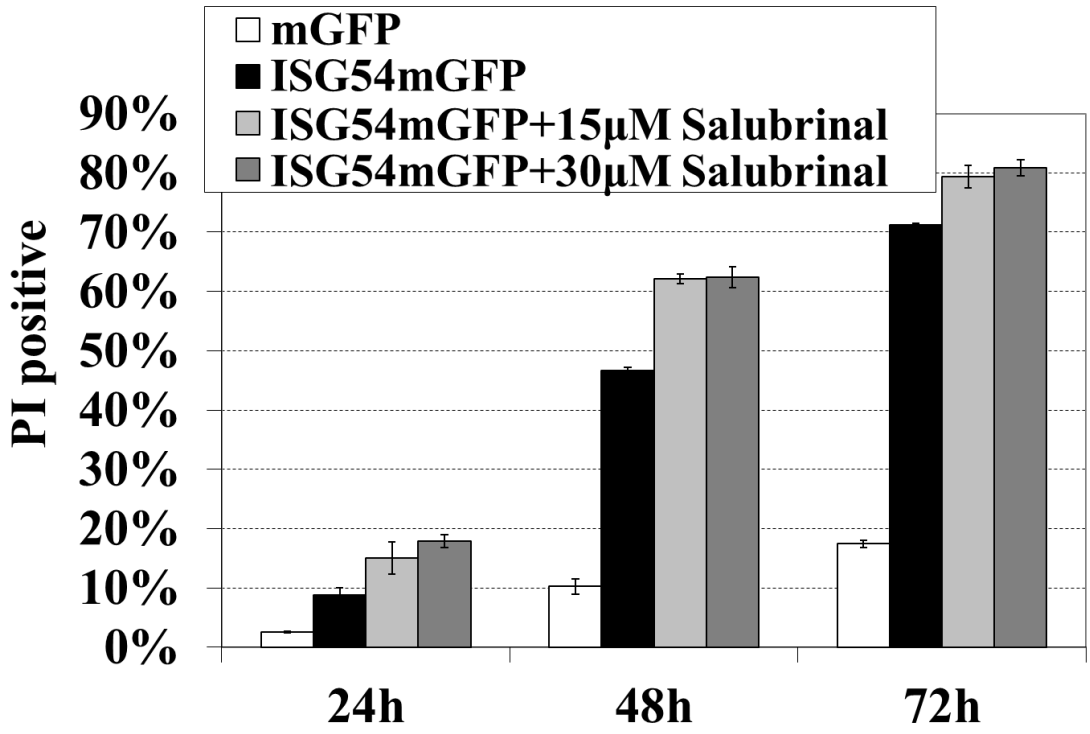

Figure 15. ER Stress inhibitor does not reduce ISG54 induced cell death. HeLa cells were transfected with mGFP or ISG54mGFP and 6 hrs after transfection cells were treated with 15μM or 30μM salubrinal, an ER stress inhibitor. Cells were harvested 24, 48, or 72 hours post transfection and analyzed for cell death with PI staining and flow cytometry. There was no noted effect of salubrinal on ISG54 induced cell death.

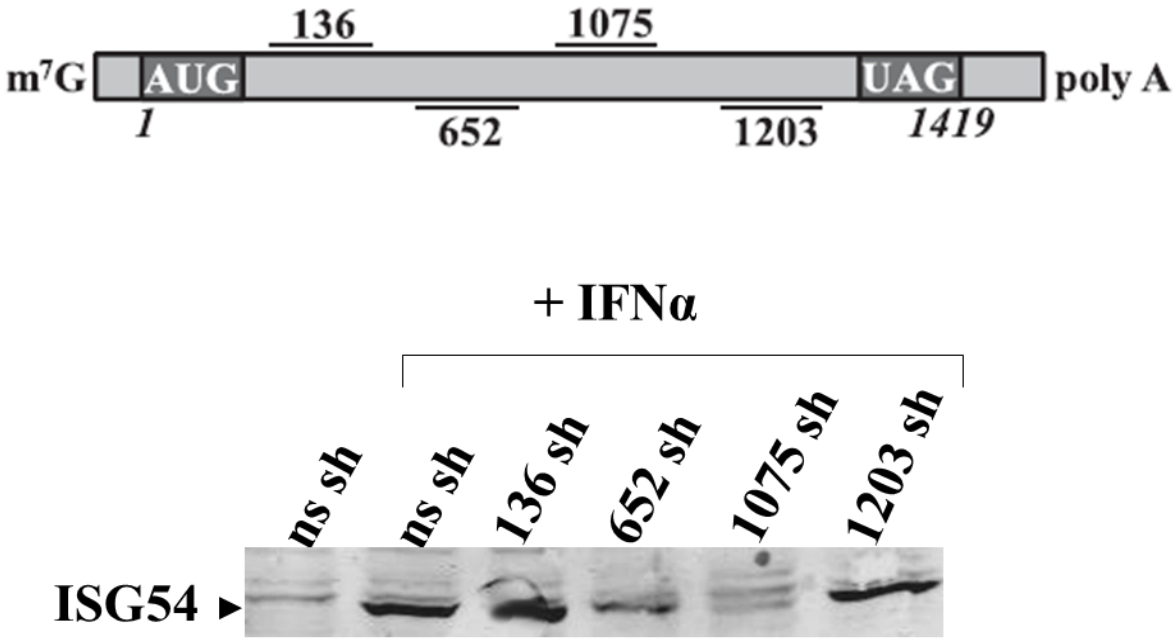

Figure 16. Knockdown of ISG54 using shRNA. *Upper panel:* Four different shRNAs were designed targeting four different regions of ISG54 mRNA. Numbers denote 5' position of mRNA sequencetargeted by each shRNA. *Lower panel:* Stable HeLa cell lines expressing each of shRNAs were established and the cells were treated overnight with interferon to induce ISG54 expression. As a control HeLa cell line expressing non-specific shRNA was used. Levels of ISG54 expression were evaluated by Western-blotting with anti-ISG54 antibodies. 1075shRNA displayed over 60% reduction in ISG54 expression measured by (Image J software)

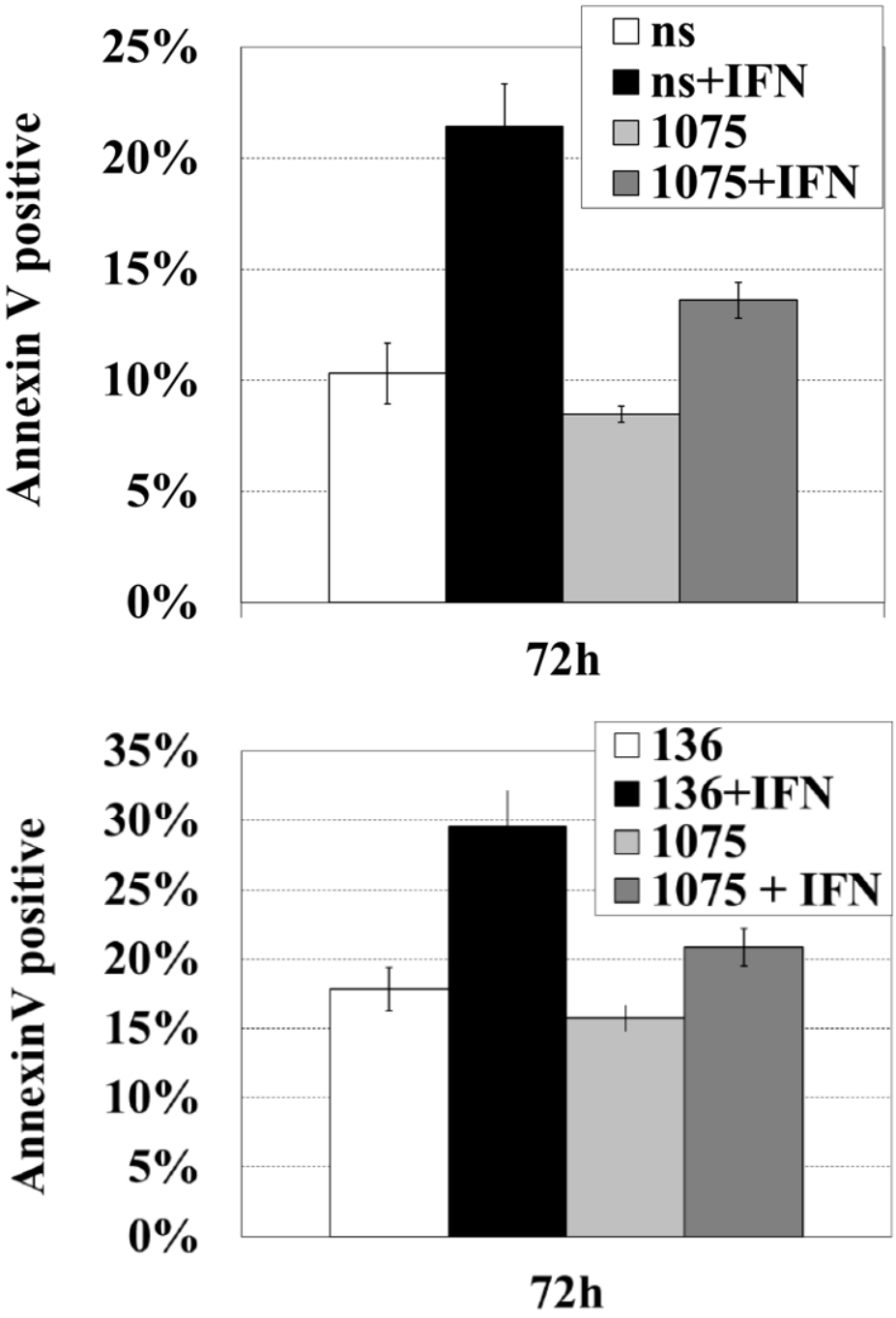

Figure 17. ISG54 knockdown reduces sensitivity of cells to IFN-induced apoptosis. Cells expressing stable knockdown of ISG54 with 1075shRNA were evaluated for their apoptotic response to IFN compared to either cells expressing non-specific shRNA (*upper panel*) or specific 136shRNA that failed to knock down ISG54 expression (*lower panel*). Calculated *p* value comparing effects of IFN in cells with 1075 shRNA or nonspecific shRNA was <0.03. *P* value comparing effects of IFN in cells with 1075 shRNA or 136 shRNA was <0.05.

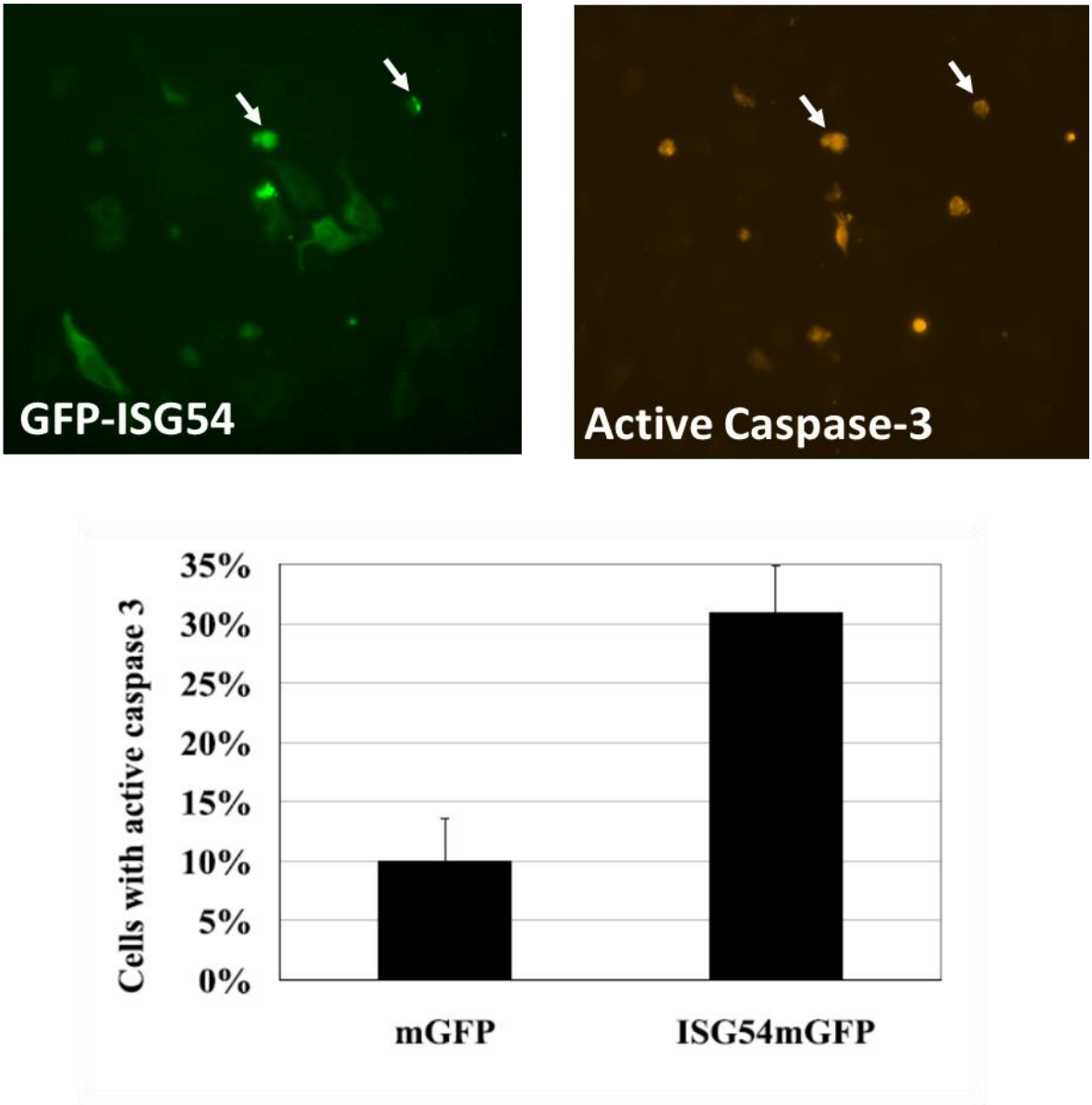

Figure 18. ISG54 induces activation of caspases. HeLa cells were transfected with ISG54mGFP or control mGFP plasmid and at 48hs after transfection they were evaluated for the activation of caspase-3 with immunofluorescence. Cells expressing ISG54mGFP showed significant activation of caspase-3 (*upper panel*). Quantitation of cells positive for GFP and active caspase-3 at 48hs showed over threefold higher number of cells with active caspase-3 in the population expressing ISG54mGFP (*lower panel*).

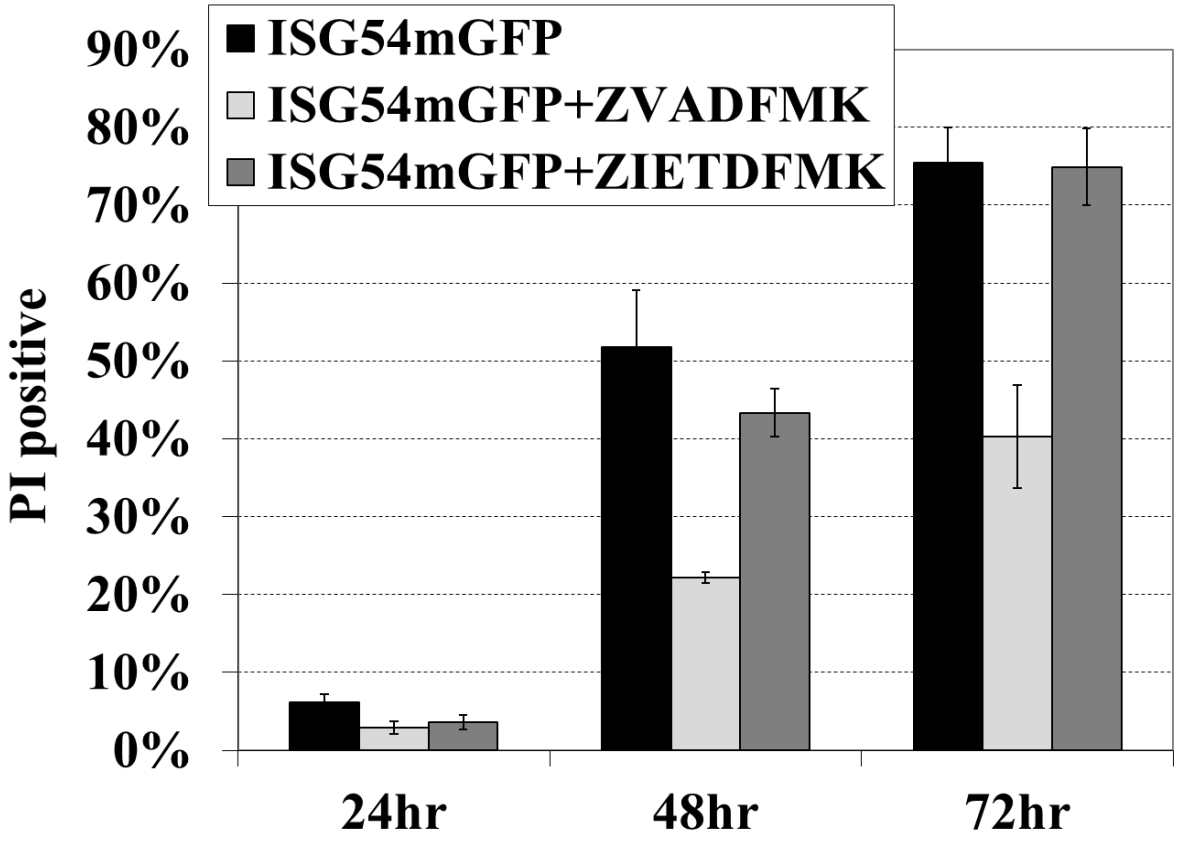

Figure 19. ZVAD-FMK inhibits ISG54-induced apoptosis. HeLa cells were transfected with ISG54mGFP and 6hs after transfection pan-caspase inhibitor ZVAD-FMK or caspase-8 inhibitor ZIETD-FMK were added to cell media at 20μM concentration. Cell death was monitored with flow cytometry by PI staining. ISG54-promoted apoptosis was inhibited by ZVAD-FMK but not by ZIETD-FMK. Calculated *p* values comparing cells treated and untreated with ZVADFMK were <0.01.

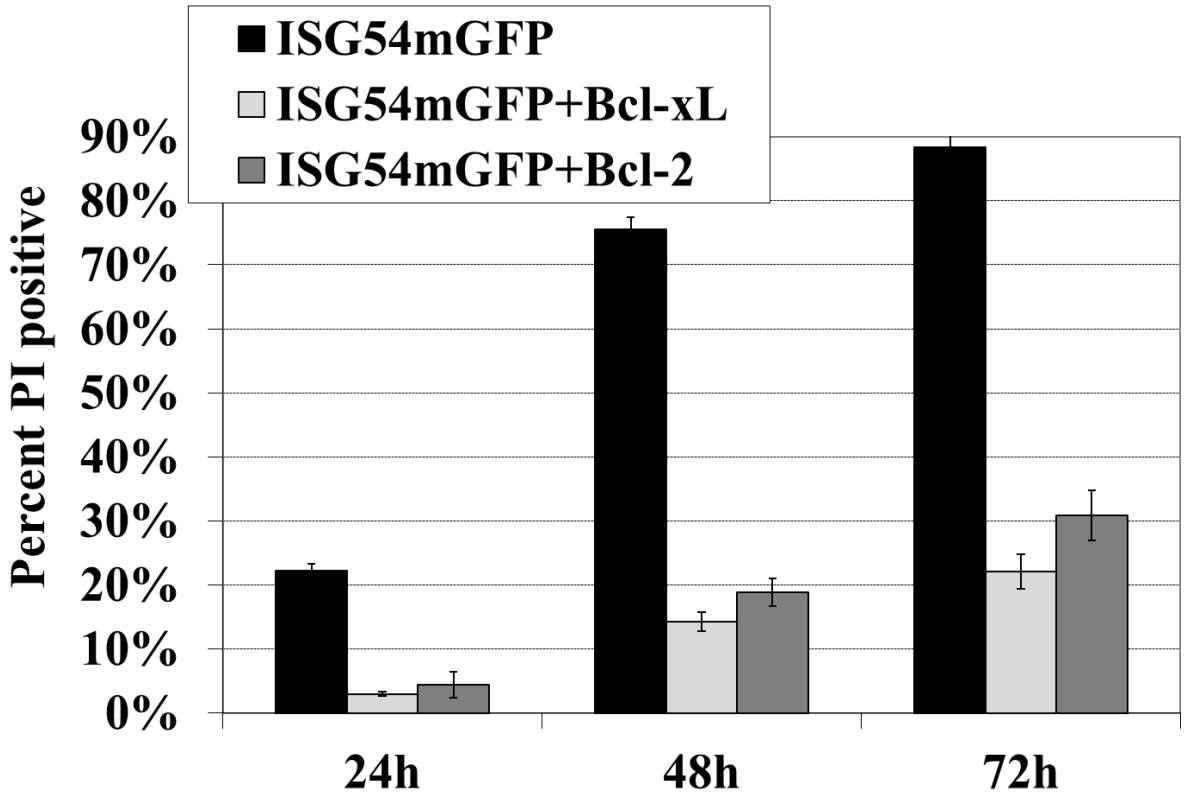

Figure 20. ISG54-induced apoptosis can be blocked by inhibitors of mitochondrial apoptotic pathway. HeLa cells were transfected with ISG54mGFP and control plasmid or with ISG54mGFP and Bcl-xL or ISG54mGFP and Bcl-2. Cell death was evaluated using flow cytometry and PI staining. Both BCl-2 and Bcl-xL potently inhibited ISG54-induced apoptosis. Calculated *p* values comparing cells transfected with ISG54mGFP with cells cotransfected with Bcl2 or Bcl-xL were < 0.0001.

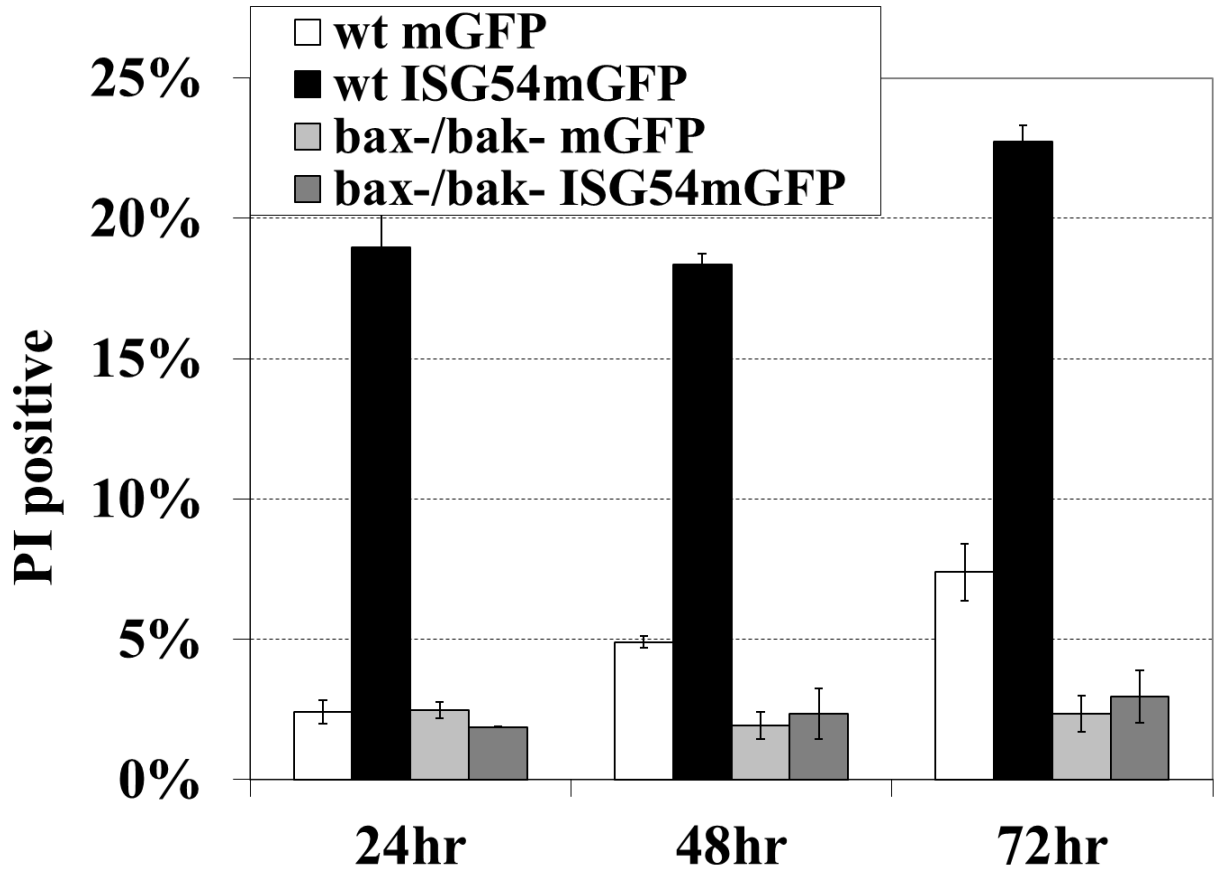

Figure 21. **Bax and Bak are necessary for apoptotic effect of ISG54.** Wild type BMK cells or *bax*$^{-/-}$ *bak*$^{-/-}$ double knock-out BMK cells were transfected with mGFP or ISG54-mGFP for the times indicated, and GFP-positive cells were analyzed by flow cytometry after PI staining. Calculated *p* values comparing apoptosis in wild-type vs *bax-/-bak-/-* cells were <0.01

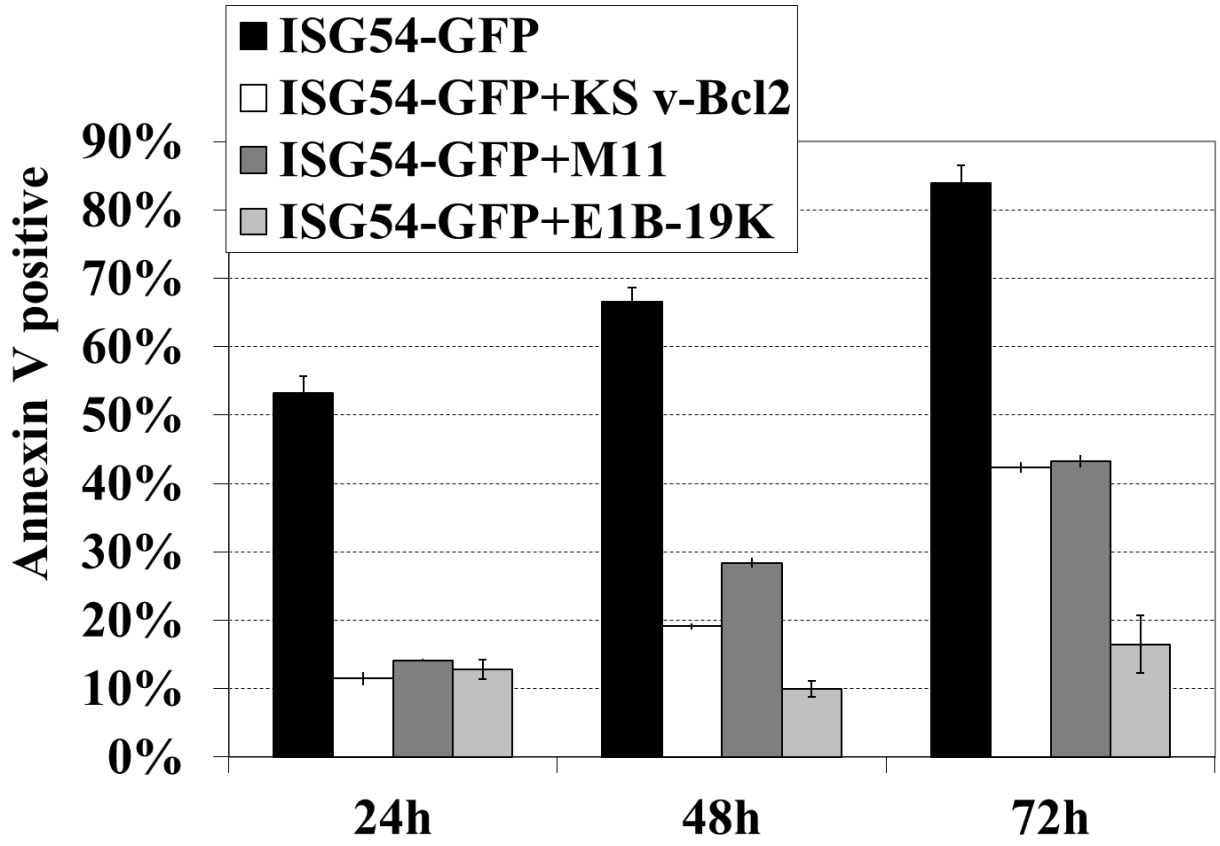

Figure 22. Viral anti-apoptotic proteins inhibit ISG54-induced cell death. HeLa cells were cotransfected with ISG54mGFP and viral proteins that are homologues of human Bcl-2: v-Bcl2 from Kaposi's Sarcoma Virus, M11 from Mouse GammaHerpesvirus-68 and adenoviral E1B19K. At 24hs,48hs and 72hs apoptosis was evaluated with annexinV staining. All the viral proteins were effective in the inhibition of apoptosis with E1B-19K having the strongest effect. Calculated *p* values comparing cells transfected with ISG54mGFP with cells cotransfected with viral anti-apoptotic proteins were < 0.01.

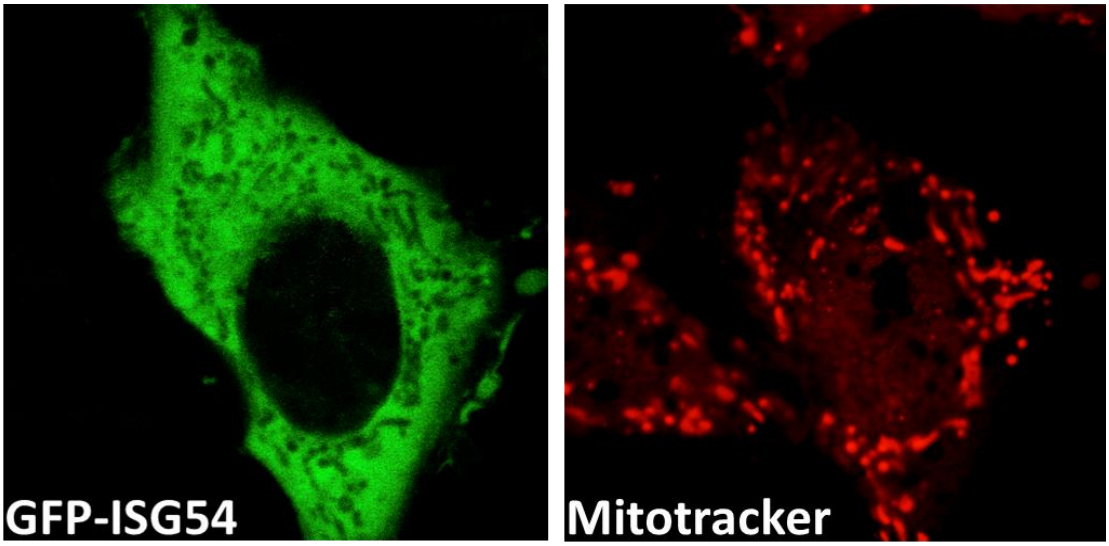

Figure 23. ISG54 does not enter inside the mitochondria. Live-cell imaging of cells expressing ISG54-mGFP (*left*) and stained with MitoTracker Orange (*right*) 24hs after transfection reveals the ISG54mGFP localizes in the cytoplasm but is excluded from mitochondrial compartment.

.

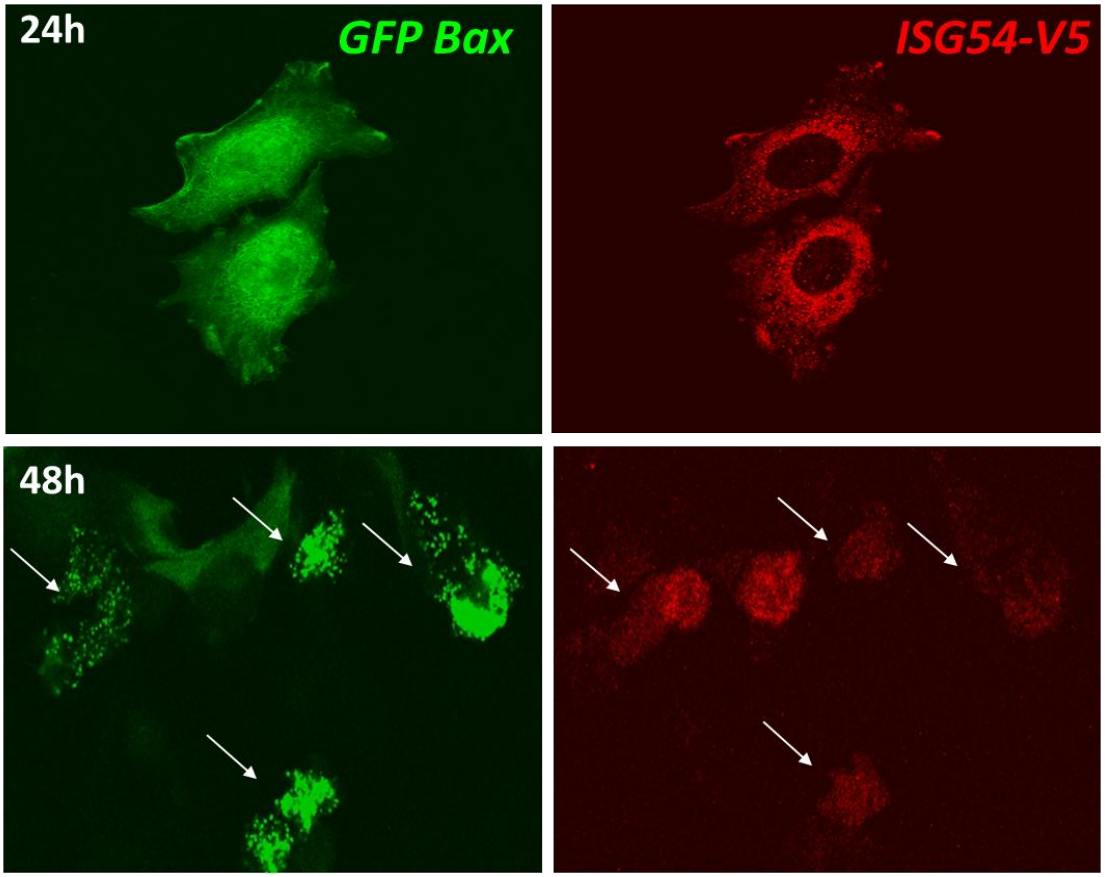

Figure 24. ISG54 stimulates translocation of Bax to the mitochondria. HeLa cells were cotransfected with Bax-GFP and ISG54-v5 and visualized with confocal microscopy 24h and 48hs after transfection. ISG54 was visualized by immunofluorescence with anti-v5 antibodies. At 24hs Bax is distributed evenly in the cells while ISG54 maintains cytoplasmic localization (*upper panel*). At 48hs *(lower panel)* cells expressing ISG54 show altered phenotype and Bax GFP forms characteristic puncta corresponding to its translocation to the mitochondria (indicated by arrows). Partially speckled pattern of ISG54 signal comes from the noise due to weak red fluorescence.

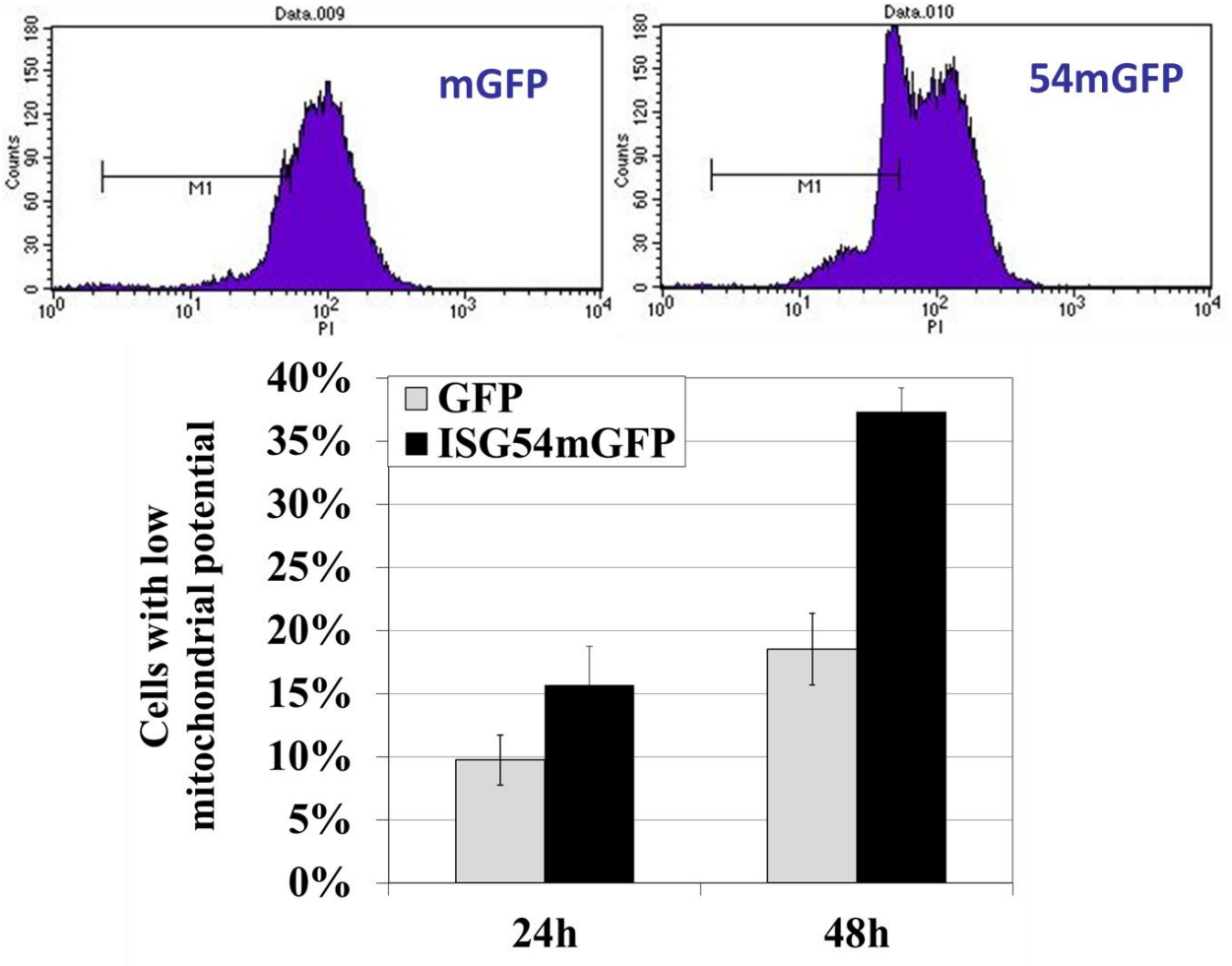

Figure 25. ISG54 expression decreases mitochondrial potential. HeLa cells were transfected with ISG54mGFP or mGFP as a control and at 24hs and 48hs their mitochondrial potential was evaluated by staining with MitoTracker Orange and analysis with flow cytometry. Distribution of cells according to the intensity of MitoTracker staining was visualized as a histogram. Dead cells displayed weak MitoTracker signal due to their low mitochondrial potential and localized in the left part of histogram. Expression of ISG54mGFP induced a characteristic peak coming from dying cells with low mitochondrial potential at 48hs (*upper panel*). Quantitative analysis of the Mitotracker staining showed that the cells expressing ISG54mGFP display lower mitochondrial potential than the cells expressing mGFP. Calculated *p* value at 48hs comparing cells expressing mGFP with cells expressing ISG54mGFP was <0.03

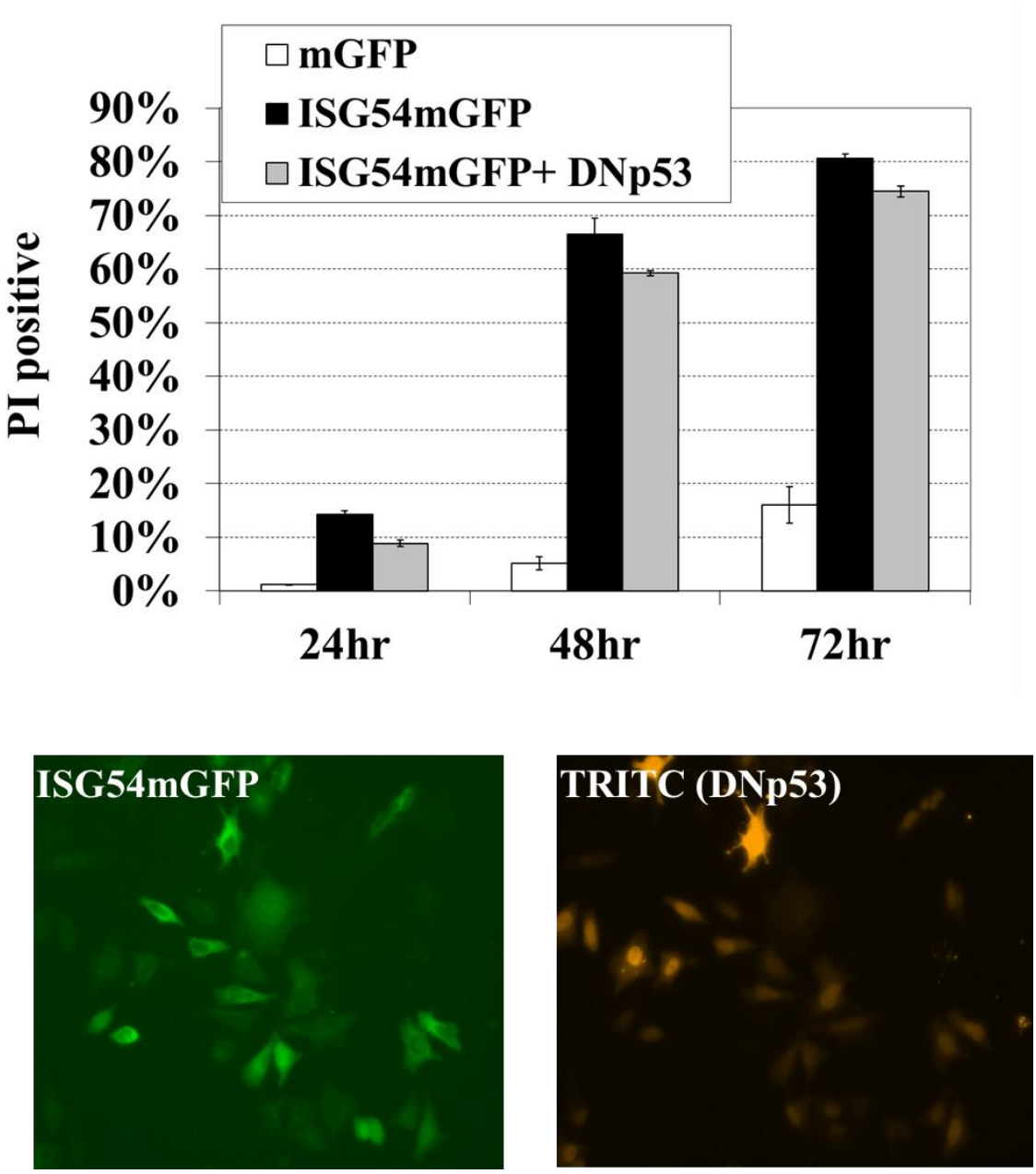

Figure 26. P53 is not required for ISG54 induced apoptosis. HeLa cells were cotransfected with ISG54mGFP and dominant negative form of p53 (DNp53). Flow cytometry analysis of cell death revealed no significant influence of DNp53 on ISG54-induced apoptosis (*upper panel*). Immunofluorescence was used to detect dominant negative p53 and showed that ISG54mGFP and p53 coexpress well in the same cells (*lower panel*)

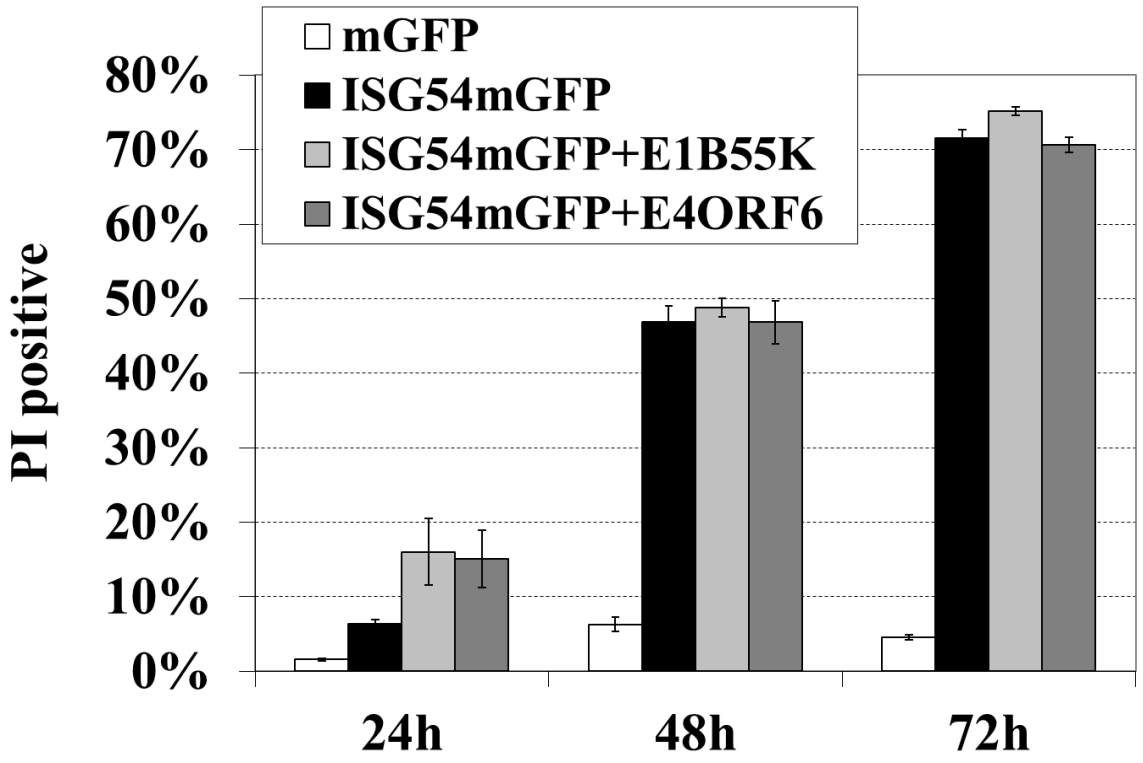

Figure 27. Viral inhibitors of p53 cannot inhibit ISG54-induced apoptosis. Cells were cotransfected with ISG54mGFP and adenoviral inhibitors of p53: E1B55K and E4ORF6. At 24hs, 48hs and 72hs cell were analyzed with flow cytometry and PI staining to evaluate levels of apoptosis. No inhibitory effect of viral proteins was observed.

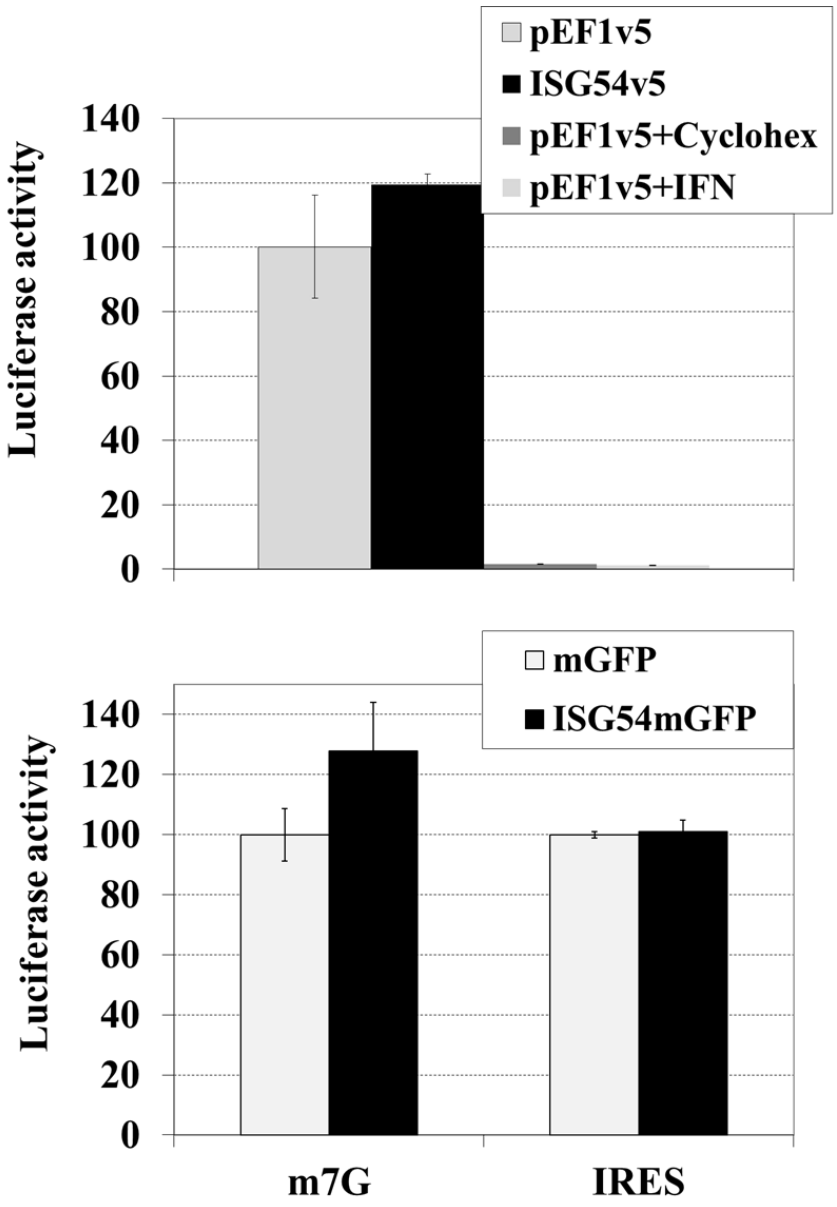

Figure 28. ISG54 does not have an effect on translation. *Upper panel*: HeLa cells were transfected with empty pEF1-v5 vector or ISG54-v5 for 12hs and subsequently transfected with m7G-capped and polyadenylated mRNA encoding luciferase. 6hs after RNA transfection cells were lysed and luciferase activity was measured Cells treated with 10 ug/ml cycloheximide or 1000U/IFN 1h prior to RNA transfection were used as a positive control for translation inhibition. *Lower panel:* HeLa cells were transfected with plasmids expressing mGFP or ISG54-mGFP for 16 h and subsequently were transfected with m7G-capped and -polyadenylated mRNA encoding luciferase (*m7G*) or with polyadenylated mRNA encoding luciferase regulated by a 5'-IRES (*IRES*). GFP-positive cells were isolated by FACS 5 h after mRNA transfection, and luciferase activity was measured

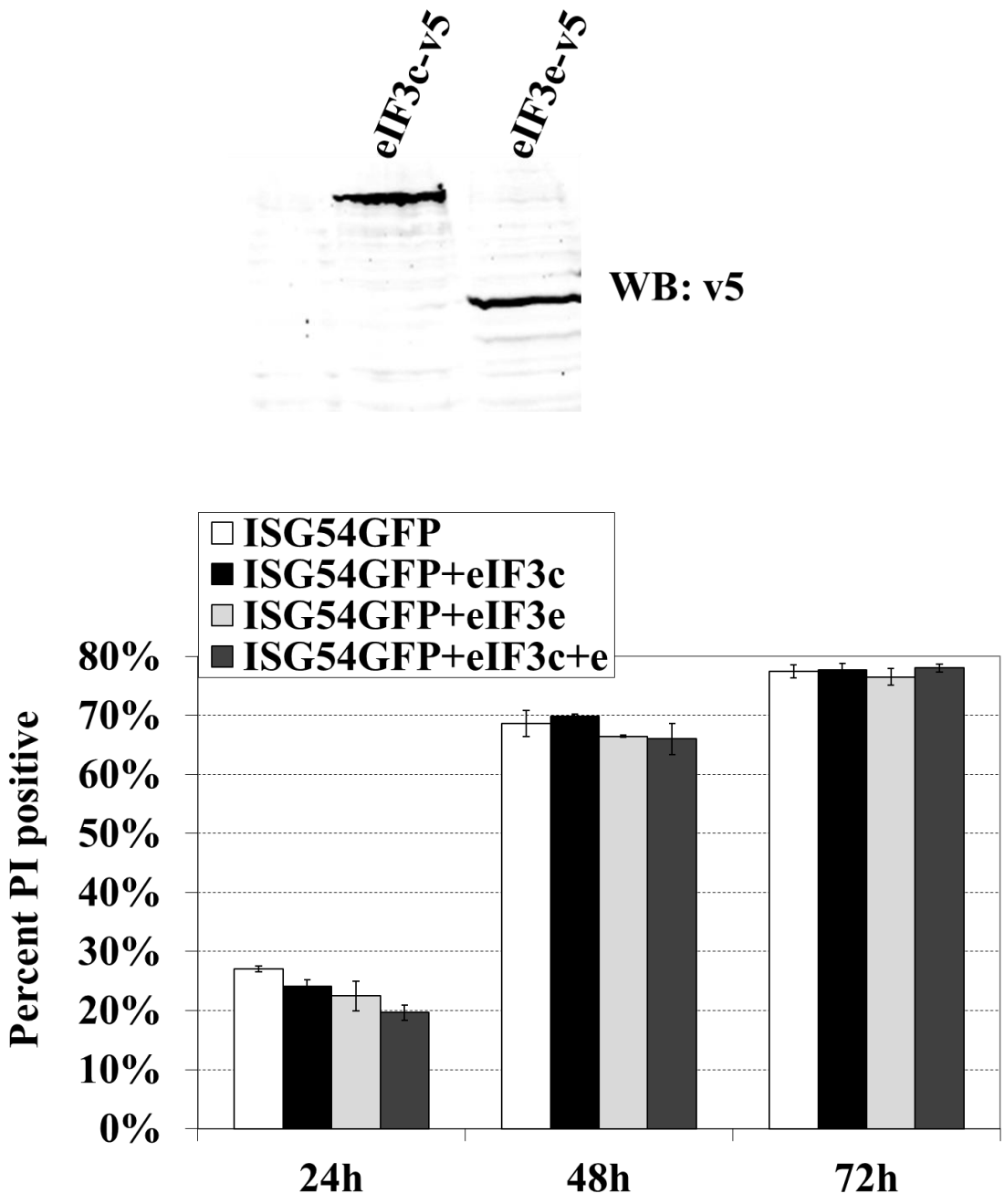

Figure 29. Ectopic expression of translation factors does not inhibit ISG54-induced apoptosis. Eukaryotic Initiation factors 3c and 3e were cloned into pEF1-v5 plasmid and their expression was verified with Western-blotting (*upper panel*). HeLa cells were cotransfected with ISG54mGFP and eIF3c-v5 or ISG54mGFP and eIF3e-v5 or ISG54mGFP and eIF3c-v5 and eIF3e-v5 together. Cells were evaluated for apoptosis with annexin V staining and flow cytometry. No influence of translation factors on ISG54 promoted apoptosis was observed *(lower panel).*

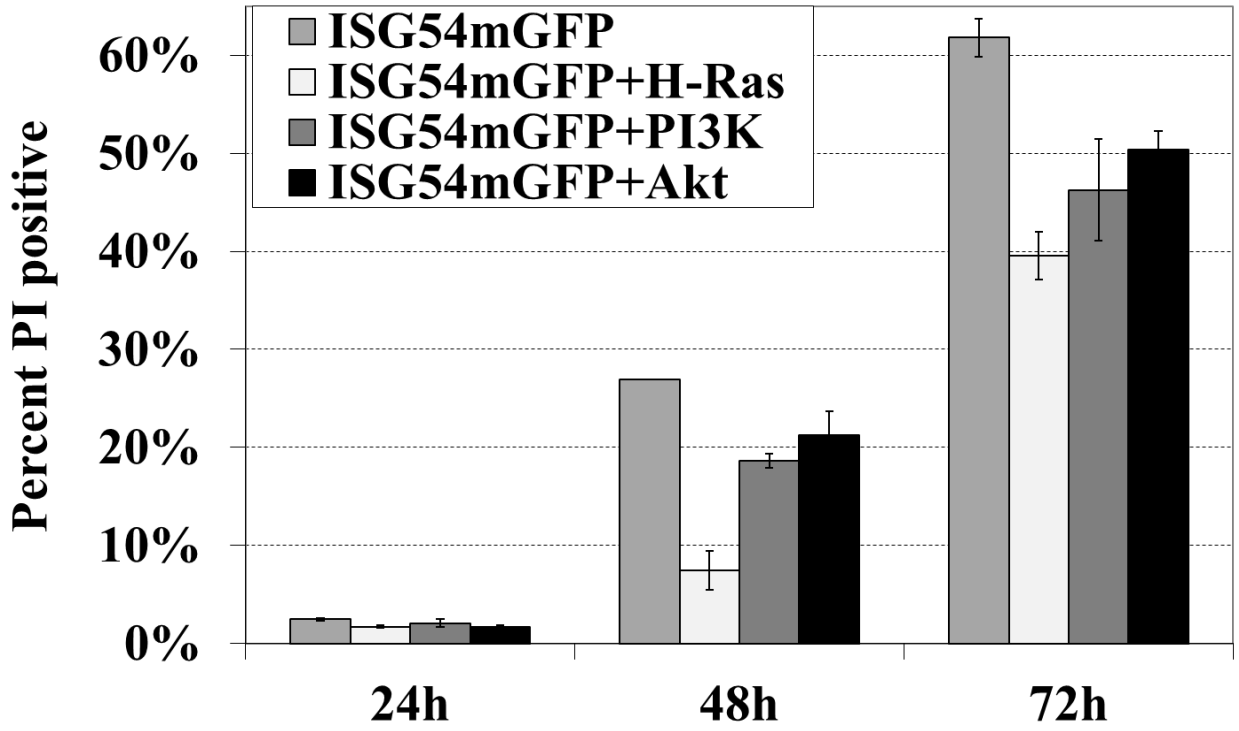

Figure 30. Components of Ras signaling pathway can partially inhibit ISG54-induced apoptosis. HeLa cells were transfected with ISG54mGFP and the constitutive active components of H-Ras signaling pathway: H-Ras-V12 mutant, constitutive active Akt kinase and constitutively active PI3K kinase. Apoptosis in cells was evaluated with PI staining and flow cytometry. H-Ras had the strongest inhibitory effect while the effect of Akt and PI3K was more moderate. Calculated *p* values comparing cells transfected with ISG54mGFP and cells cotransfected with ISG54mGFP and components of Ras signaling pathway were < 0.05.

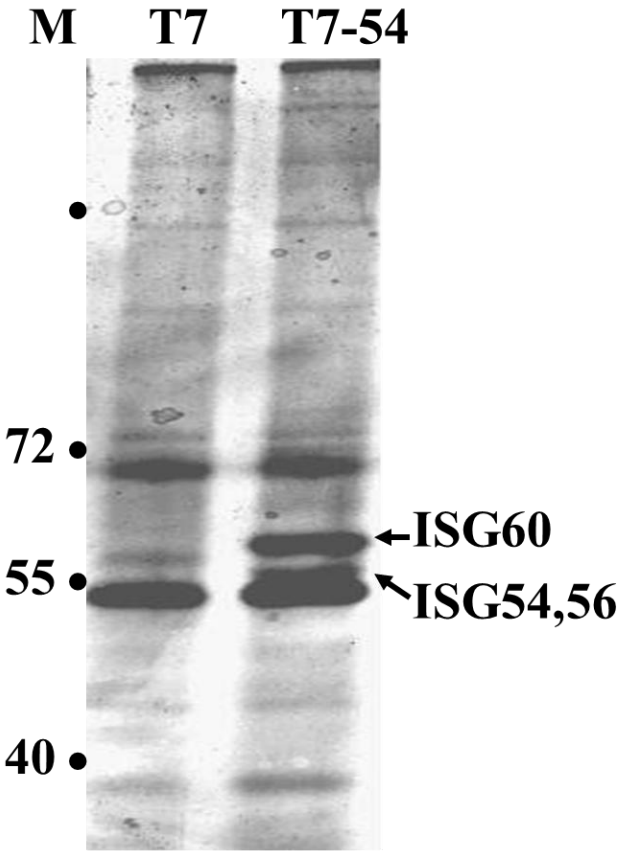

Figure 31. ISG54 forms oligomers with itself, ISG56 and ISG60. HeLa cells were transfected with T7-ISG54 or T7-empty vector for 24 h, and immunocomplexes were collected from cell lysates with anti-T7 antibodies. Proteins were separated by SDS-PAGE and silver-stained, and proteins specific to ISG54 expression were identified by mass spectrometry as ISG60 (*upper band*) and ISG56 and ISG54 (*lower band*). Molecular mass standards are indicated (*M*) in kDa.

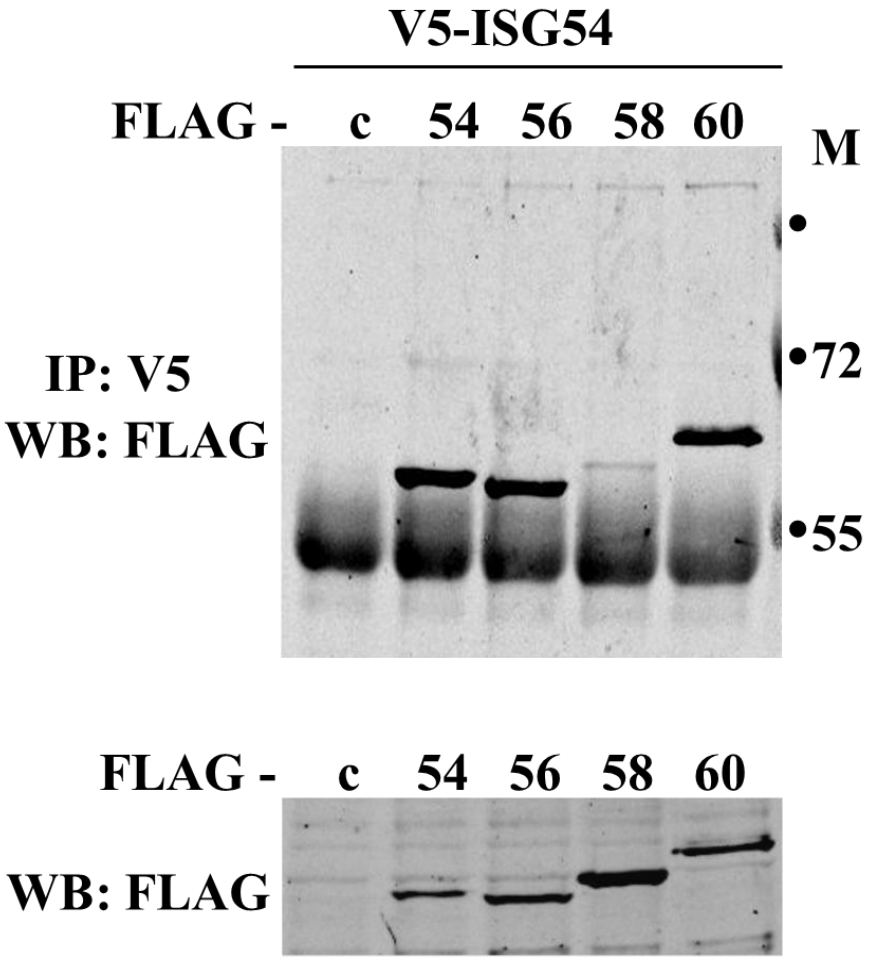

Figure 32. ISG54 interacts with itself, with ISG56 and ISG60. HeLa cells were co-transfected with V5-ISG54 and FLAG-empty vector (*c*) or FLAG-ISG54 (54), FLAGISG56 (56), FLAG-ISG58 (58), or FLAG-ISG60 (60). *Upper panel:* ISG54 protein was immunoprecipitated (*IP*) with anti-V5 antibodies, and associated proteins were detected by Western blot with anti-FLAG antibodies. *Lower panel:* Input expression of all FLAG-tagged ISG constructs was evaluated by Western blot with anti-FLAG antibodies.

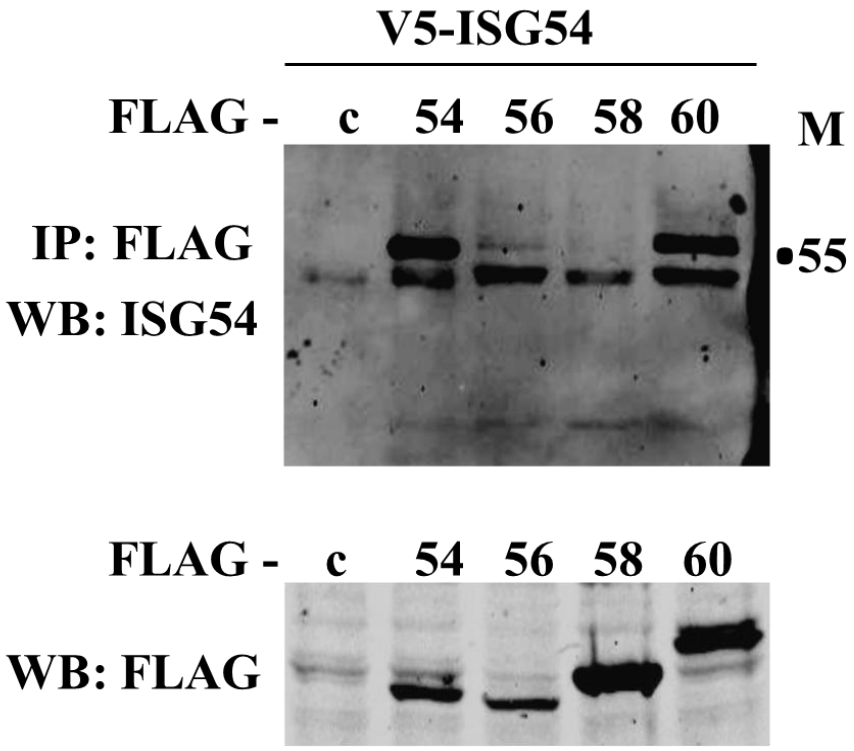

Figure 33. ISG54 interacts with ISG56, ISG60 and with itself. HeLa cells were co-transfected with V5-ISG54 and FLAG-empty vector (*c*) or FLAG-ISG54 (54), FLAG ISG56 (56), FLAG-ISG58 (58), or FLAG-ISG60 (60). *Upper panel:* FLAG-tagged ISG proteins were immunoprecipitated (*IP*) with anti-FLAG antibodies, and associated ISG54 was detected by Western blot with anti-ISG54 antibodies. *Lower panel:* Expression of all FLAG-tagged ISG constructs was evaluated by Western blot with anti-FLAG antibodies.

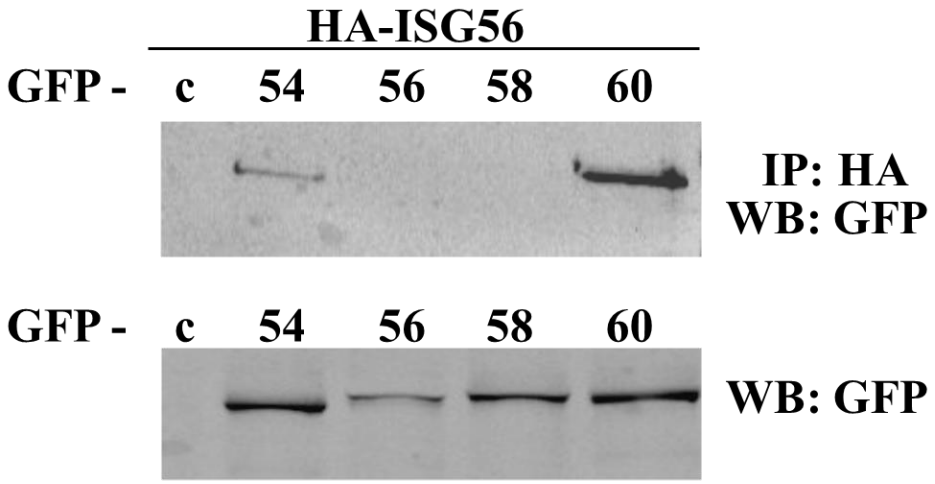

Figure 34. ISG56 interacts with ISG54 and ISG60. HeLa cells were co-transfected with HA-ISG56 and GFP-empty vector (*c*) or GFP-ISG54 (54), GFP ISG56 (56), GFP-ISG58 (58), or GFP-ISG60 (60). *Upper panel:* GFP-tagged ISG proteins were immunoprecipitated (*IP*) with anti-GFP antibodies, and associated ISG56 was detected by Western blot with anti-HA antibodies. *Lower panel:* Expression of all GFP-tagged ISG constructs was evaluated by Western blot with anti-GFP antibodies.

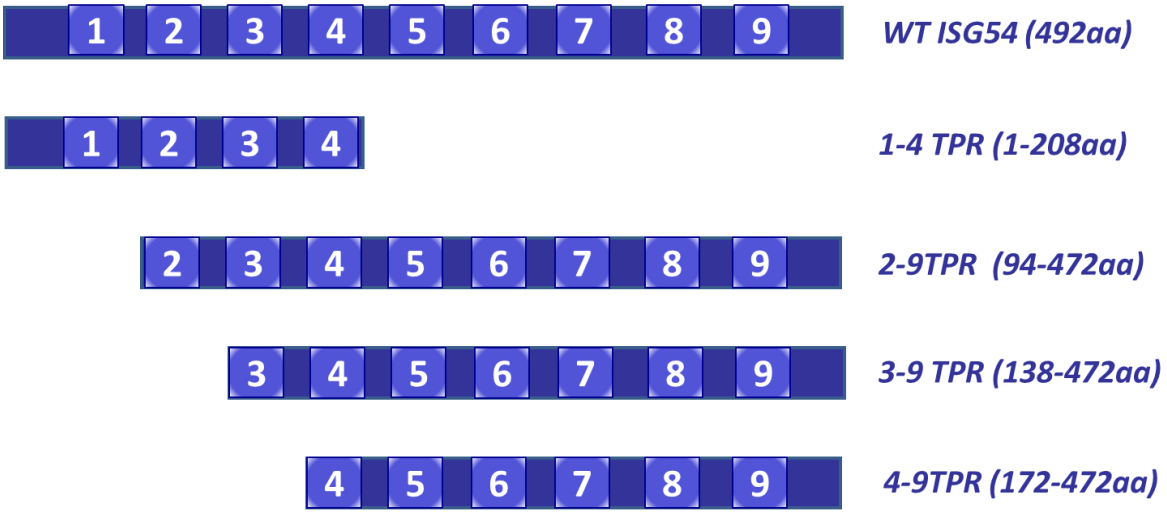

Figure 35. Truncations of ISG54. A schematic diagram of full length ISG54 and four truncated constructs that were v5-tagged and used to study interactions with other members of ISG54 family. Diagram shows amino acid positions and TPR content of each of deletion mutations.

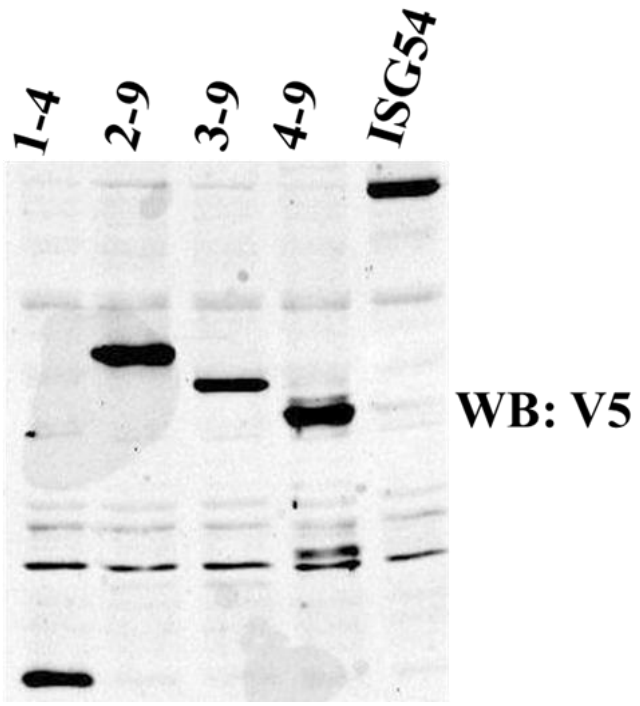

Figure 36. Expression of V5-tagged ISG54 truncations that were presented on figure 33. All the constructs expressed well and were easily detectable by Western blot. Numbers correspond to TPR domain within ISG54

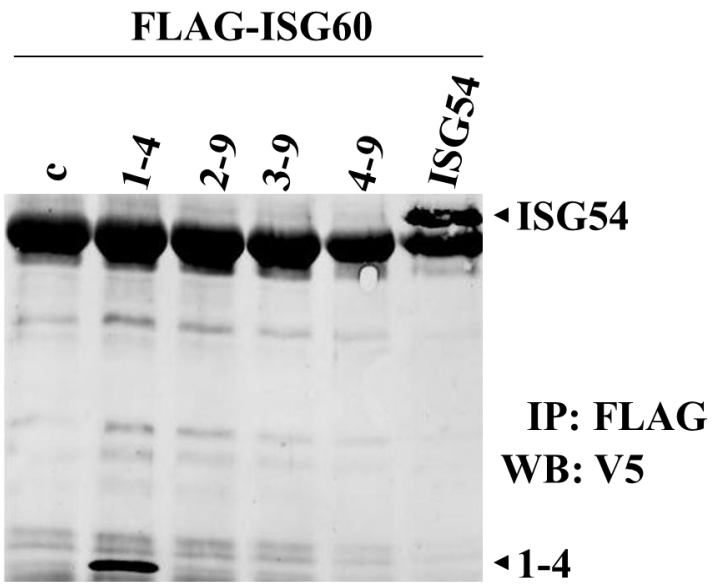

Figure 37. First TPR domain of ISG54 is necessary for binding to ISG60. HeLa cells were co-transfected with FLAG-ISG60 and either empty vector (c), one of the truncations of ISG54-V5 (noted by TPR content), or full-length ISG54-V5. Immunoprecipitation (IP) of ISG60 was performed with anti-FLAG antibody, and Western blot was performed with anti-V5 antibody to detect associated ISG54 fragments.

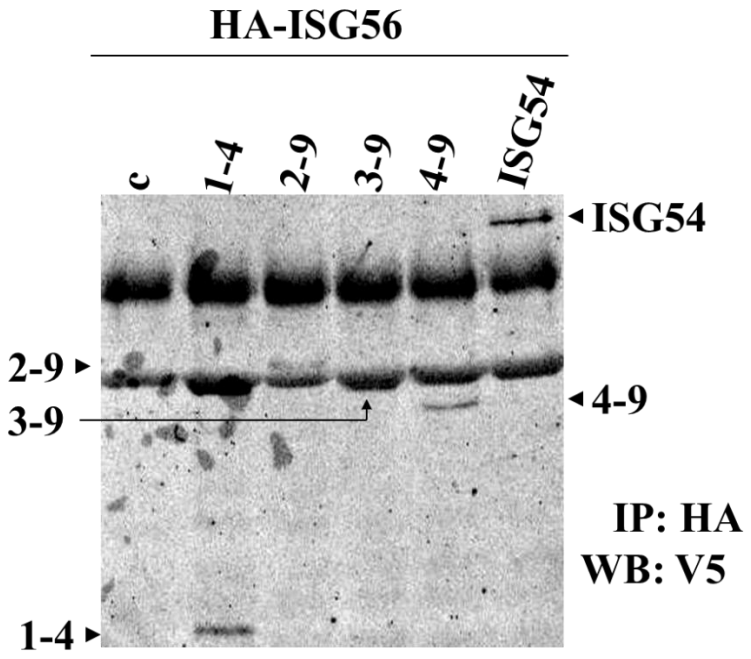

Figure 38. Both N and C-terminal regions of ISG54 participate in its binding to ISG56. HeLa cells were co-transfected with HA-ISG56 and one of the truncated versions of ISG54-V5 as in Figure 35. Immunoprecipitation of ISG56 was performed with anti-HA antibody, and associated ISG54 fragments were detected by Western blot with anti-V5 antibody.

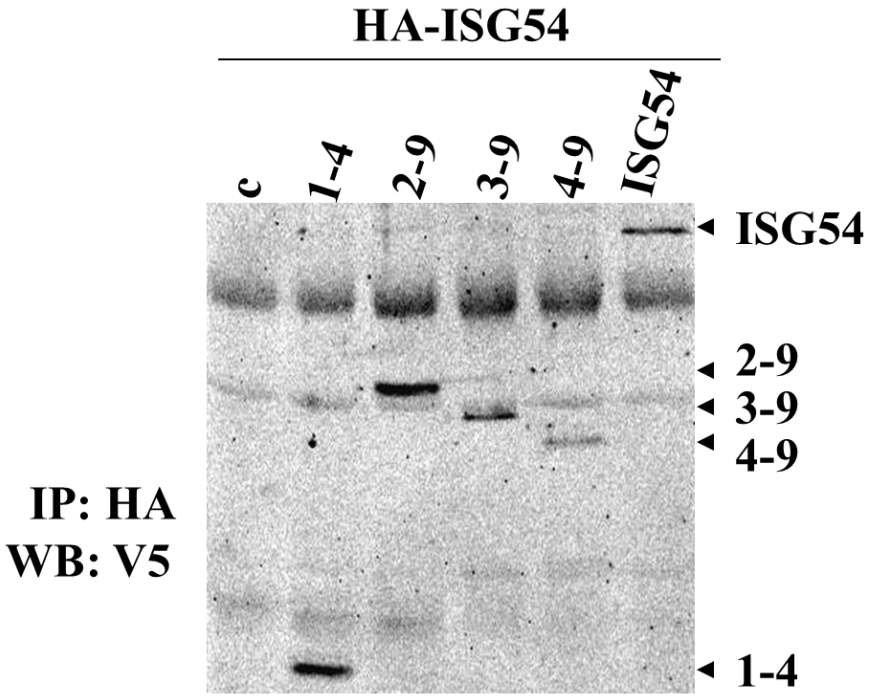

Figure 39. Both N and C-terminal part of ISG54 participate in its self-oligomerization. HeLa cells were co-transfected with HA-ISG54 and truncated versions of ISG54-V5 as in the Figures 35,36. Immunoprecipitation of ISG54 was performed with anti-HA antibody, and associated ISG54 fragments were identified by Western blot with anti-V5 antibody.

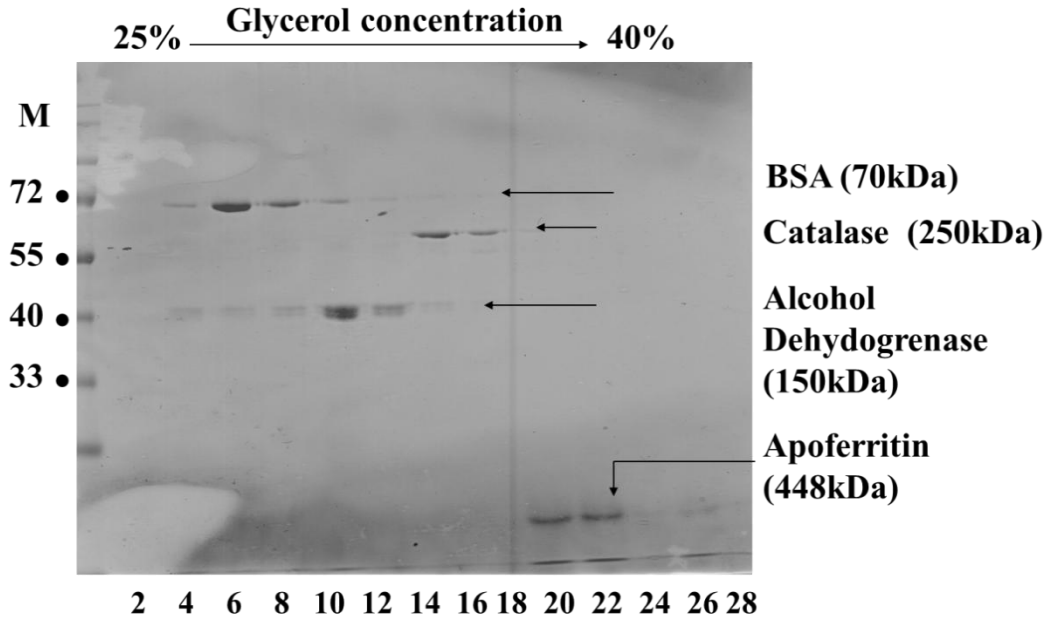

Figure 40. Glycerol gradient sedimentation of protein markers. 50ug of bovine serum albumin (70 kDA), alcohol dehydrogenase (150kDa), catalase (250kDa) and apoferritin (448kDa) were loaded on the top of 25-40% glycerol gradient and centrifuged overnight at 40000 rpm. Fractions were collected from the top of the gradient, and applied on an SDS-PAGE gel. During electrophoresis subunits of oligomeric proteins dissociate: catalase, alcohol dehydrogenase and apoferritin. SDS-PAGE gel was stained with Coomassie Blue to visualize proteins and their positions in fractions served as a reference standard. Numbers of fractions are indicated at the bottom and molecular mass markers for Western blot (M) are indicated on the side in kDa.

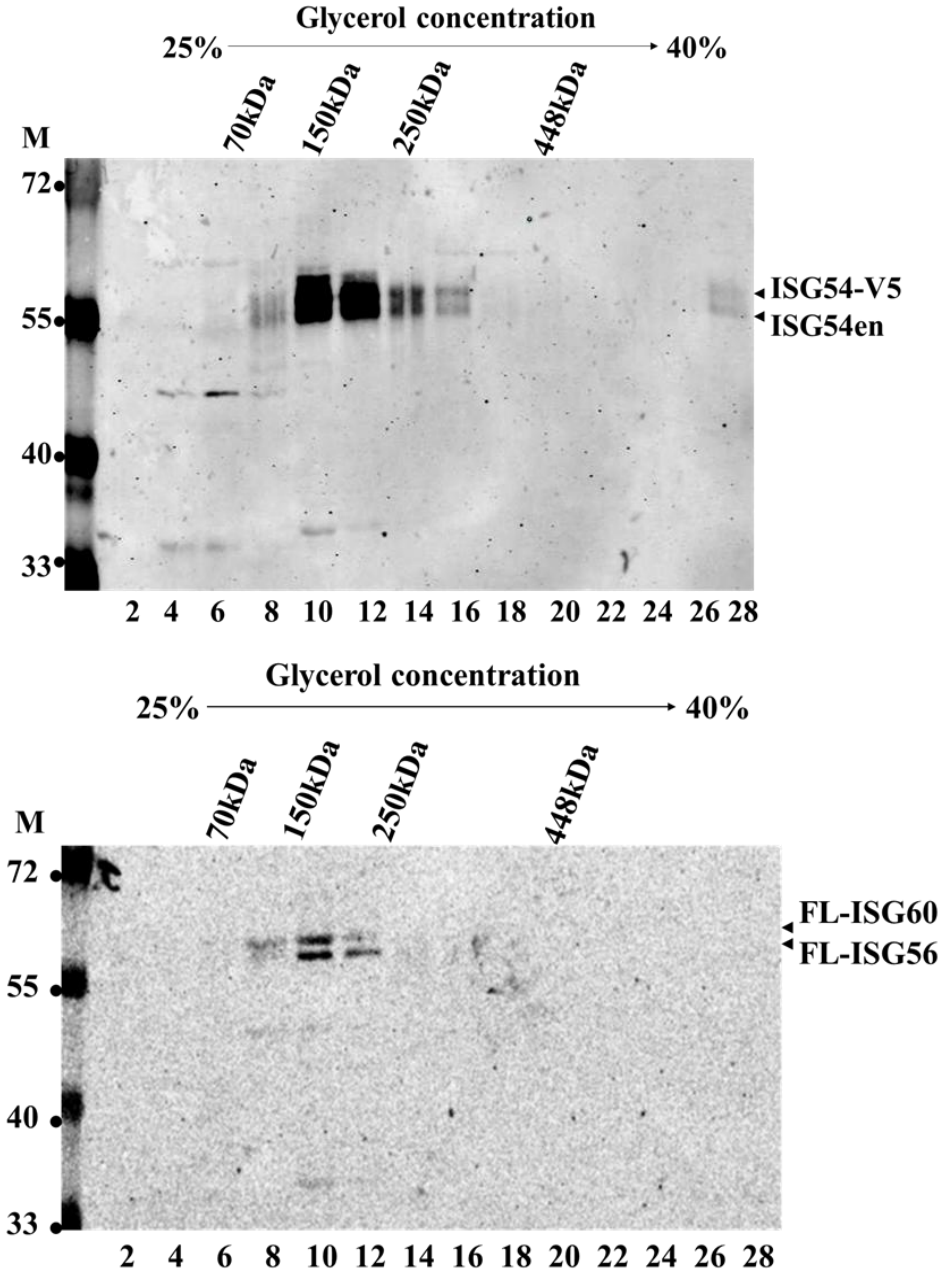

Figure 41. ISG54, 56 and 60 colocalize in the same fractions. HeLa cells were co-transfected with ISG54-V5, FLAG-ISG56, and FLAG-ISG60 plasmids and treated with IFN for 18 h. Lysates were sedimented through 25–40% glycerol gradients in parallel with mass markers present in figure 38, and fractions were collected Western blot with anti-ISG54 antibody was used to detect ISG54-V5 and endogenous ISG54 (ISG54en). (*upper panel*). Western blot with anti-FLAG (FL) antibody detected both FLAG-ISG56 and FLAG-ISG60 (*lower panel*). The sedimentation positions of molecular mass markers in the gradients are indicated at the top and molecular mass markers for Western blot (M) are indicated on the side in kDa. Numbers of fractions are displayed on the bottom

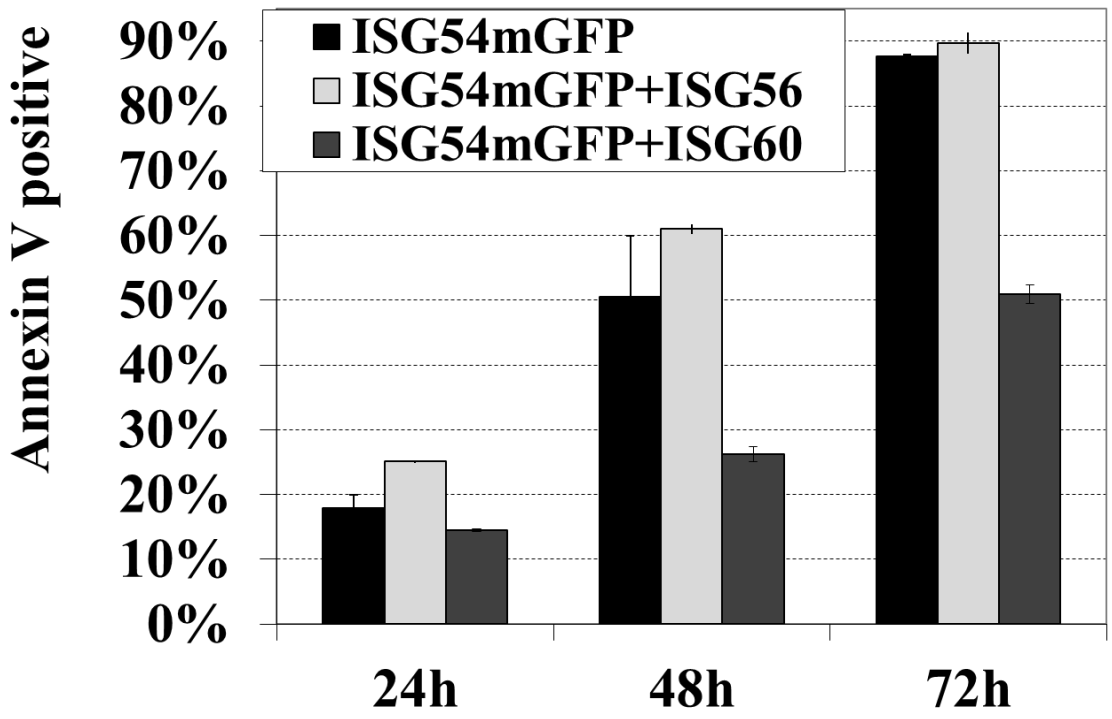

Figure 42. ISG60 inhibit ISG54 induced apoptosis. HeLa cells were cotransfected with ISG54mGFP and either control plasmid or ISG56-v5 or ISG60-v5. GFP positive cells were analyzed for annexin V staining with flow cytometry. While ISG56 had weak effect on ISG54 induced apoptosis, ISG60 significantly reduced ISG54 promoted cell death. Calculated *p* values for the inhibitory effect of ISG60 were <0.02 and <0.007 at 48 and 72 h, respectively.

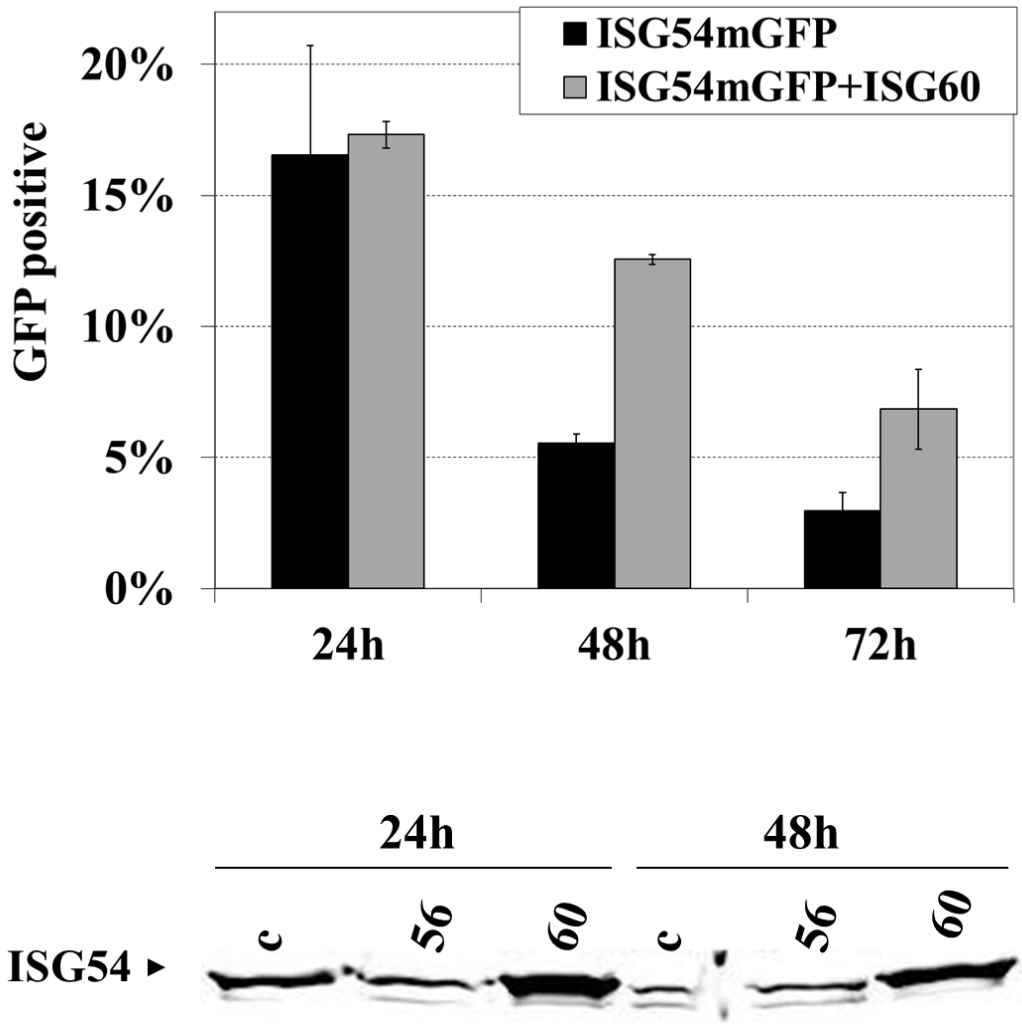

Figure 43. ISG60 stabilizes the levels of ISG54. *Upper panel:* HeLa cells from the experiment presented in figure 40 were analyzed with flow cytometry regarding number of GFP positive cells. In the presence of ISG60 number of the cells that express ISG54mGFP increased. *Lower panel:* Western blot from the cells that were cotransfected with ISG54mGFP and either control vector (c), or ISG56 or ISG60. In the presence of ISG60 levels of ISG54 are elevated.

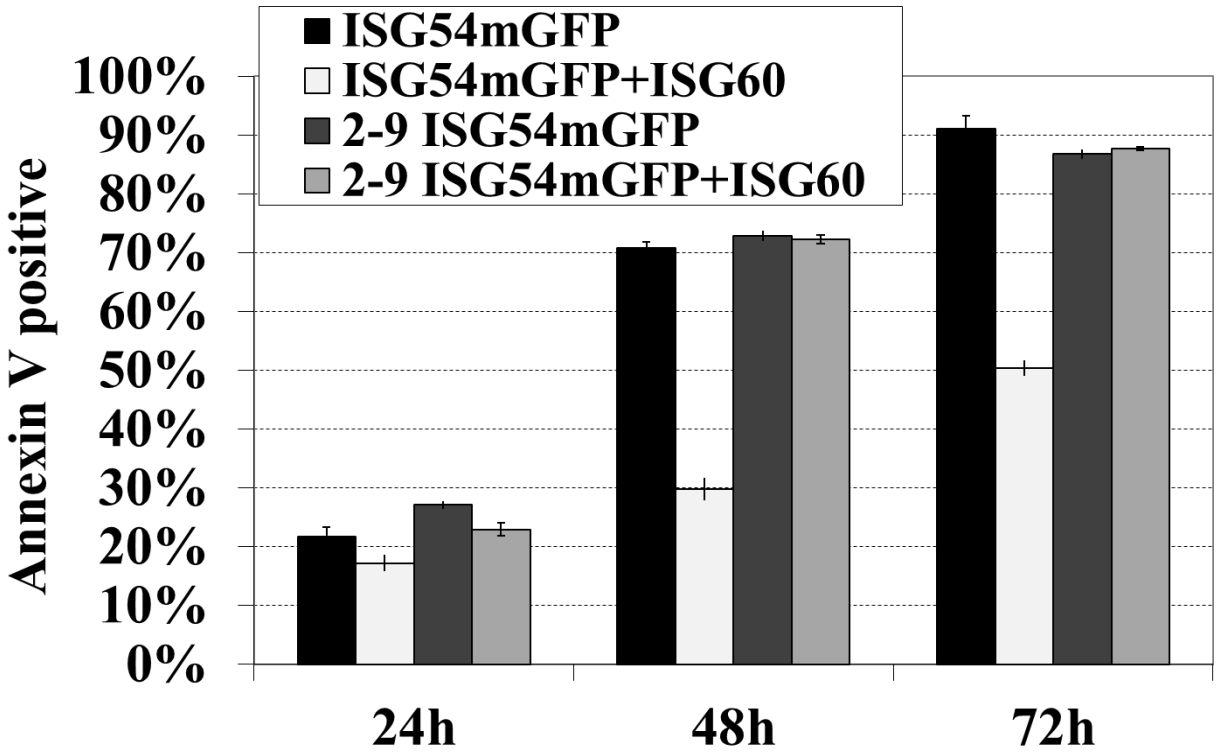

Figure 44. ISG60 inhibits apoptosis by binding to the first TPR domain of ISG54. HeLa cells were transfected with either ISG54-mGFP and empty vector, ISG54-mGFP and ISG60-V5, 2–9TPR-ISG54-mGFP and empty vector, or 2–9TPR-ISG54-mGFP and ISG60-V5. GFP-positive cells were analyzed for annexin V staining by flow cytometry after 24, 48, or 72 h post-transfection. ISG60 effectively inhibited apoptosis caused by full-length ISG54 but not by the mutant lacking first TPR domain. Calculated *p* values for the inhibitory effect of ISG60 were <0.003 and < 0.01 at 24h and 48h respectively.

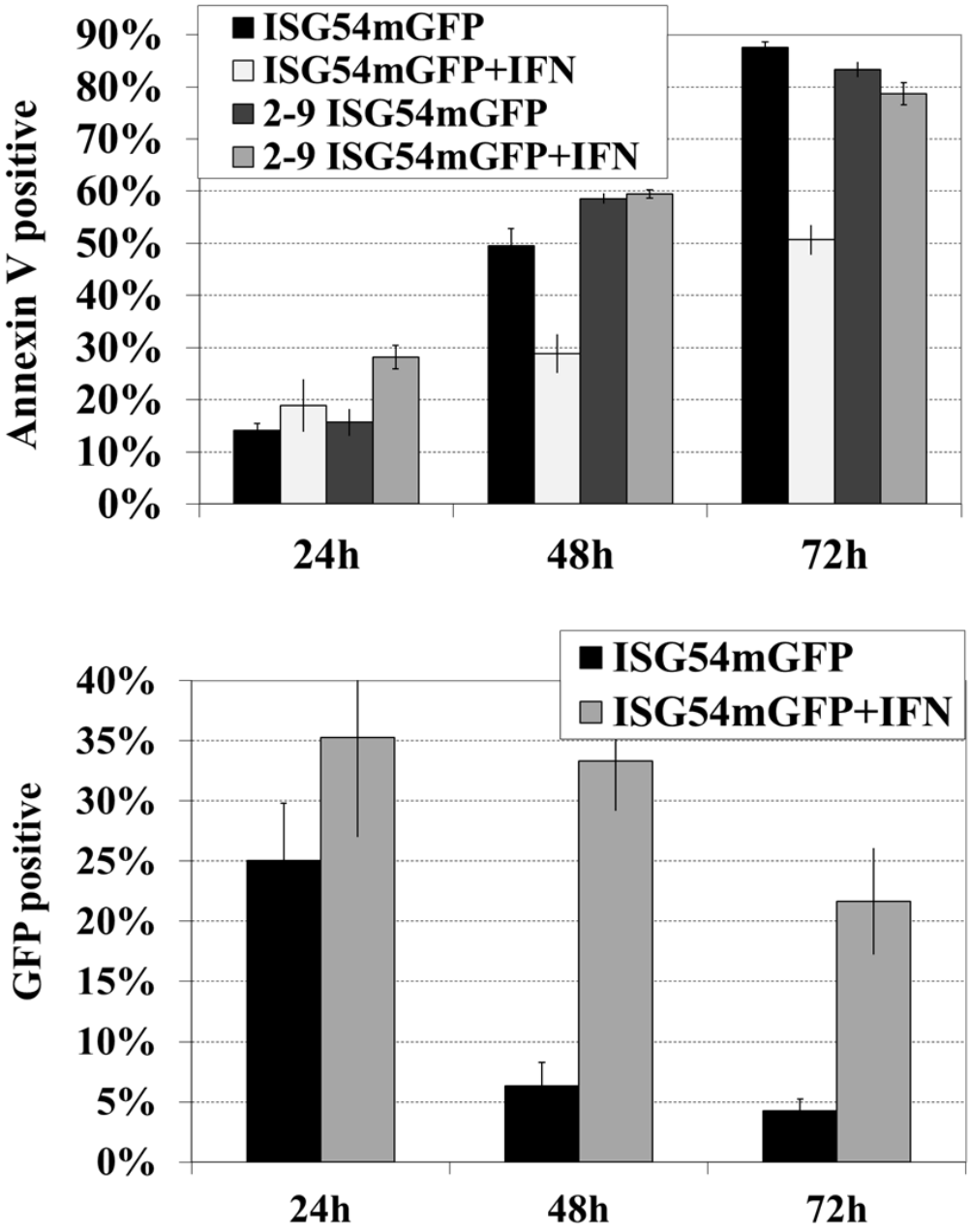

Figure 45. Interferon stimulation inhibits ISG54-induced apoptosis. Cells were transfected with ISG54mGFP or 2-9TPR-ISG54mGFP and after 12 hours the cells were untreated or treated with 2000 U/ml IFNα. GFP-positive cells were analyzed for annexin V staining by flow cytometry after 24, 48, or 72 h post-transfection. *Upper panel:* IFN treatment effectively inhibited apoptosis caused by full-length ISG54 but not by the mutant lacking first TPR domain. *Lower panel:* IFN treatment stabilized the number of cells expressing ISG54mGFP in culture. Calculated *p* values for the inhibitory effects of IFN were <0.01 and <0.008 at 48 and 72 h, respectively.

Figure 46. Truncations of ISG54 used for studying apoptosis. A schematic diagram of full length ISG54 and six truncated constructs that were mGFP-tagged and used to study their ability to induce cell death. Diagram shows amino acid positions and TPR content of each of deletion mutations.

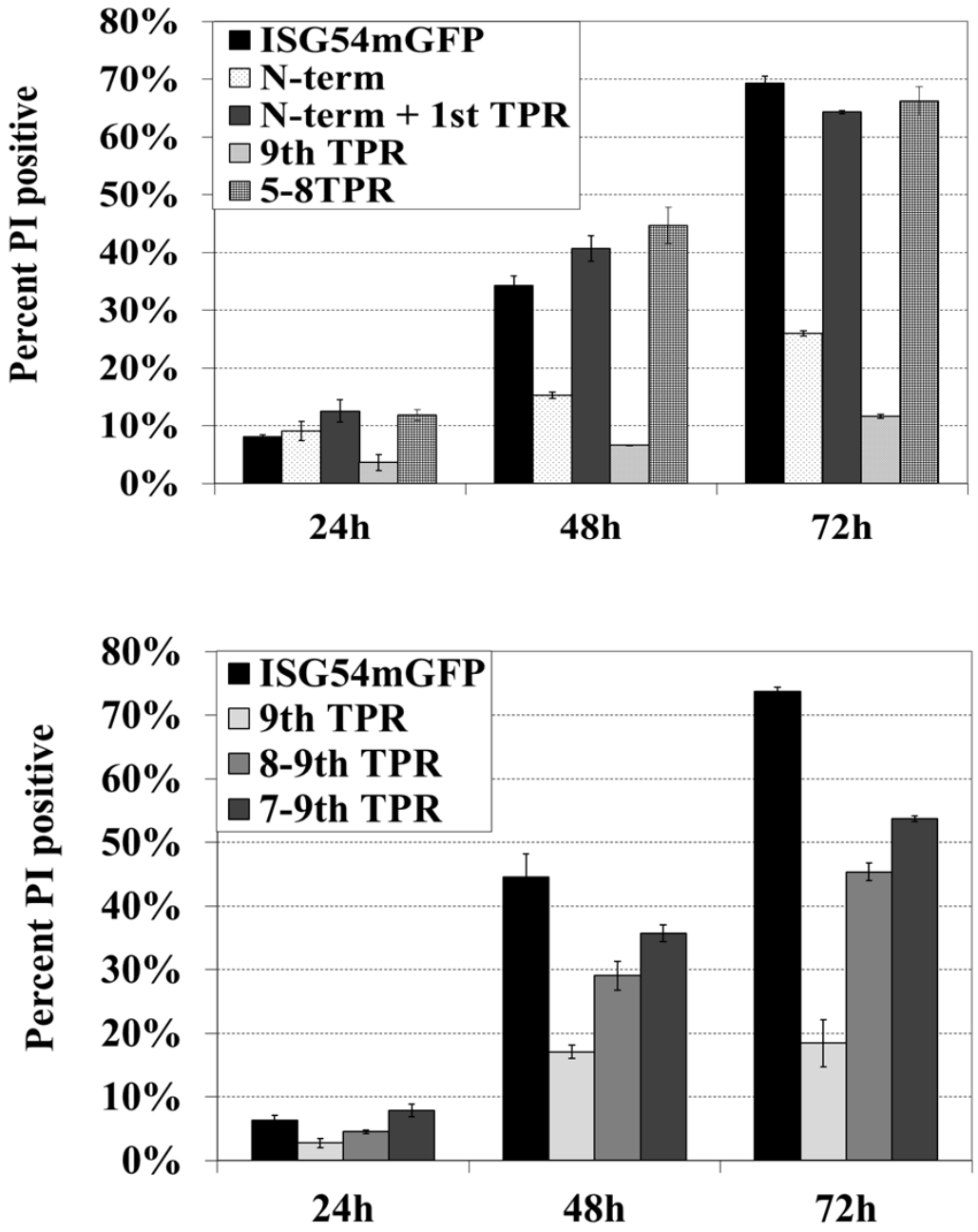

Figure 47. Ability of ISG54 truncations to induce apoptosis. HeLa cells were transfected with either ISG54mGFP or each of mGFP tagged truncations presented in Figure 44. *Upper panel*: Presence of the first TPR domain was sufficient to induce apoptosis as strong as full-length protein while the 9th TPR domain had no apoptotic effect. Fragment containing four TPR domains: 5-8 caused apoptosis similar to the full-length protein. *Lower panel:* 9th TPR domain of ISG54 displays limited pro-apoptotic effect but this effect increases proportionally to the number of added TPR domains. Calculated *p* values comparing apoptosis caused by full-length ISG54 with apotosis induced by truncated versions of the protein were <0.05.

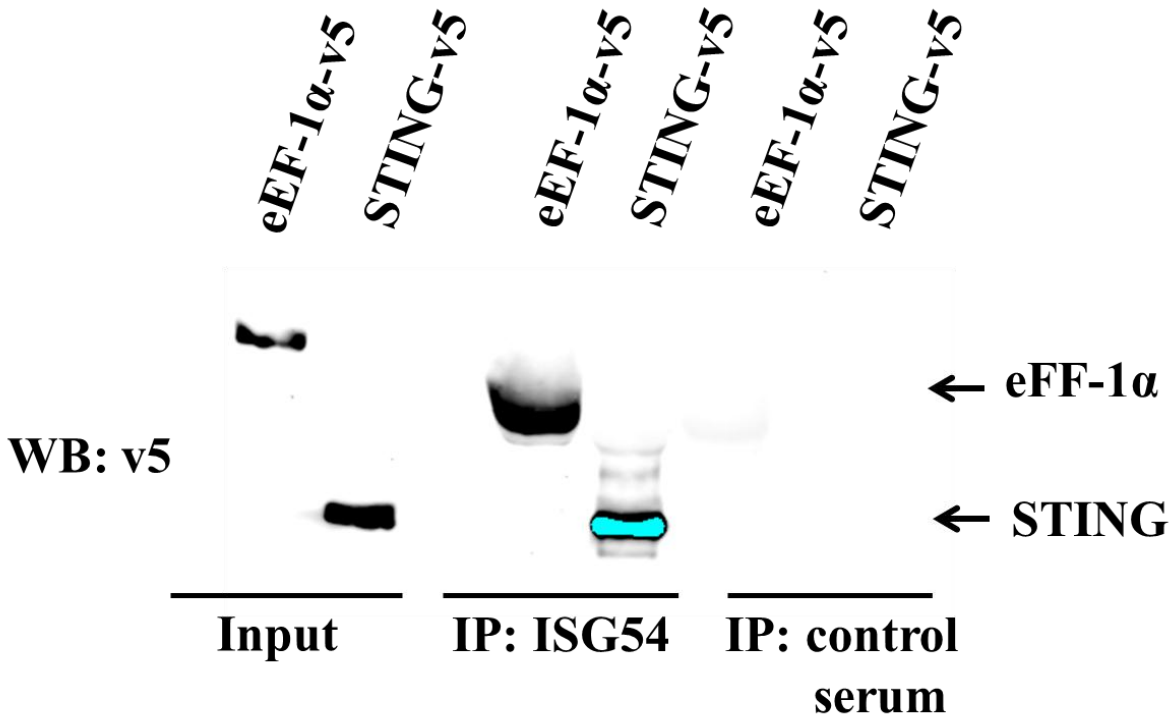

Figure 48. ISG54 interacts with eukaryotic elongation factor-1α (eEF1-α) and STING. HeLa cells were transfected with eEF-1α or STING-v5 and stimulated overnight with IFNα at 1000U/ml. The next day cells were lysed and endogenous ISG54 was immunoprecipitated with anti-ISG54 rabbit serum. As a control, non-specific rabbit serum was used. Associating proteins were detected by Western blot using anti-v5 antibodies.

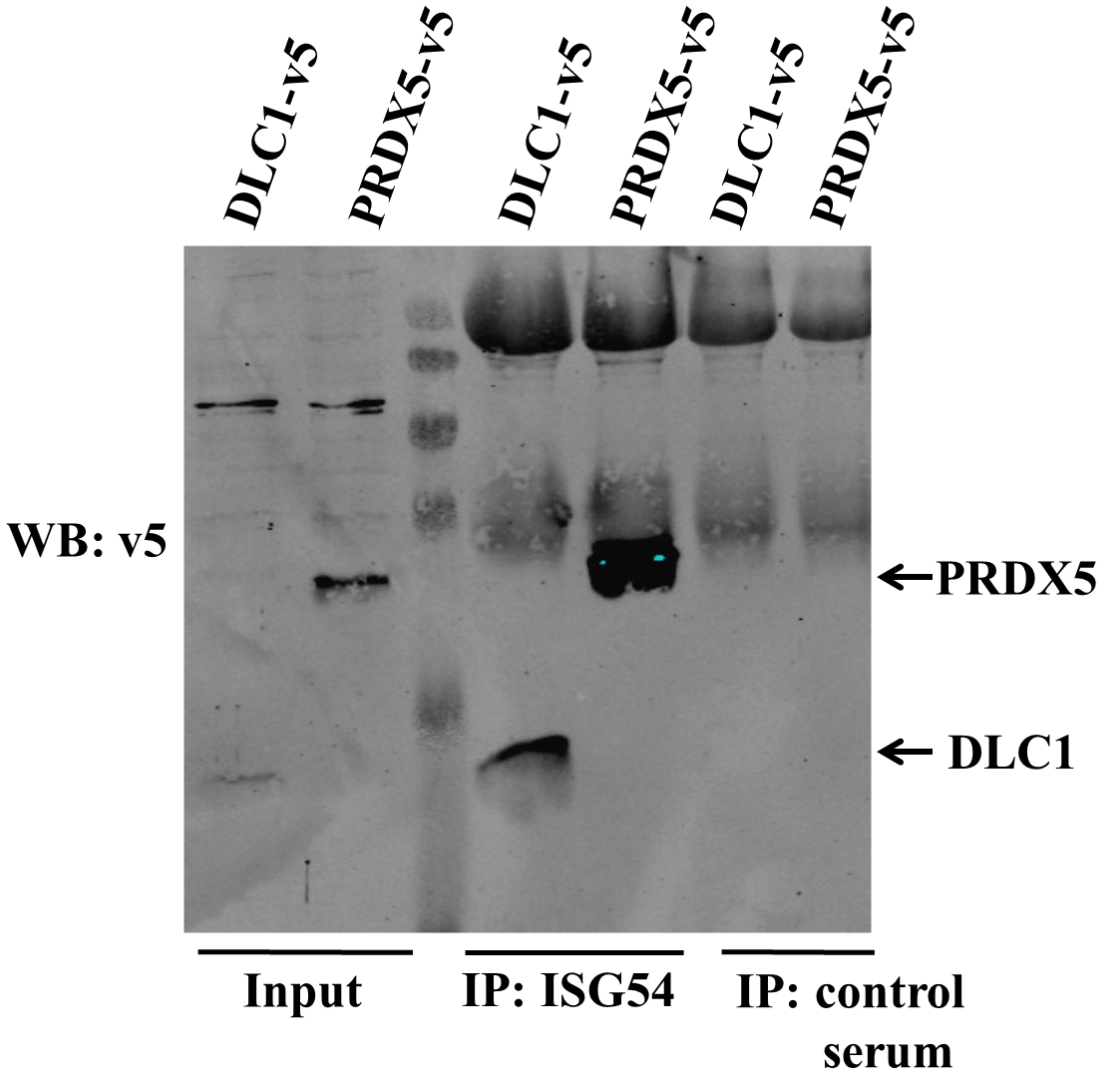

Figure 49. ISG54 interacts with dynein light chain 1 (DLC1) and peroxiredoxin 5 (PRDX5). HeLa cells were transfected with DLC1-v5 or PRDX5-v5 and stimulated overnight with IFNα at 1000U/ml. The next day cells were lysed and endogenous ISG54 was immunoprecipitated with anti-ISG54 rabbit serum. As a control, non-specific rabbit serum was used. Associating proteins were detected by Western-blot using anti-v5 antibodies.

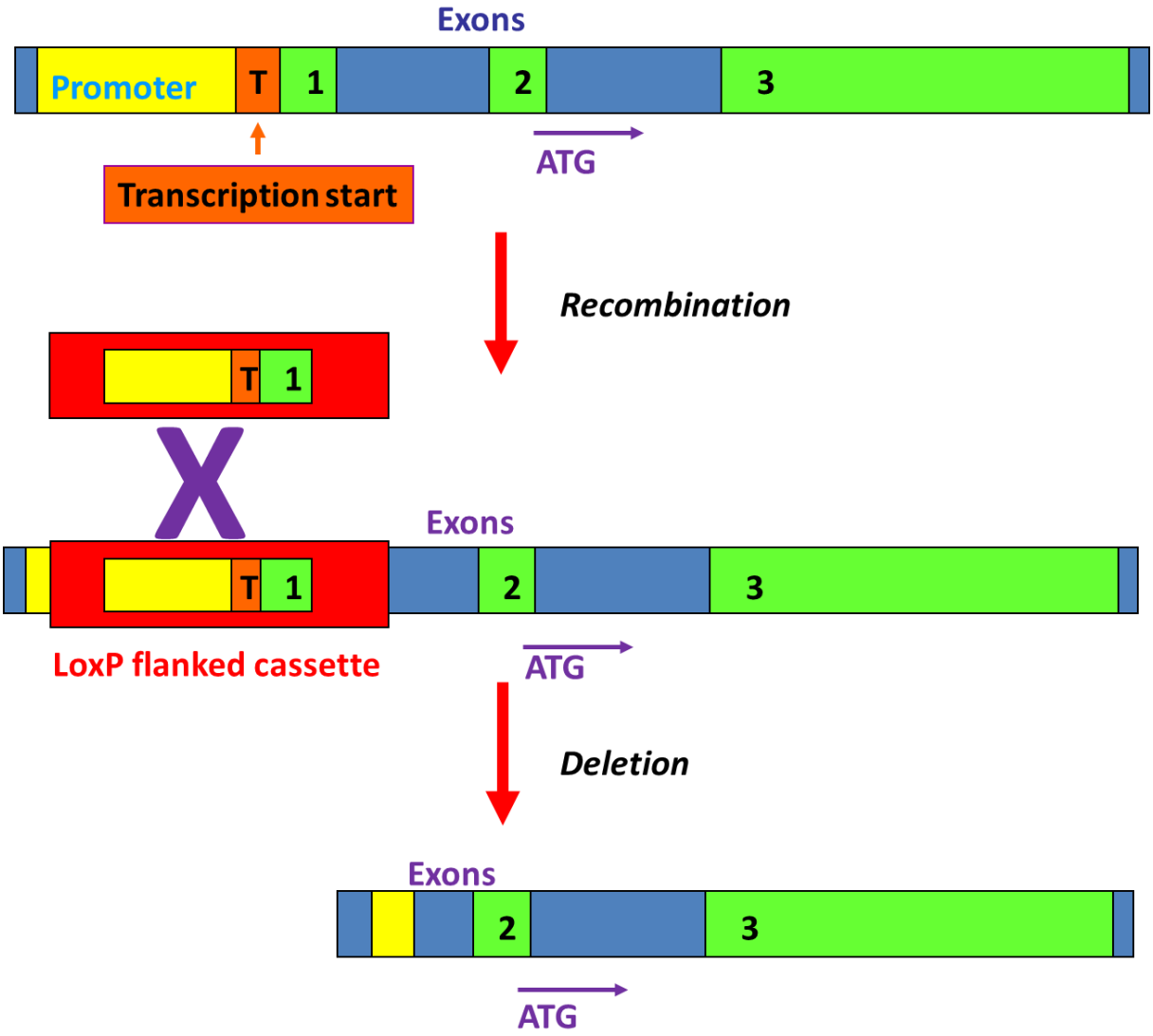

Figure 50. Schematic diagram of ISG54 knockout. Top diagram shows a simple layout of ISG54 gene with promoter, transcription start site (T), three exons (1-3) and translational start site (ATG). The targeting replacement plasmid consisted of LacZ gene and loxP flanked *neo* cassette was inserted through recombination into promoter region of ISG54 gene. Deletion of the insert was performed by Cre recombinase and as a result the promoter sequence and the first exon of ISG54 were removed. The entire coding sequence of the gene including the start codon remained intact.

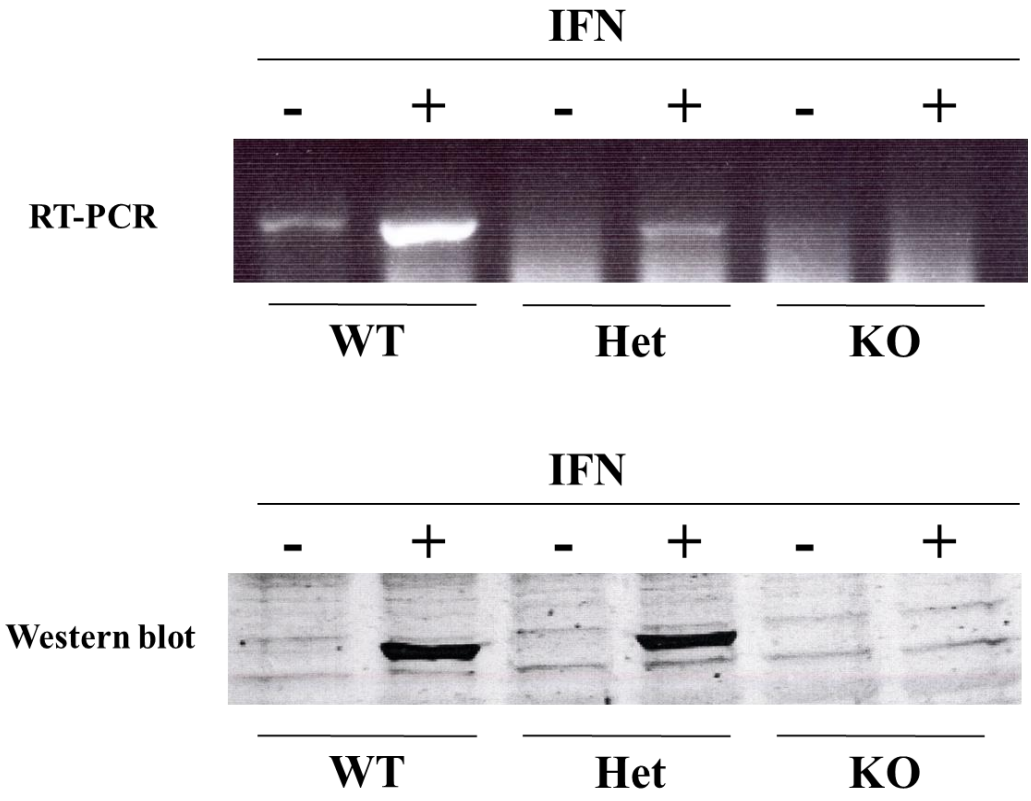

Figure 51. ISG54 knockout (KO) mice do not express ISG54. Splenocytes from wild-type, heterozygous or ISG54 knockout mice were collected lysed and analyzed for ISG54 expression both on the RNA (RT-PCR, *upper panel*) and the protein (Western-blot, *lower panel*) level. ISG54 knockout animals failed to produce ISG54 mRNA or protein.

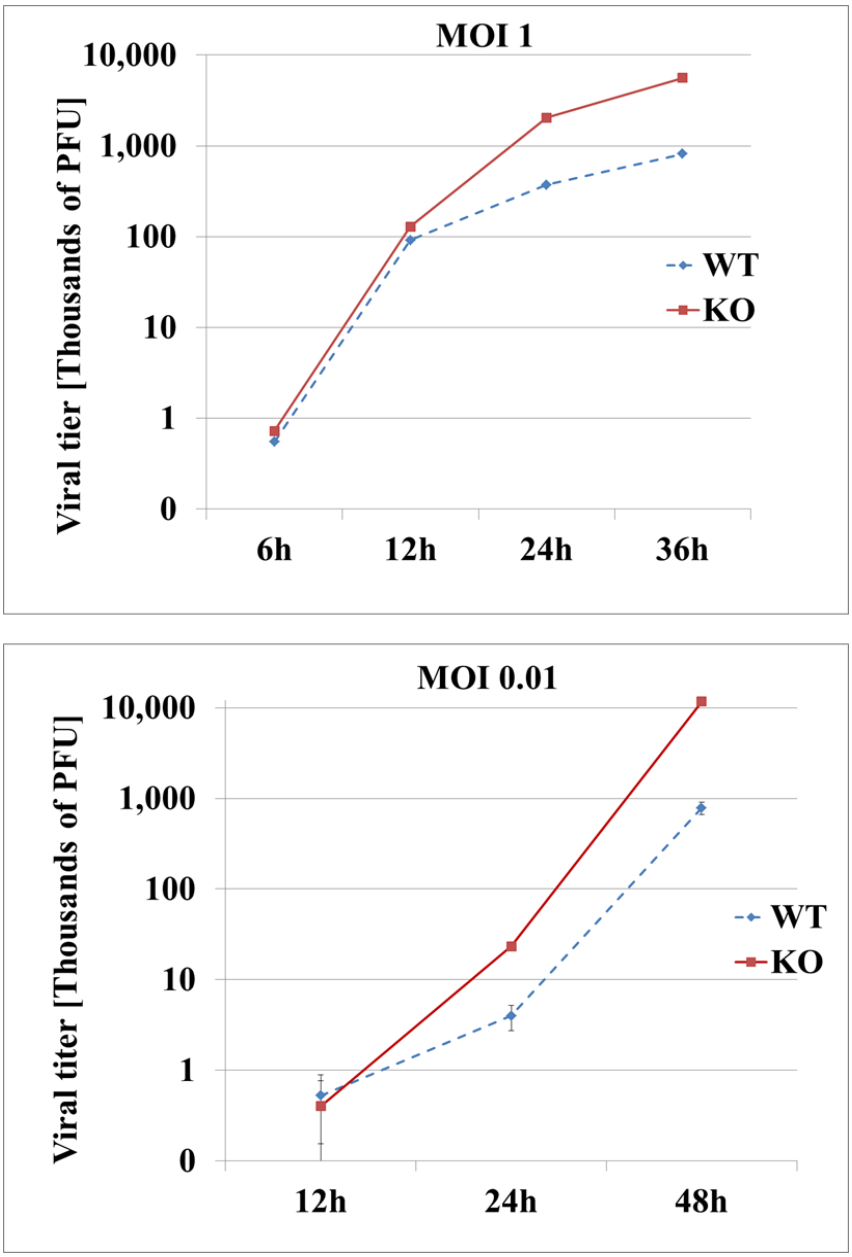

Figure 52. MHV68 replicates to higher titer in ISG54KO MEFs. Wild-type or ISG54 knockout Mouse Embryo Fibroblasts (MEFs) were infected with MHV68 at MOI 1.0 (*upper panel*) or MOI 0.01 (*lower panel*). Cells were harvested at different timepoints after infection and the viral titer was determined with plaque assay. ISG54 knockout MEFs display over five times higher viral titer at MOI1 and over tenfold higher viral titer at MOI 0.01. Calculated *p* values at 24hs and 48hs were <0.03 and <0.01 respectively

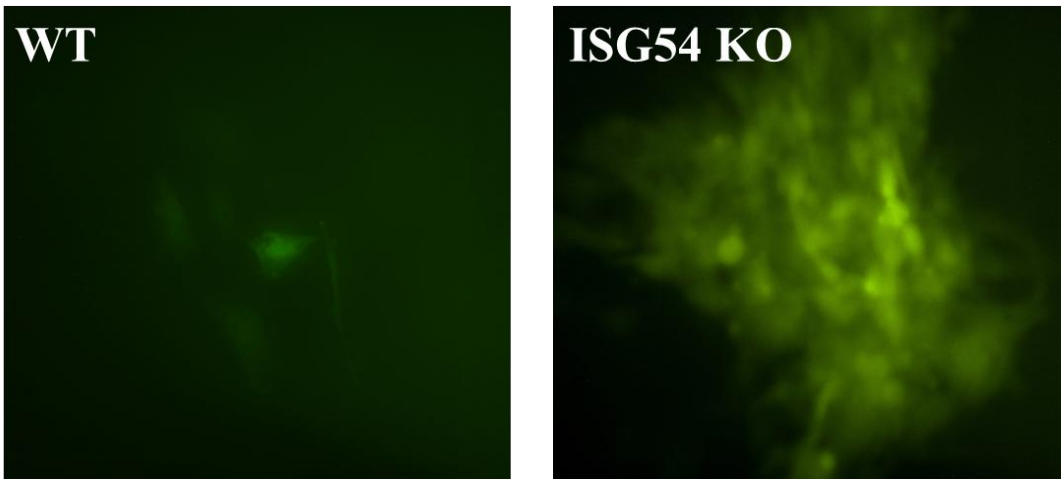

Figure 53. Spreading of MHV68 infection is increased in ISG54KO MEFs. Wild-type or ISG54 knockout (KO) MEFs were infected with MHV68 coding for YFP protein at MOI 0.01. At 48 hs cells were studied with fluorescence microscopy to evaluate the infection progression and spreading of the virus. ISG54 deficient MEFs displayed wide areas infected with the YFP virus (*right*) while in the wild-type culture only single cells showed yellow fluorescence (*left*). These observations suggested that infection progresses faster and virus spreads more rapidly in ISG54 knockout MEFs

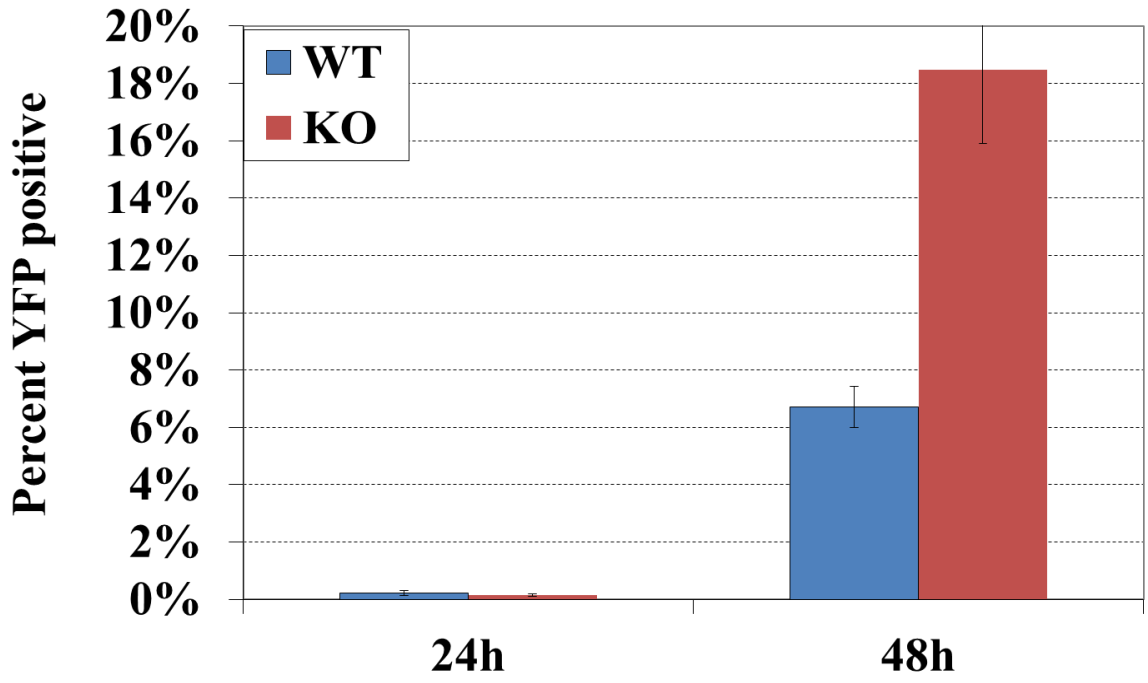

Figure 54. Quantitation of MHV68-YFP spreading in WT vs. ISG54KO MEFs Wild-type or ISG54 knockout MEFs were infected with MHV68 coding for YFP protein at MOI 0.01. At 24hs and 48hs after infection MEFs were analyzed with flow cytometry to evaluate the number of YFP positive cells. At 24hs number of infected cells was low and no significant difference could be observed. However, at 48hs ISG54 knockout MEFs displayed over twofold higher percentage of cells infected with MHV68. Calculated *p* value comparing number YFP positive cells between WT and KO MEFS was < 0.001.

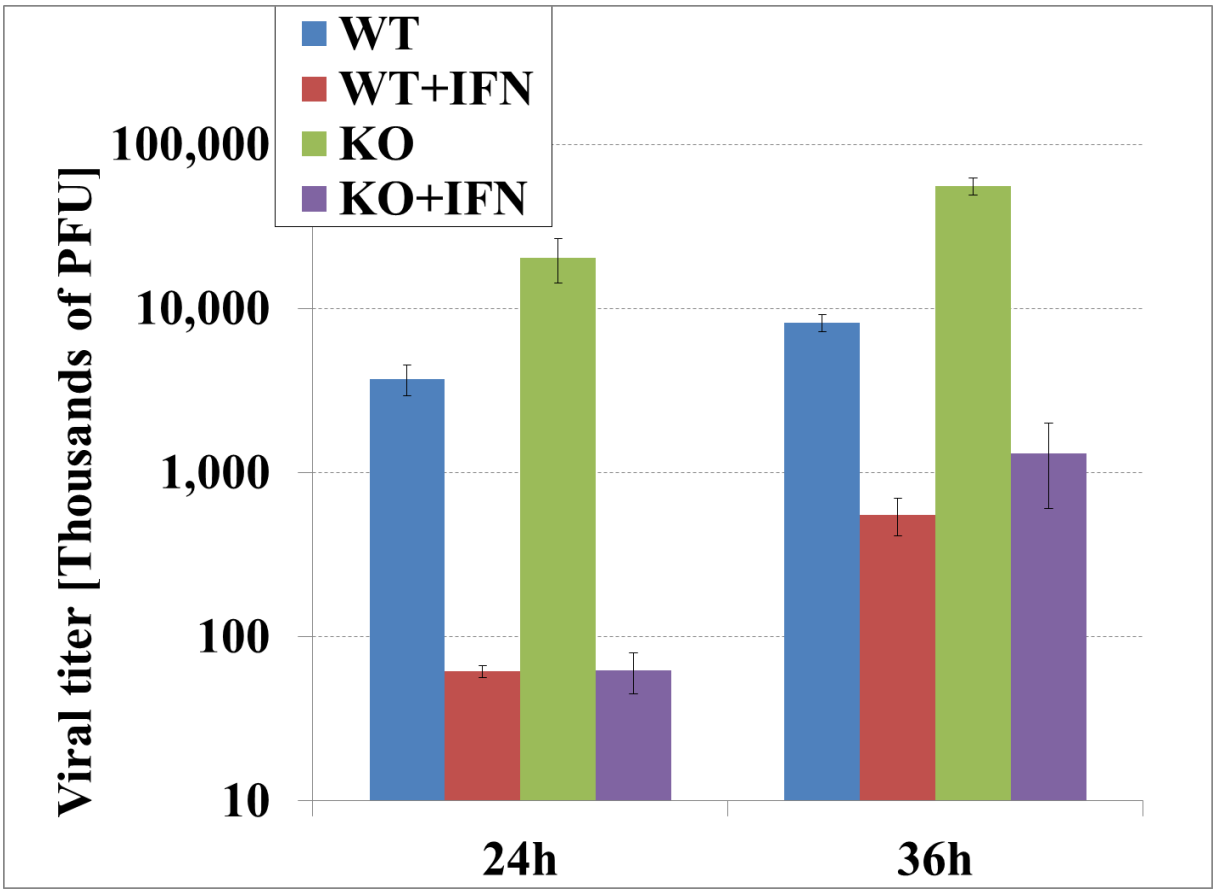

Figure 55. Effect of IFNβ on MHV68 replication in WT and ISG54KO MEFs. Wild-type or ISG54 KO MEFs were pretreated overnight with 100U/ml murine IFN-β and the next day infected with MHV68 at MOI 1. Viral titer was determined at 24hs and 36hs after infection with plaque assay and compared to the viral titer in the cells that were not treated with IFN. Calculated *p* values comparing viral titer in cells treated vs untreated with IFN were <0.01 IFN treatment decreased MHV68 replication at similar rate in wild-type and knockout cells.

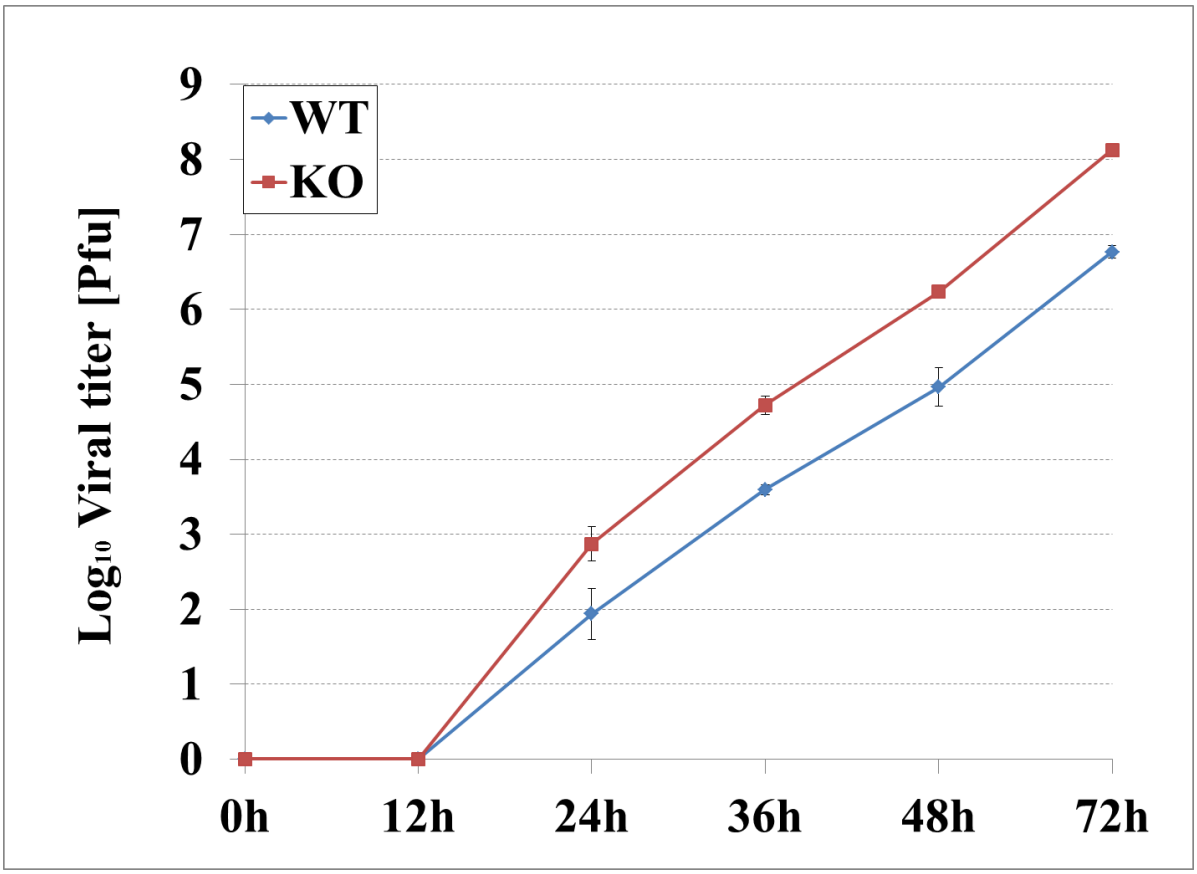

Figure 56. MHV68 mutant lacking M11 protein replicates better in ISG54 knockout cells than WT cells. Wild type or ISG54 knockout MEFs were infected with mutated MHV68 virus that lacked M11 protein at MOI 0.01. Viral titer was determined at different timepoints after infection using plaque assay. Viral titer was more than ten times higher in the ISG54 knockout versus wild-type cells. Calculated *p* value comparing viral titer in WT vs ISG54KO cells at 48h and 72hs were <0.001 and <0.0001 respectively.

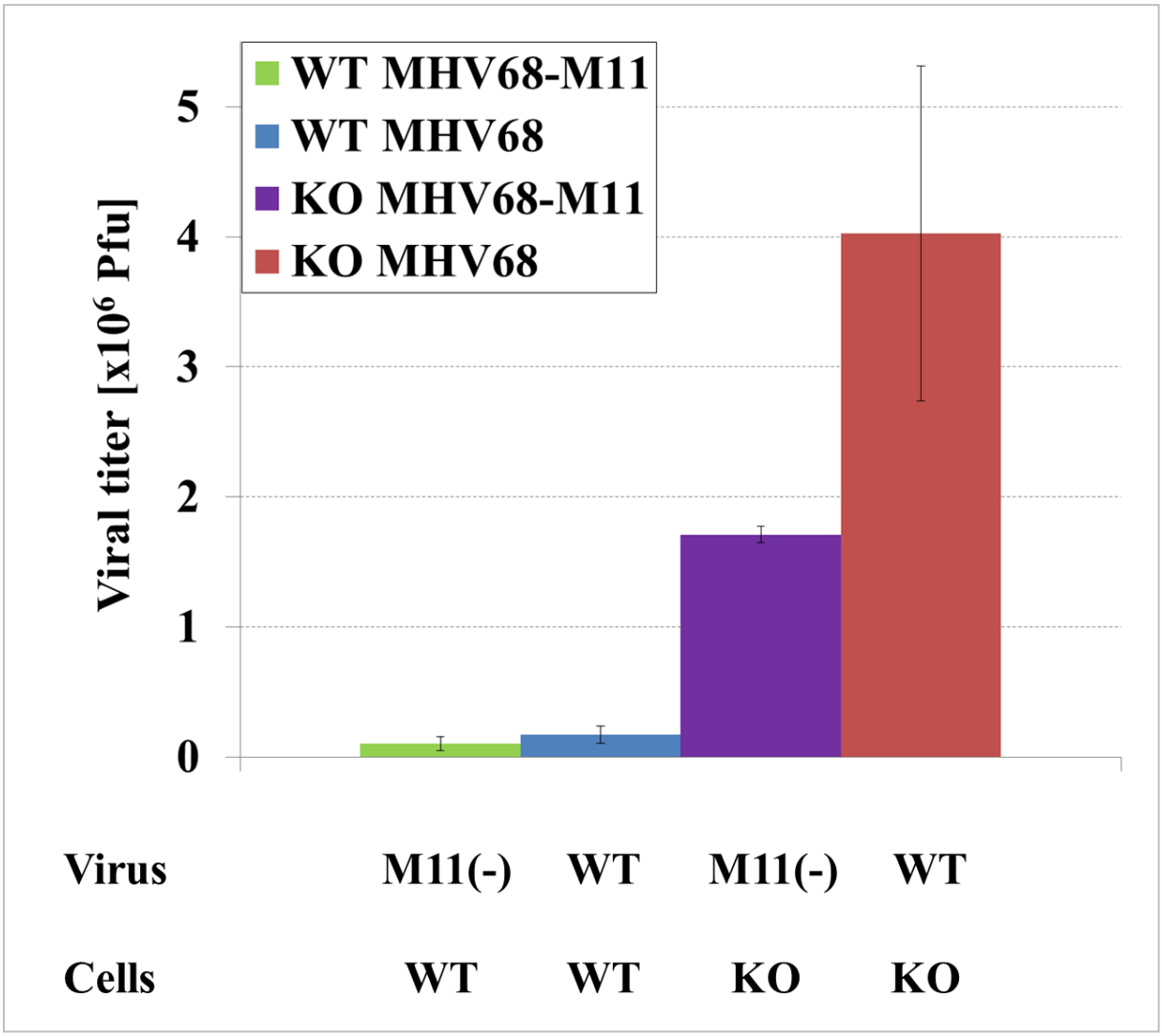

Figure 57. ISG54 counteracts action of viral antiapoptotic M11 protein. Wild-type or ISG54 knockout cells MEFs were infected with wt MHV68 virus or MHV68 that lacks M11 protein (MHV68-M11) or with control wild-type virus with the same backbone. Infection was performed at MO I 0.01 for 48hs and the viral titer was evaluated with plaque assay. While in the wild type MEFs difference between replication of wild-type and M11 deficient virus was not significant (*p* value = 0.11), in ISG54 KO MEFs wild type virus produced over two-times higher titer than M11 deficient virus (*p* value <0.02)

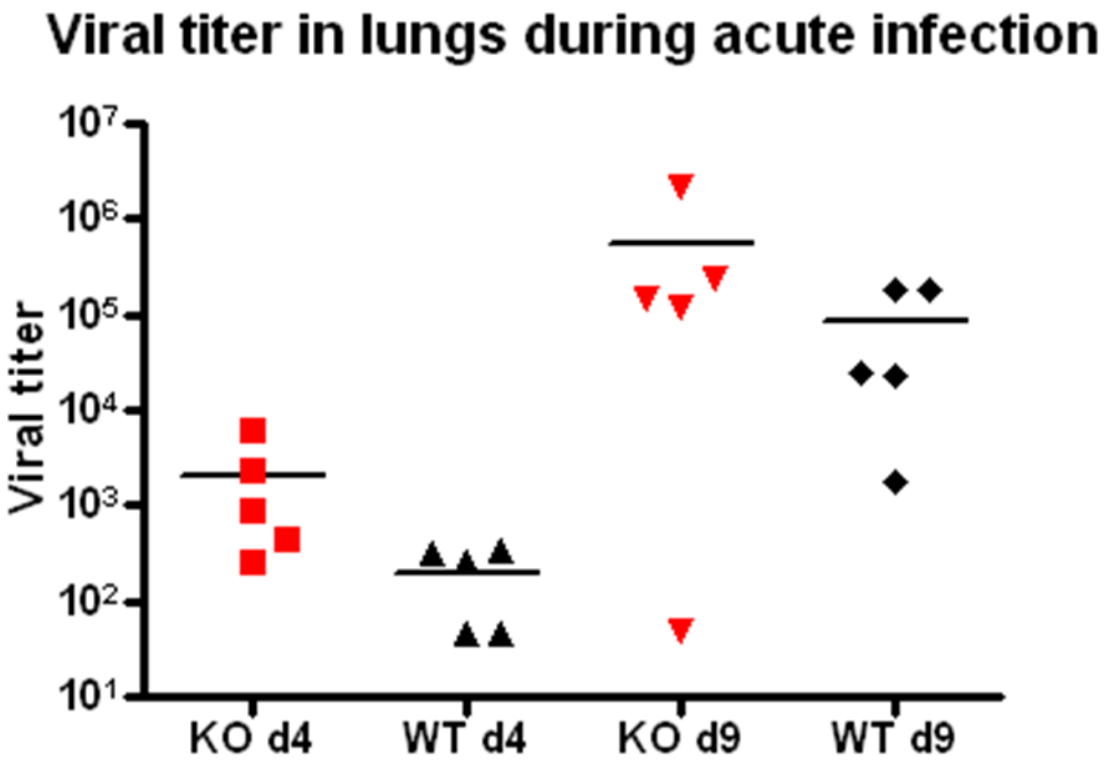

Figure 58. MHV68 acute replication in the lungs. Wild-type (WT) or ISG54-knockout (KO) mice were infected intranasally with 1000Pfu of MHV. At day 4 (d4) and day 9 (d9) after infections the lungs were removed, homogenized and viral titer was determined with plaque assay.

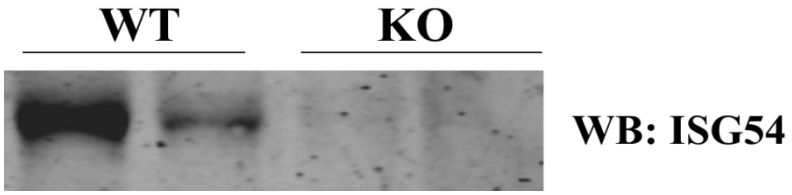

Figure 59. ISG54 is expressed in the lungs during MHV68 infection. Lung samples from two wild-type or two ISG54 knockout animals removed at day 9 post infection were homogenized, lysed and analyzed with Western-blotting for ISG54 expression. Wild-type mice showed expression of ISG54 while no ISG54 protein was detected in knockout animals.

\

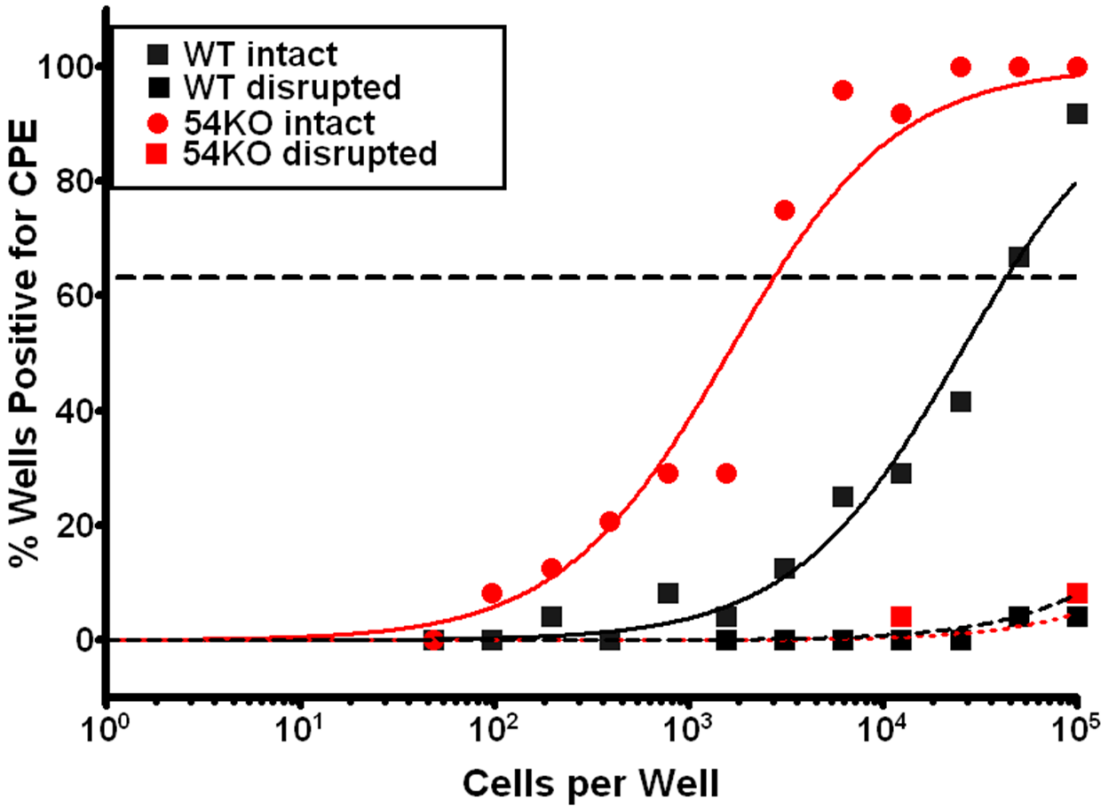

Figure 60. MHV68 splenic reactivation is elevated in ISG54 knockout mice. Wild type (WT) or ISG54 knockout (54KO) mice were infected intranasally with MHV68 at Pfu 1000. 16 days after infection mice were sacrificed, spleens harvested and the intact splenocytes were plated at 12 serial dilutions on the monolayer of mouse embryo fibroblasts (MEFs). In parallel, mechanically disrupted cells were plated to detect the presence of preformed infectious virus. 2 weeks after plating the wells were examined under microscope for the cytopathic effect. Percentage of wells positive for reactivation was calculated, plotted and analyzed with non-linear regression fit. ISG54 knockout animals displayed over ten times higher reactivation comparing to the wild-type mice. The levels of preformed virus were insignificant both in wild-type and knockout mice. Dashed line at 63% corresponds to the minimal number of cells required to obtain at least one reactivating virus (according to Poisson's distribution)

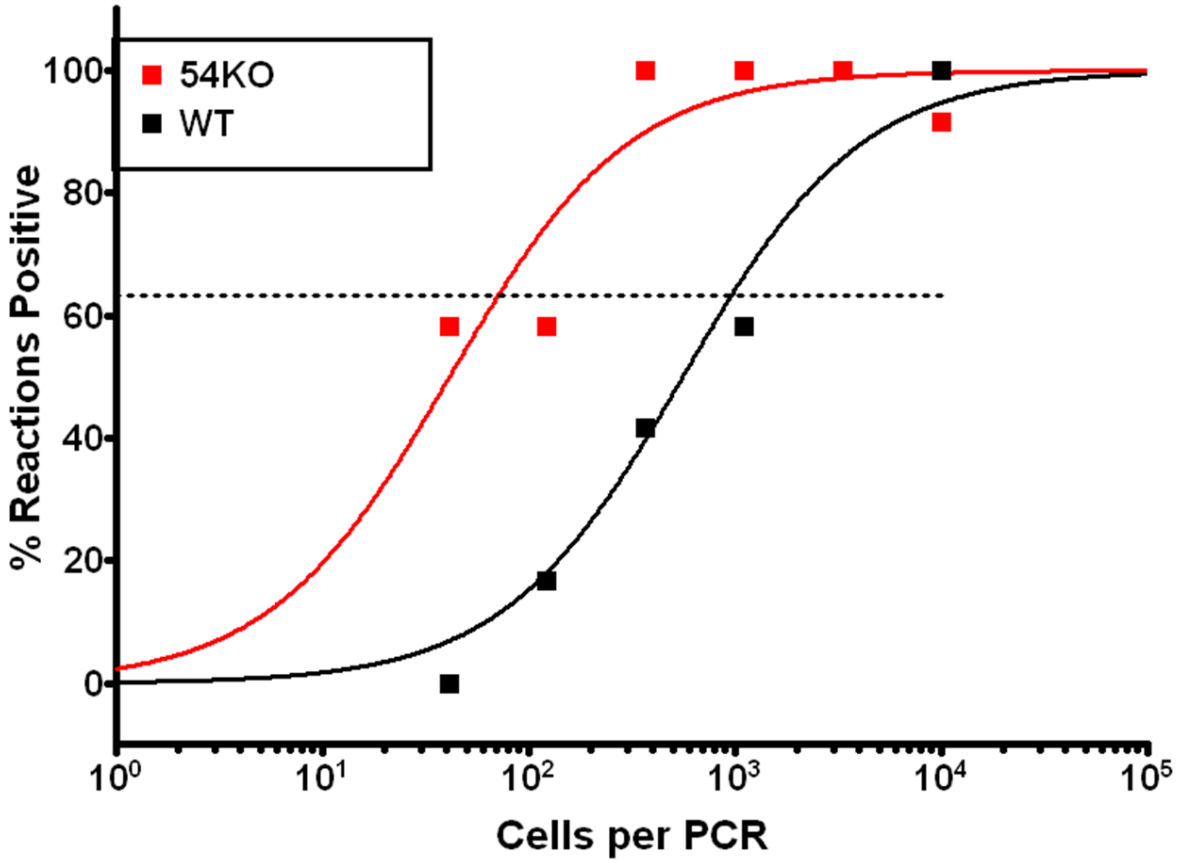

Figure 61. MHV68 splenic latency is elevated in ISG54 knockout mice. Wild type (WT) or ISG54 knockout (54KO) mice were infected intranasally with MHV68 at Pfu 1000. 16 days after infection mice were sacrificed, spleens harvested and the level of viral latency was evaluated with Limited Dilution PCR (LD-PCR). ISG54 knockout animals displayed more than ten times higher latency comparing to the wild-type mice. Dashed line 63% corresponds to the minimal number of cells required to obtain at least one latent virus (according to Poisson's distribution).

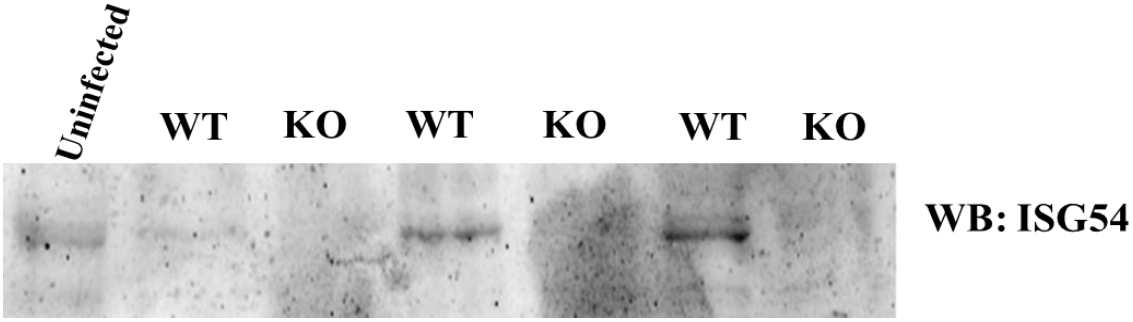

Figure 62. ISG54 is expressed in the spleens during MHV68 infection. Combined pools of wild-type or ISG54 knockout splenocytes isolated at day 16 after viral infection (Pfu 1000) in three independent experiments were lysed and analyzed with Western-blotting for the presence of ISG54. ISG54 was induced in the wild-type splenocytes but not in ISG54-deficient cells.